MEASUREMENT OF pH IN AQUEOUS SOLUTIONS AT ELEVATED TEMPERATURES

by

Gary Douglas Manning, B.Sc., A.R.C.S.

A Thesis submitted for the Degree of

Doctor of Philosophy of the University of London

January 1975

ABSTRACT

The pH of three standard buffer solutions has been measured using a hydrogen electrode versus a silver-silver chloride electrode in a cell without a liquid-liquid junction. The measurements have been carried out at 95-120°C for 0.05 m Potassium Tetroxalate, 100-160°C for Saturated (at 25°C) Potassium Hydrogen Tartrate and at 100-200°C for 0.05 m Potassium Hydrogen Phthalate.

The precipitation of compounds from aqueous 0.5 M solutions of divalent metal sulphates at 150° and 200°C has been studied. Three different basic nickel sulphates have been prepared, their formulae determined and their X-ray powder patterns correlated to those of previously reported solids. In addition, two basic cobalt sulphates and one basic manganese sulphate have been shown to exist. Their probable formulae and their powder patterns are reported.

CONTENTS

	ABSTRACT	2
1.	INTRODUCTION	6
1.1	Theoretical pH Scales	6
1.2	The Operationally Defined pH Scale	11
1.3	pH Measurement at Elevated Temperatures: Proposed Work	12
1.4	The pH_S Scale	14
1.5	The Measurement of pa_H in Buffer Solutions	16
2.	APPARATUS AND TECHNIQUES	21
2.1	The Autoclave	21
	Pressure Connections	23
	Electrical Connections	23
2.2	The Potential Measuring Circuit	27
	Digital Voltmeter	29
	Back-off Circuit	29
	Vibron Electrometer	29
	Potential Recorder	31
	Circuit Calibration	31
2.3	Pressure Measurement	32
2.4	Temperature Measurement	34
	Thermocouple Calibration	35
	B. Point of Water	36
	M. Points of Metals	38
2.5	Silver-Silver Chloride Electrodes	42
	Types and Preparation	42

	Solubility of AgCl in Chloride Solutions	44
	Protection of the Ag-AgCl Electrodes	47
	Standard Potential of the Ag-AgCl Electrode	50
2.6	Hydrogen Electrodes	55
	Palladium Electroplating	58
	Iridium Electroplating	59
2.7	Reagents and Solutions	61
	Water Evaporation	65
2.8	Experimental Procedure	68
3.	ANALYSIS OF EXPERIMENTAL DATA	71
3.1	The Hydrogen Gas Activity	71
	Vapour Pressure of the Solutions	71
	Saturated Water Vapour Pressure	76
	Fugacity Coefficient of Hydrogen	76
3.2	The Dielectric Constant of Water: the Debye-Huckel Constants	85
3.3	General Analysis of $p(a_H \gamma_{Cl})$ Data	89
	Statistical	89
	Calculation of $p(a_H \gamma_{Cl})^\circ$	93
4	RESULTS	96
4.1	Stability of Standard Buffer Solutions	96
4.2	0.05 m Potassium Tetroxalate	100
	Ionic Strength	110
	γ°_{Cl} in the Solution	112
4.3	Saturated (25°C) Potassium Hydrogen Phthalate	114
	Ionic Strength	127

4.4	0.05 m Potassium Hydrogen Phthalate	133
	Ionic Strength	154
4.5	0.025 m Potassium Dihydrogen Phosphate - 0.025 m Disodium Hydrogen Phosphate	158
4.6	Accuracy and Comparison with Previous Work	158
4.7	Standard Buffers at Elevated Temperatures	160
5.	SYMBOLS AND THE PHYSICAL CONSTANTS	162
6.	REFERENCES	164
	Acknowledgements	175
Appendix A.	The Calculation of the Minimum Dimensions of the Autoclave.	176
Appendix B.	The Reduction of AgCl by H_2 and some Considerations of the Requirements for Reference Electrodes at Elevated Temperatures.	181
Appendix C.	Precipitation of Metal Compounds from Aqueous Solutions at Elevated Temperatures.	197

1. INTRODUCTION

1.1 Theoretical pH Scales[1]

Eversince Sørensen described, in 1909, the unique influence of the hydrogen ion concentration in biochemical reactions its importance as a major parameter for describing aqueous equilibria has steadily increased. Sørensen also drew attention to the significance of the 'degree of acidity' of a solution compared to its 'total acidity' and proposed the 'hydrogen ion exponent' as a convenient notation to cover the wide range of hydrogen ion concentrations encountered, i.e. $10 - 10^{-15}$ $m.l^{-1}$. Thus

$$c_H = 10^{-p}$$

(where 'p' derived from Potenz, puissance or power) and therefore

$$pcH = - \log c_H$$

or on the molal scale

$$pmH = - \log m_H$$

both of which are totally physically defined quantities.

To measure pH, Sørensen proposed the cell

$$Pt(H_2) \,|\, \text{Soln. X} \,\|\, \text{Conc. KCl soln. } (c_{KCl}) \,\|\, 0.1\overset{M}{\backslash} \text{Calomel electrode.} \qquad \text{— (1)}$$

In an attempt to minimise the liquid junction potentials, different KCl concentrations were used in the salt bridge and the cell's potential plotted versus $1/c_{KCl}$ and extrapolated to $1/c_{KCl} = 0$, i.e. infinite KCl concentration, at which point the junction

potentials were assumed completely nullified. (This was the so-called Bjerrum extrapolation). Now if E_0 and E_1 were the cell potentials so obtained from using two solutions X_0 and X_1 then according to classical Arrhenius and Nernst theories

$$E_1 - E_0 = \frac{RT}{F} \ln \frac{(c_H)_0}{(c_H)_1} \qquad — (2)$$

and if E_0 was the potential of the cell obtained when X_0 was a solution with $c_H = 1.0\ m.l^{-1}$ then

$$E_1 = E_0 + \frac{RT}{F} psH_1 \qquad — (3)$$

and E_1 became directly proportional to the psH (the original Sørensen pH scale) of the unknown solution, X_1. To obtain E_0, Sørensen used solutions containing either HCl or mixtures of HCl and NaCl and assumed that in such solutions c_H was given by

$$c_H = \alpha\, c_{HCl}$$

where α was the fractional dissociation of HCl which he obtained from conductance measurements using classical Arrhenius theory. In this manner he obtained $E_0(25^\circ C) = 0.3376$ V and therefore equation (3) became generally

$$psH = \frac{E - 0.3376}{0.05916} \qquad — (4)$$

However, following the advent of G.N.Lewis' theory of the activity of electrolytes, which was strongly supported by the Debye-Huckel theory, it was seen that the above argument contained flaws. Firstly, the hydrogen ion concentrations in the Nernst equation (2)

should really be activities and secondly, the hydrogen ion concentration in a strong acid, such as hydrochloric acid, is actually equal to the concentration of the acid, i.e. the acid is totally dissociated. The initial Sørensen pH scale, psH, measured therefore neither hydrogen ion concentration nor activity and was merely a conventional scale following equation (4).

Sørensen subsequently proposed a new pH scale based on hydrogen ion activity,

$$pa_H = -\log a_H = -\log c_H\gamma_H.$$

Such a definition, however, immediately involved the difficulty that single ion activities are not uniquely defined by thermodynamics. Thinking was rather confused on this point at the time but in 1929 Guggenheim[2] had summed up the situation: "It has long been realised that one cannot accurately determine in a solution the activity or chemical potential of an individual ion, because of the existence of liquid junction potentials whose magnitude cannot be computed without a previous knowledge of the individual ionic activities that one wishes to measure. This vicious circle has generally been regarded as an unfortunate accident...." The accident did not, of course, exist the relevant point being that single ion activities are never required in any thermodynamic expression to describe a physically measurable quantity. Therefore no physical measurement of any thermodynamic quantity can ever yield values of single ion activities. Because of this Guggenheim went on to somewhat forcefully dismiss single ion activities as a concept without unique physical definition, a view which, although certainly true within equilibrium thermodynamics, might be regarded by some authors as rather extreme when some

extra-thermodynamic assumptions are made. (See, for example, references (3) and (4)). Indeed Guggenheim later relented somewhat and, in common with other researchers, admitted the usefulness of the idea. Moreover, the problem of deciding on sensible, conventional values for single ion activity coefficients is not as hopeless as at first it seemed. For example, the mean ionic activity coefficients, $\gamma_{\pm}$ of all 1:1 electrolytes tend to become equal in dilute solutions and therefore the obvious convention is to assume that all single ion activity coefficients in such solutions are also equal. In more concentrated solutions, in which values of $\gamma_{\pm}$ for different 1:1 electrolytes are no longer similar a more complicated convention would have to be assumed.(5,6)

Thus to precisely define the pa_H scale, a choice, to some extent arbitary, has to be made for the value of one particular single ion activity coefficient, although it will be seen that this need not be for the hydrogen ion. Once this has been done, however, an entirely self-consistant pH scale is defined which uniquely describes true thermodynamic quantities, e.g. equilibrium constants.

Guggenheim(5) and Hitchcock(7) have suggested the function

$$p(a_H\gamma_{Cl}) = -\log (m_H\gamma_H\gamma_{Cl})$$

a special case of the more general function

$$p(a_H\gamma_A) = -\log (m_H\gamma_H\gamma_A)$$

in which A is any univalent anion. These are totally physically defined functions containing the product of two single ion activity coefficients. Unfortunately, however, in certain types of solution

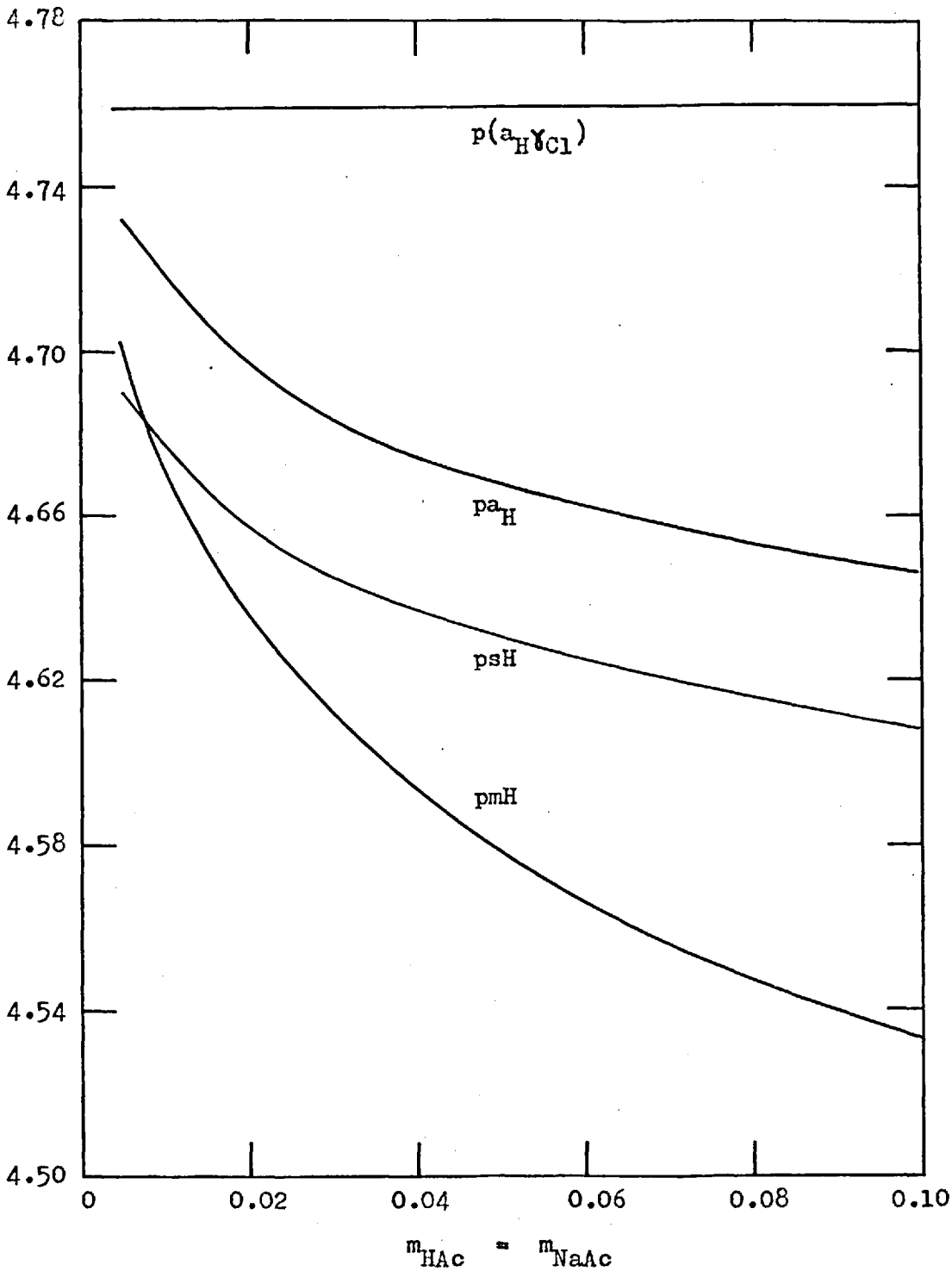


Fig. (1) Acidity of acetate buffer solutions at 25°C on four different scales, as a function of molality

such functions are not very good measures of the degree of acidity. Fig. (1) (after Bates[1,8,9]) shows the functions pmH, psH, pa_H and $p(a_H\gamma_{Cl})$ in solutions containing equimolar quantities of sodium acetate and acetic acid and it can be seen that $p(a_H\gamma_{Cl})$ is virtually constant despite a change of 0.16 units in pmH.

1.2 The Operationally Defined pH Scale

In order to circumvent the theoretical difficulties, modern practical pH measurement employs an operationally defined pH scale. Thus the internationally agreed operational definition of pH, as recommended by Bates and Guggenheim[6] and recognised by IUPAC is as follows. If two cells are considered, at constant temperature, T

$$Pt(H_2)\,|\,\text{Soln. X}\,||\,\text{Conc. KCl soln.}\,||\,\text{Reference electrode}$$

$$Pt(H_2)\,|\,\text{Soln. S}\,||\,\text{Conc. KCl soln.}\,||\,\text{Reference electrode}$$

whose potentials are E_X and E_S respectively, then

$$pH_X = pH_S + \frac{(E_X - E_S)\,F}{RT \ln 10} \qquad -(5)$$

It is to be understood that the two hydrogen electrodes may be replaced by two quinhydrone or glass electrodes, although corrections may have to be applied at high and low pH when using the latter. The KCl salt bridge, which is usually part of the reference electrode assembly, is either saturated or 3.5 M.

Thus the operational pH of a solution, X, becomes a function of a cell's E.M.F. and the pH_S of some standard (buffer) solution, S, and the operational pH of two solutions, X_1 and X_2 may be

conveniently compared without having recourse to the precise meaning and value of pH_S as long as it is sensible and constant.

Although this may seem theoretically unsatisfactory it may be pointed out that in practice it is rare in the laboratory and probably unheardof in industry for the pH of a solution to be considered in terms of solution theory. What is required, in far the majority of cases, is a sensible, quantitative measure of acidity and alkalinity to perhaps $\pm$ 0.05 pH units.

1.3 pH Measurement at Elevated Temperatures: Proposed Work

The commercial availability of glass electrode assemblies and pH meters has made pH measurement in all types of aqueous solutions routine up to the boiling point. At above 100°C, however, the situation alters radically. It has been seen that for practical pH measurement three things are required: i) a pH monitoring electrode (almost invariably glass) ii) a reference electrode (usually either Ag-AgCl or $Hg-Hg_2Cl_2$) and iii) a standard buffer solution. At below 100° all these are readily available but at above 100° this is no longer the case. Glass electrodes become increasingly attacked by aqueous solutions at elevated temperatures, drastically shortening their working life. This effect alone makes pH measurement, at present, virtually impossible at >150°C using anything other than a hydrogen electrode, which is generally unsuitable. Reference electrodes can cause problems at elevated temperatures because of competing side reactions, e.g. hydrolysis, disproportionation or reduction (if hydrogen is present). However, a suitably designed Ag-AgCl reference electrode could almost certainly be used up to at least 200°C in the absence of hydrogen.

This point is more fully discussed in Appendix B.

Regarding buffers, there is very little data on the pH of buffer solutions at elevated temperatures across the main region of the pH scale. In 1930, Stene,[10] using a rather ingenious apparatus incorporating a balanced-pressure electrolytic bridge, measured the pH of HCl-KCl, phthalate, phosphate and borate buffers up to 150°C with a hydrogen electrode versus a cold calomel reference electrode. More recently Le Peintre[11] has measured the pH of HCl, tartrate, acetate, phosphate and borate buffers up to 250°C using one hydrogen electrode versus another hydrogen electrode in a HCl reference solution. However, his cell contained a saturated KCl salt bridge and therefore involved unknown liquid junction potentials. Kryukov, et al,[12] have also calibrated similar buffer solutions plus tetroxalate and phthalate buffers up to 150°C using a hydrogen electrode. The precise nature of their reference electrode, based on thallium, is unclear, but was probably a 'Thalamid' type electrode comprising of thallium (or thallium amalgam) in contact with solid thallous chloride in a saturated KCl solution which would also have involved liquid juntion potentials. Indeed the only pH measurements in buffer solutions, at elevated temperatures, obtained from a cell not containing a liquid junction seems to be those of Greeley,[13] who has calibrated 0.001-1.0 m HCl solutions from 25 to 275°C. In fact the pH of these solutions change little over this temperature range although the solutions are not particularly useful as standards, having little buffering capacity and their pH being too low for convenience.

In view of the above situation regarding practical pH measurement at elevated temperatures it was proposed to extend the

calibration of known buffers from 100° to 200°C using a cell without a liquid junction.

The standardisation of buffer solutions at elevated temperatures before a convenient method of pH measurement is available may seem a little premature but this is not so. Any electrode which is to measure pH usefully at above 100°C (be it a modified glass electrode or otherwise) will have to obey the Nernst equation more or less closely, i.e. its potential must change by RT ln 10/F per pH unit over a significant pH range and the only way that this can be checked is by using previously standardised buffers. Thus the developement of a pH electrode and buffer calibration must proceed simultaneously.

1.4 The pH_S Scale

To calibrate buffers for the practical, pH_S scale it is necessary to decide on which theoretical pH scale the measurements are to be based and in making the choice previous workers have taken both the theoretical and practical aspects into account. Practical measurement according to equation (4) and lately to (5) has been so widely carried out that a scale closely following the potential response of the cells from which these expressions have been derived is virtually essential. It has been seen that the function $p(a_{H}\gamma_{Cl})$ can be an unsuitable measure of the degree of acidity and must therefore be rejected. The psH scale, although very convenient, has unfortunately virtually no theoretical meaning. A similar criticism may be leveled at the pa_H scale although its role in chemical equilibria and the precise point in its definition at which it departs from a purely thermodymamic, physically defined

function can be clearly seen. It obviously differs from the pmH scale by log γ_H (although they are identical at infinite dilution) and in Fig. (1) it seems to parallel the psH scale. That this will always tend to be so may be demonstrated by considering Sørensen's original cell (1) more fully. The two half-cell reactions will be

$$H^+ + e^- = \tfrac{1}{2}H_2$$

$$\tfrac{1}{2}Hg_2Cl_2 + e^- = Hg + Cl^-(\text{in 0.1 M KCl}) \pm \text{ion transfer across liquid junction}$$

and the half-cell potentials,

$$E_{H^+} = E^o_{H^+/H_2} - \frac{RT}{F} \ln \frac{a_{H_2}^{\frac{1}{2}}}{a_{H^+}}$$

$$E_{Hg_2Cl_2} = E^o_{Hg_2Cl_2} - \frac{RT}{F} \ln \frac{a_{Hg}a_{Cl^-}}{a_{Hg_2Cl_2}} + E_j$$

where E_j is a liquid junction potential, clearly necessary because a_{H^+} and a_{Cl^-} do not refer to the same solution. If E is the observed full-cell potential, then on assuming normal standard states

$$pa_H = -\log a_{H^+}$$

$$= \frac{F}{RT \ln 10}(E - E^o_{Hg_2Cl_2} - E_j) + \log a_{Cl^-}$$

log a_{Cl^-} is constant and if E_j is assumed to be at least approximately so, then

$$pa_H = \frac{E - E'}{0.05916} \qquad -- (6)$$

where E' is the standard potential of the reference half-cell

$$Hg\text{-}Hg_2Cl_2 \,|\, 0.1\ M\ KCl \,\|\, \text{Salt bridge} \,\|$$

Equation (6) is of the same form as Sørensen's definition of psH (equation (4)) and since $E'(25^\circ C) = 0.3356$ V

$$pa_H = psH + 0.04$$

Thus the pa_H scale has the advantages of closely following both the Operation and Sørensen pH scales and in particular of being linearly related to the many previous measurements made on the latter. It can also be handled theoretically, even if it is not actually precisely thermodynamically defined.

It is for these reasons that Bates and his co-workers chose the pa_H scale as the basis for their calibration of standard buffers. They have measured the pa_H of a series of primary standards and for these solutions,

$$pH_S = pa_H$$

1.5 The Measurement of pa_H in Buffer Solutions

The present measurement of pa_H in buffer solutions at elevated temperatures was carried out using basically the same method that Bates employed at below 100°C. The cell

$$Pt,Pd \text{ or } Ir(H_2)\,|\,\text{Buffer, } KCl(m_{KCl})\,|\,Ag\text{-}AgCl,Pt$$

was used. This has no liquid junctions and therefore its half-cell reactions are

$$H^+ + e^- = \tfrac{1}{2}H_2$$

$$AgCl + e^- = Ag + Cl^-$$

with half-cell potentials,

$$E_{H^+/H_2} = E^o_{H^+/H_2} - \frac{RT}{F} \ln \frac{a_{H_2}^{\frac{1}{2}}}{a_{H^+}}$$

$$E_{Ag/AgCl} = E^o_{Ag/AgCl} - \frac{RT}{F} \ln \frac{a_{Ag}a_{Cl^-}}{a_{AgCl}}$$

Conventional standard states make $a_{Ag} = a_{AgCl} = 1$ and $E^o_{H^+/H_2} = 0$ at all temperatures and therefore if E is the full-cell potential,

$$E = (E_{Ag/AgCl} - E_{H^+/H_2})$$

$$= E^o_{Ag/AgCl} - \frac{2.303RT}{F} \log \frac{a_{Cl^-}a_{H^+}}{a_{H_2}^{\frac{1}{2}}} \qquad -- (7)$$

But $a_{Cl^-} = m_{Cl^-}\gamma_{Cl^-} = m_{KCl}\gamma_{Cl^-}$, therefore substituting into (7) and rearranging gives

$$p(a_H\gamma_{Cl}) = -\log (a_{H^+}\gamma_{Cl^-})$$

$$= \frac{(E - E^{\circ}_{Ag/AgCl})}{2.303RT/F} - \log m_{KCl} + \tfrac{1}{2}\log a_{H_2} \qquad -- (8)$$

$p(a_H\gamma_{Cl})$ was measured for a series of chloride concentrations in each buffer and then extrapolated (at constant temperature) to zero chloride concentration to give

$$p(a_H\gamma_{Cl})^{\circ} = \lim_{m_{KCl} \to 0} p(a_H\gamma_{Cl}) \qquad -- (9)$$

which is still a totally thermodynamically defined function. The pa_H of the buffer solution in the absence of chloride is

$$pa_H = p(a_H\gamma_{Cl})^{\circ} + \log \gamma^{\circ}_{Cl} \qquad -- (10)$$

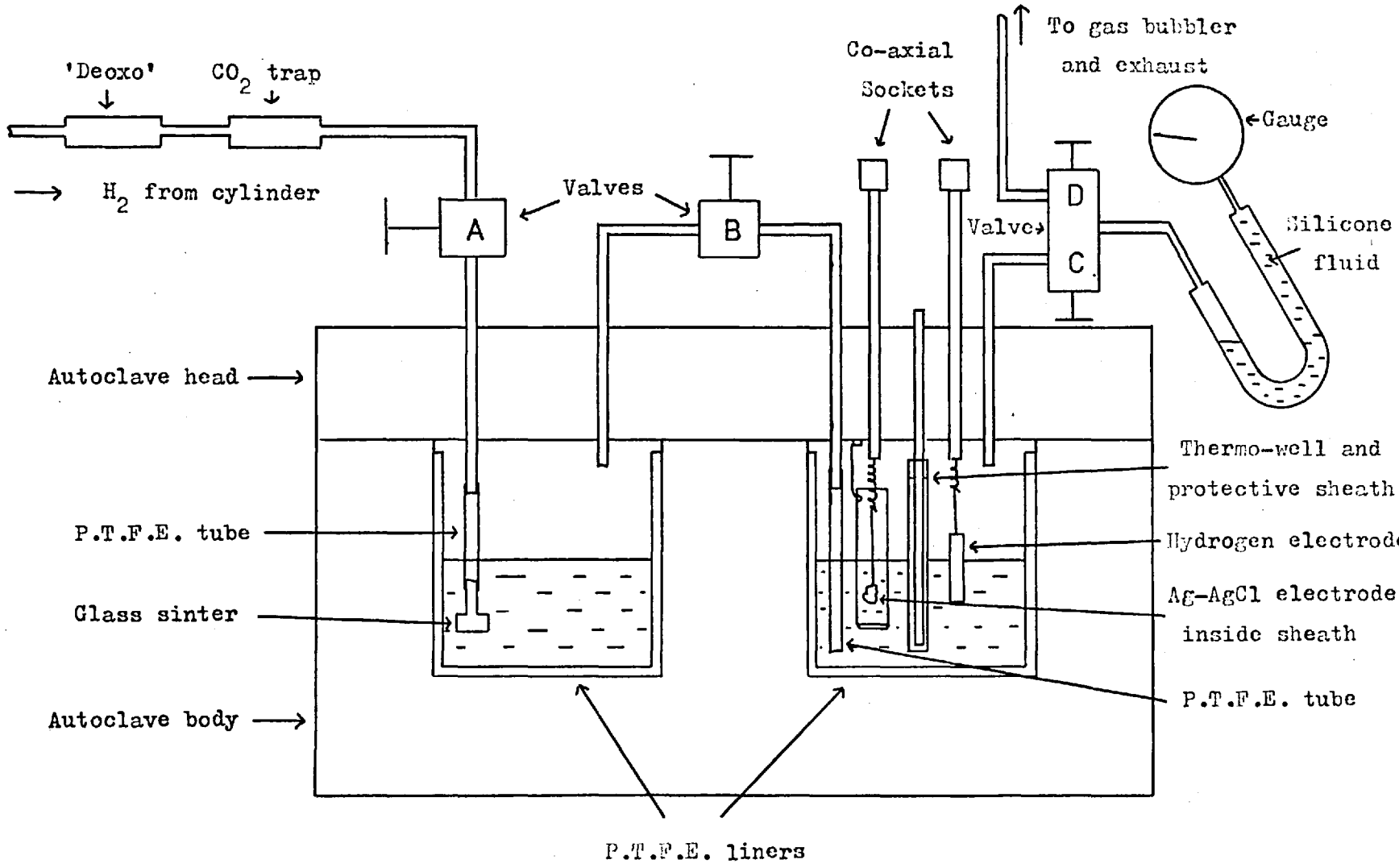
where γ°_{Cl} is the activity coefficient of the chloride ion in the buffer solution at infinitely dilute chloride concentration and is assumed to be given by,

$$\log \gamma^{\circ}_{Cl} = \frac{-AI^{\frac{1}{2}}}{1 + 1.5I^{\frac{1}{2}}} \qquad I \leq 0.1 \qquad -- (11)$$

in which A is the Debye-Huckel limiting slope and is temperature dependant. This final assumption, due to Bates and Guggenheim[6], is the only non-thermodynamic part of the definition of pa_H and in fact makes γ°_{Cl} effectively equal to the mean ionic activity coefficient of NaCl in solutions up to 0.1 m.

The value of I, the ionic strength of the buffer solution in the absence of KCl, can be calculated with sufficient accuracy ($\pm$ 10%) from the $p(a_H\gamma_{Cl})^\circ$ data and relevant equilibrium constants (if any). Details of the calculation are shown in the section on each respective buffer.

Fig. (2) Schematic cross-section of experimental arrangement.



2. APPARATUS AND TECHNIQUES

A schematic cross-section of the autoclave showing the essential gas pipelines, valves, pressure gauge, electrical connections, electrodes etc. is shown in Fig. (2).

2.1 The Autoclave

The reaction vessel was machined from a single block of EN 58J (B.S. 970 Pt. 4 Type 316 S16) stainless steel and had two adjacent cylindrical reaction pots, 3 in. diameter and 3 in. deep. This design seemed potentially the most useful for the present and possible future work. The vessel head, also made from stainless steel, was bolted to the main body by fifteen Socket Head Cap Screws and was equipped with seven through-holes, with pressure unions, above each pot. The pressure seal between head and body was achieved using two Viton rubber O-rings concentric with the reaction pots. These O-rings were found perfectly satisfactory up to 200°C and could be reused several times, despite considerable distortion during their first run, as long as some care was taken to avoid any surface scratching.

The whole vessel was surrounded by a substantial aluminium heat sink made, for convenience, in two halves and bolted together. The stainless vessel was a sliding fit in the aluminium at slightly above room temperature.

The assembly was heated by three Kel Co-planar heating elements (Thermic Products Co.) with power ratings of 1 kw.ft.$^{-2}$ Two identical heaters at opposite ends of the heat sink and one larger one beneath gave a total power of $3\frac{1}{4}$ kw.

The total specific heat of the stainless steel and aluminium was rather large, approximately 22.8 kcal.deg.$^{-1}$; therefore some provision for artificial cooling was made. Two cooling plates were constructed and bolted onto the remaining opposite sides of the heat sink. These plates were originally designed for use with the inert heat transfer medium 'Thermex' (a eutectic of diphenyl and diphenyl oxide) and were therefore constructed of mild steel. However, water was eventually found a more convenient coolant and was subsequently employed. The designs for these plates and for the stainless autoclave are given in Appendix A.

The whole assembly was enclosed in a box constructed of Syndanio sheet packed with Kao-wool thermal insulation and supported, at a convenient height above floor level, on a trolley made from Handy-Angle.

The power to the heaters was controlled by a Eurotherm temperature controller, whose monitoring iron-constantan thermocouple was inserted into a hole drilled in one of the aluminium blocks. Thus the temperature of the heat sink was controlled rather than that of the reaction vessel. This was the better arrangement because despite the high total heat capacity of the aluminium its temperature always initially overshot the nominal set temperature by up to 10°, but because of thermal lag this effect did not occur inside the reaction pot whose temperature rose smoothly to its equilibrium value. Because no allowance was made for the error (about 1°) in the monitoring thermocouple this final equilibrium temperature was always rather higher than that set on the Eurotherm.

To protect the stainless vessel from the hot chloride solution used (albeit dilute) each pot was fitted with a 1/8 in. thick P.T.F.E.

liner machined from a block of the plastic. Although very successful from the protection point of view unfortunately P.T.F.E. has a low thermal conductivity and heat transfer across plastic-liquid boundaries seemed particularly poor leading to an increase in the time for the internal solution to come to thermal equilibrium.

Pressure Connections

These were standard pressure unions manufactured by Autoclave Engineers Ltd. taking 1/8 in. O.D. stainless tubing. All pressure seals between the autoclave head and piping (including that of the through-electrodes) used these unions.

Electrical Connections

The electrical connections from the external potential measuring circuit through the autoclave head were particularly successful over the limited temperature and pressure ranges employed (i.e. <210°C, <300 p.s.i.). These 'through-electrodes' were designed so that their pressure seals and electrical connections were independant and either could therefore be broken and remade without disturbing the other. In fact in practice, once the pressure seals had been made they rarely needed to be disturbed and only then for cleaning purposes whereas the electrical connections to the measuring circuit needed to be broken and remade every run.

Each through-electrode was based on a floating co-axial socket 'araldited' to a stainless steel tube through which passed an insulated platinum wire. A schematic cross-section of such an electrode (twice actual size) is shown in Fig. (3) but because its

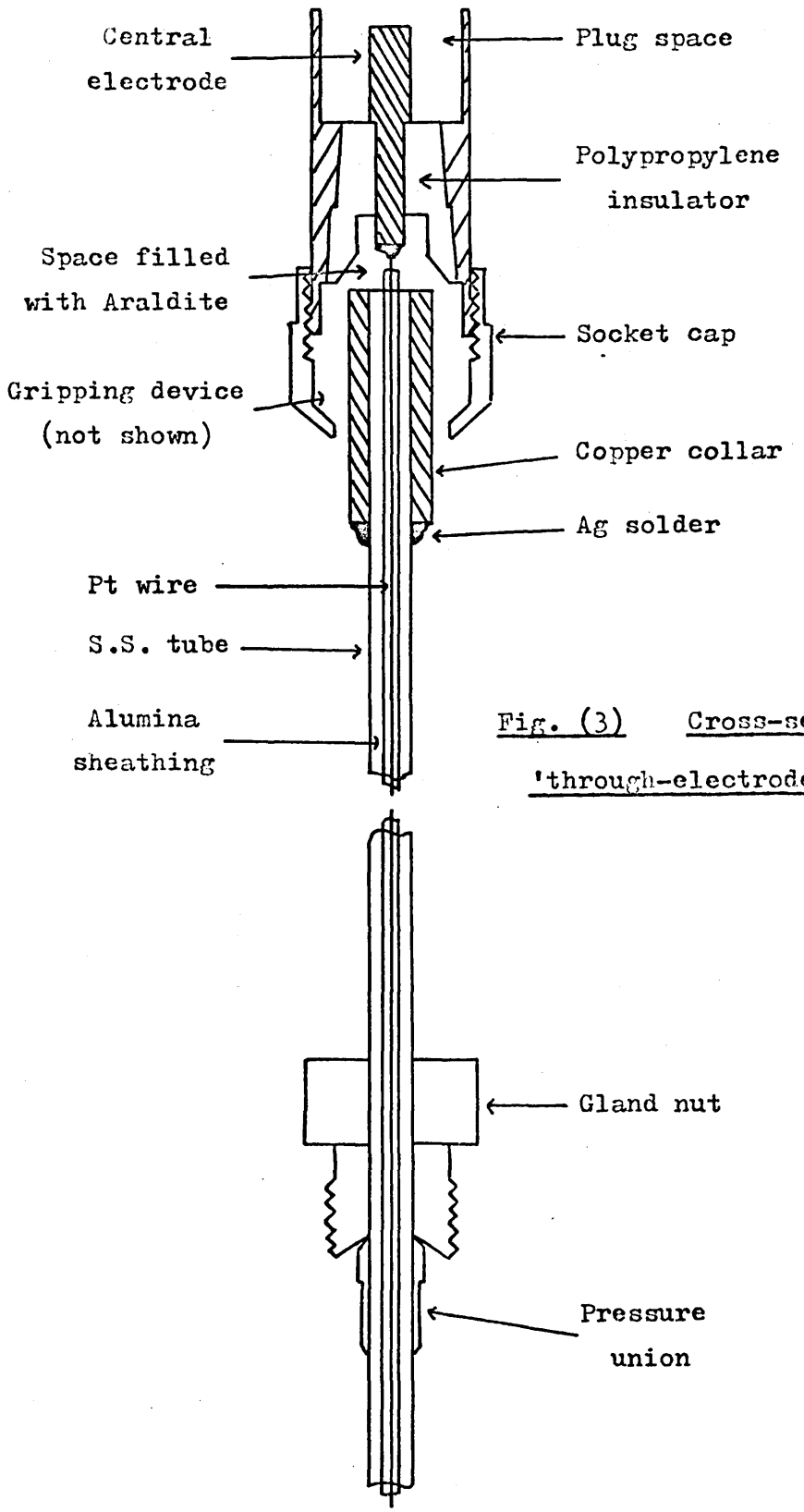


Fig. (3) Cross-section of a 'through-electrode' (x2)

assembly is not totally straightforward it will be described in some detail.

The actual electrical lead was a length of 0.3 mm. diameter platinum thermocouple wire silver-soldered to the co-axial socket's central elctrode which was then assembled, with its polypropylene insulator, in the socket's shell in the usual way. The plug space (see Fig.) was filled with a paste of alumina thermal cement (used normally for covering furnace windings) and the socket supported vertically in an oven at 60°C until the cement set hard. This acted as a support for the polypropylene during a later stage.

A $\frac{3}{4}$ in. long section of copper tubing ($\frac{1}{4}$ in. O.D.) was silver-soldered onto a 3 in. length of thin-walled stainless tubing (1/8 in. O.D.) to form a collar. Short lengths of alumina thermocouple sheathing (about 1 mm. O.D.) were slid over the platinum wire to act as electrical insulation and this then threaded through the stainless tubing so that the copper collar entered the co-axial socket as shown. The socket assembly was then completed in the usual manner and its cap screwed tight so that its internal gripping device (not shown in the Fig.) tightened onto the copper collar. The space around this collar in the socket and in the stainless tube was then filled with powdered 'high-temperature' Araldite resin (prepared by crushing solid sticks of Araldite AT 1 after cooling in liquid nitrogen) by inverting and adding through the neck of the socket cap and down the stainless tubing. Settling was aided by vibrating with a mechanical etching tool. The assembly was heated in an oven at 120° for 1-2 hours, during which time the Araldite melted to a viscous liquid. On cooling more powder was added and reheated, the process being repeated until all the space was filled. The unit

was then heated over-night at 130-140°C to completely cure the resin and it was during this period that the polypropylene insulator would have softened to such an extent as to make it unable to support the weight of the only partially solidified resin without the added support of the alumina cement.

On cooling this cement was easily removed from the plug space by washing with water and the socket could then be connected to a co-axial plug in the usual manner. A sleeve and gland nut of a pressure union were then fitted on the stainless tube which then screwed into the autoclave head giving a pressure seal. It was arranged that the tube went completely through the head and just protruded to ensure insulation of the platinum lead from the autoclave body.

The unit has several advantages: not only is the cell circuit (i.e. the platinum wire) completely insulated but it is also effectively screened by the stainless tube connected to the co-axial cable screening and autoclave body which is itself insulated from the solution by the P.T.F.E. liner. The pressure seal is standard and may be easily screwed into other autoclaves. Solid, cured Araldite AT 1 is fairly resistant to chemical attack and will withstand temperatures up to at least 240°C and anyway in this unit there is a considerable temperature gradient along the stainless tube so that even when the autoclave was at 200° the co-axial socket was at $<60^{\circ}C$ there therefore being no danger of failure. It seems likely that these through-electrodes could be successfully used up to 300°C and several thousand p.s.i. with certain modifications e.g. longer tube, replacing the polypropylene with a more thermally stable plastic, etc.

It will be seen below that both the hydrogen and Ag-AgCl electrodes used were themselves supported on platinum thermocouple wires and therefore connecting them to their respective through-electrodes amounted to joining pairs of 0.3 mm. platinum wires at the outset of each run to produce connections which had not only good electrical contact but which also could be broken easily at the end of each run (so that the electrodes might be re-prepared) without breaking the wires. However, it was found that perfectly satisfactory connections could be made by winding the platinum wires of the through-electrodes into loose spirals about 1 cm. long and quite simply bending the hydrogen or Ag-AgCl electrodes' platinum support wires to form hooks and hanging them onto one of the loops of a spiral. Moreover, although the wires were initially given a light gold plating to aid contact this was found unnecessary and when the gold eventually wore off it was not replaced.

2.2 The Potential Measuring Circuit

There were two main requirements of the potential measuring circuit. Firstly, it should measure the potential to better than 0.1 mV in 1 Volt and secondly, the resistance of the circuit should be as high as possible. This latter requirement was originally to avoid any polarisation of the electrodes but latterly enabled the system to work when the cell's internal resistance became very large due to the low porosity P.T.F.E. sinter.

To obtain a very high resistance in the measuring circuit a vibron electrometer had to be used. However, such instruments do not have the necessary significant figure accuracy required so a six digit digital voltmeter plus a back-off circuit were incorporated.

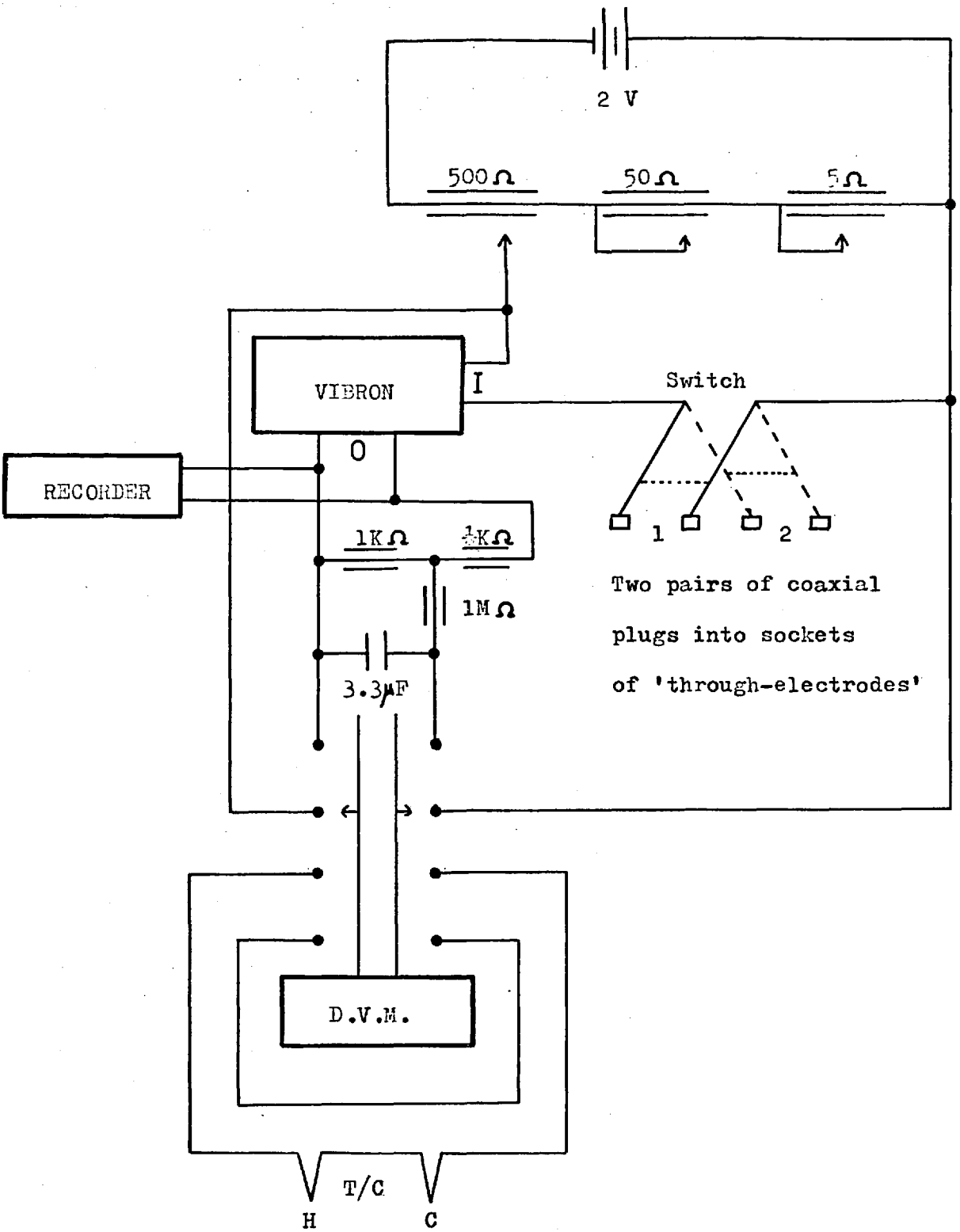


Fig. (4) Potential Measuring Circuit

A potential recorder was also added to enable the change of potential with time to be followed. The whole circuit, including a potential divider and a filter on the electrometer output (see below) and the thermocouple (whose potential was also measured by the DVM) is shown in Fig. (4).

The Digital Voltmeter

A Solartron A210 Digital Voltmeter was used having five D.C. voltage ranges from 119.999 mV to 1199.99 V. There was no standard cell incorporated and none was used throughout this work. The instrument is guaranteed to a long term accuracy of 0.001 % full scale (F.S.)

The Back-off Circuit

This consisted simply of three potentiometers in series with resistances of 500, 50 and 5 ohms giving coarse and fine control and was driven by a heavy duty 2 V lead accumulator. The back-off potential was measured by the DVM.

The Vibron Electrometer

The vibron electrometer was an E.I.L. Model A 33C, which had a maximum internal resistance of around 10^{16} ohms enabling readings to be taken from sources with resistances of up to 10^{12} ohms. The actual internal resistance of the instrument, found by measuring the current leakage rate, was $>10^{15}$ ohms throughout this work. The instrument was always used on the most sensitive of its five ranges, 10 mV F.S.

The stated accuracy of the electrometer was better than $\pm$ 1 % F.S. ($\pm$0.1 mV) reading capability plus better than $\pm$ 2 % F.S. ($\pm$0.2 mV) due to amplification error.

To minimise the reading error the electrometer's output (1 ma into 1.5 kohm) was fed (via a potential divider) into the DVM with a simple filter interposed to stabilise the digital reading. Various time constants were tried and one of 3.2 seconds (plus the low pass filter on the DVM) reduced the noise to a flicker in the third digit (equivalent to 0.01 mV). This combination of filters meant that about 30 seconds were required for the final digital value to be displayed.

The potential for the recorder had to be taken from the circuit before the filter because if the recorder was put directly in parallel with the DVM then the combination of the recorder's internal resistance (2 Mohm) and the filter's resistance (0.1 Mohm) acted as a second potential divider causing the DVM to read 5 % low (i.e. 2/2.1 of the true value). This arrangement was no inconvenience, however, because the recorder's own damping was sufficient to eliminate any electrometer noise from the potential-time trace. The internal resistance of the DVM ($>10^{10}$ ohm) was large enough for the filter's resistance to be negligible in comparison.

This combination of the electrometer and DVM meant that 10 mV input to the former was equivalent to 1 V on the latter. All subsequent potential measurements using the electrometer were read on the DVM.

The Potential Recorder

A Honeywell single pen potentiometric recorder was used on its 1 V F.S. range. No readings were taken using this instrument, which was used only to indicate when the cell potential had reached its equilibrium value.

Circuit Calibration

The whole circuit was calibrated as follows. The electrometer's input was short circuited and its zero set. 10.00 mV were then applied and the electrometer set at full-scale deflection using its own internal calibration potentiometer. The zero flutuated considerably (up to $\pm$ 0.05 mV) over the duration of a normal experimental run (10 hours) possibly due to mains flutuations, therefore when any readings were subsequently taken the zero was also measured. The linearity was tested by appling known potentials (<10 mV) measured by the DVM and comparing the electrometer readings (also measured by the DVM). Typical values are shown in Table (1). It can be seen that the linearity was very good and that

$$E = \frac{-(V_E - V_O)}{100} \pm 0.01 \text{ mV}$$

the difference in sign being due to the circuit arrangement. Thus the electrometer could be calibrated and read to an accuracy of $\pm$ 0.01 mV in the short term an increase of an order of magnitude on the stated limits of the instrument.

Table (1)

Calibration of the Potential Measuring Circuit

Applied Potential	Vibron		
E(mV)	V_E(V)	V_0(V)	V_E-V_0
-0.677	0.061	-0.006	0.067
-2.901	0.284	-0.006	0.297
-5.127	0.508	-0.005	0.513
-7.638	0.758	-0.005	0.763
-9.853	0.979	-0.005	0.984

2.3 Pressure Measurement

The pressure was measured with a simple stainless steel Bourdon Tube gauge manufactured by Budenberg Gauge Co. Ltd. Its scale was 0-300 p.s.i. graduated in 2 p.s.i. divisions and could be read to 0.1 $\pm$ 0.1 p.s.i. For the present work the gauge was mounted on a short iron U-tube and the whole filled with a silicone fluid (DC 200/20 c.s.) to protect the bourdon tube and to stop major distillation of water from the autoclave. (In fact water did eventually distil into the U-tube but merely collected at the bottom, the silicone fluid having a density slightly less than 1.0)

The manufacturer's calibration indicated that the gauge was correct to within 0.5 p.s.i., however, when recalibrated using a dead-weight tester (Barnet Instruments Ltd.) it was found linear across its scale to rather better than this. Unfortunately, although this linearity remained constant the gauge showed different zero errors on different days, presumeably due to temperature

Table (2)

Pressure Gauge Calibration

True Pressure*	Scale Reading	Corrected Reading
p.s.i.	p.s.i.	p.s.i.
0	1.6	0.0
10	11.8	10.2
25	26.8	25.2
50	51.6	50.0
75	76.6	75.0
100	101.6	100.0
125	126.5	124.9
150	151.5	149.9
175	176.6	175.0
200	201.6	200.0
225	226.6	225.0
250	251.6	250.0
275	276.6	275.0
299	300.6	300.0

* The dead-weight tester was quoted accurate to $\pm$0.05%

changes, but because it had no zero adjustment facility (the pointer merely resting against a zero stop) daily calibration would have been required to take advantage of its full potential accuracy. To overcome this inconvenience the gauge and U-tube were mounted such that the gauge dial was in a vertical plane as normal but the whole assembly was rotated anticlockwise about its central axis by about 40°. In this position the gauge pointer no longer rested against the stop at atmospheric pressure but was held by the tension of the gauge's hair-spring just on the scale. A zero correction could then be read which during this work ranged from 1.6 to 2.1 p.s.i. A typical calibration of the gauge thus mounted is given in Table (2). It can be seen that it is correct to $\pm$ 0.2 p.s.i. when the zero correction is applied.

2.4 Temperature Measurement

The temperature of the buffer solutions in the autoclave was measured by an iron-constantan thermocouple inserted down the stainless steel thermo-well through the central pressure union in the autoclave head above the reaction pot. This thermo-well was protected from the hot solutions by a pyrex or P.T.F.E. sheath.

An iron-constantan thermocouple was chosen because of its high thermoelectric E.M.F., i.e. 50-56 $\mu V.deg.^{-1}$ or $<0.02^{\circ}$ per μV, between 0 and $200^{\circ}C$.

The 'hot' junction was made by merely welding the two thermocouple wires in an air/gas flame (using borax flux) and annealing in a pure gas flame for a few minutes.

The 'cold' junction consisted of the two wires welded separately

to two tin-plated copper leads which were then inserted into silicone fluid filled thin glass tubes. These tubes were immersed in an ice/water slurry in a vacuum flask and were assumed to be at the ice point at thermal equilibrium.

Thermocouple Calibration

Iron-constantan thermocouples deviate considerably from the average given in the International Reference Tables[14] and need frequent calibration. Temperature Fixed Points were therefore chosen which could be quickly and easily maintained.

The International Practical Scale of Temperature (1948)[15] (I.P.S.T. 48) has now been superceeded by the I.P.S.T. of 1968.[16] In the latter the relationship between t (^{o}C) and T (K) is defined by

$$T - t = 273.15$$

and the triple point of water is defined as 273.16 K (0.01^{o}C). Primary fixed points in the relevant temperature range are the boiling point of water and the melting point of tin. Both scales have various secondary fixed points including

	I.P.S.T. 48	I.P.S.T. 68
	t^{o}C	t^{o}C
Triple Pt. Benzoic Acid	122.36	122.37
Melting Pt. In	156.61	156.635
" Sn	231.91	231.9681
" Pb	327.3	327.502
" Zn	419.505	419.58

and for the Boiling Pt. of water:

$$t_{48} = 100 + 28.012\left(\frac{P}{P_o} - 1\right) - 11.64\left(\frac{P}{P_o} - 1\right)^2 + 7.1\left(\frac{P}{P_o} - 1\right)^3$$

(P_o = 760 mm: P = 660–860 mm Hg; 96.1–103.5°C)

$$t_{68} = 100 + 28.026\left(\frac{P}{P_o} - 1\right) - 11.641\left(\frac{P}{P_o} - 1\right)^2 + 7.1\left(\frac{P}{P_o} - 1\right)^3$$

(P_o = 760 mm: P = 757–773 mm Hg; 99.9–100.1°C)

In addition I.P.S.T. 48 gives the boiling points of Naphthalene ($218.0°C^{(760mm)}$) and Benzophenone ($305.9°C^{(760mm)}$) as functions of pressure.

It was found that these latter two boiling points were not easily maintained nor was the triple point of Benzoic Acid. The boiling point of water was found satisfactory, although because it was measured under atmospheric pressure, P ranged over wider limits than those covered by the function of I.P.S.T. 68 and therefore that of I.P.S.T. 48 was used. (The difference between the two scales was not significant in the present work). The melting points of In, Sn, Pb and Zn were all satisfactory and their I.P.S.T. 68 values used for the thermocouple calibration.

Measurement of the B. Pt. of Water

The simple apparatus shown in Fig. (5), used normally for melting point determinations, was found satisfactory if shielded from draughts. The thermocouple was protected from the hot water

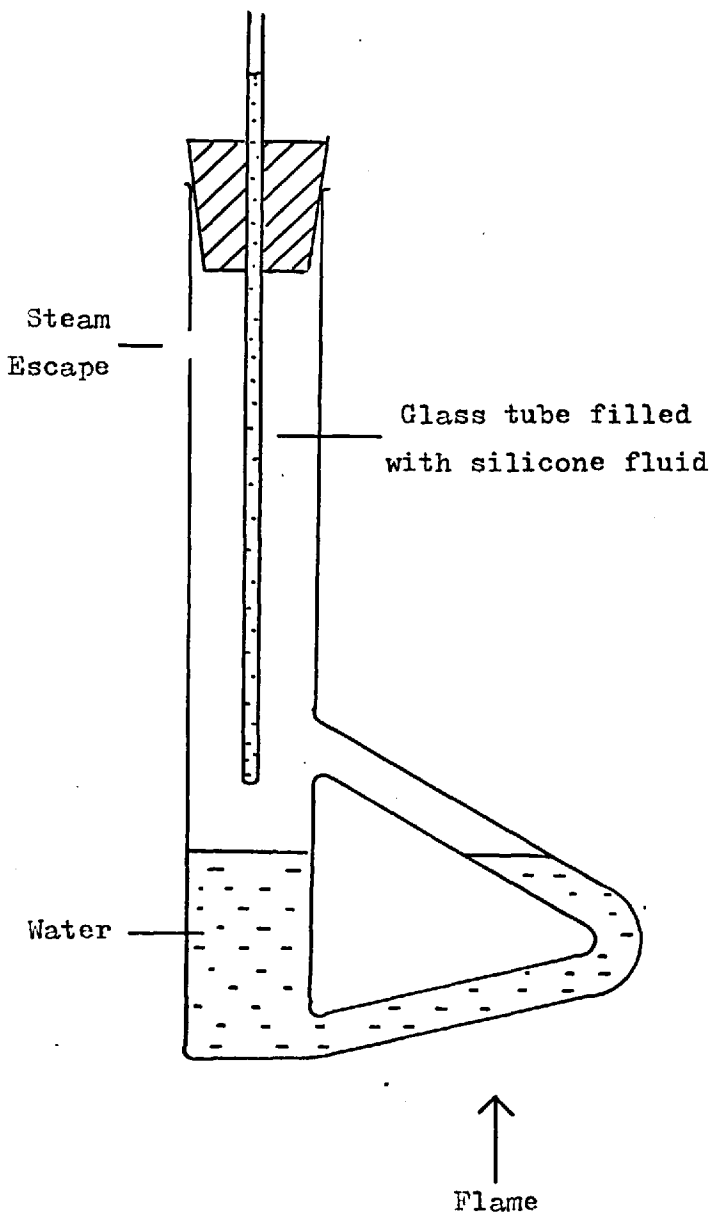


Fig. (5) Apparatus for determining the boiling point of water under atmospheric pressure.

by immersion in a silicone fluid in a thin, glass tube. The flame was adjusted so that gentle boiling in the side-arm caused boiling water to be ejaculated onto the thermocouple tube and the liquid was assumed to reach equilibrium with steam as it ran down it thus avoiding superheating. The thermoelectric E.M.F. for the boiling point was taken when the temperature remained stable for at least two minutes. Care had to be taken because it was possible to obtain a stable spurious high value by strong boiling. The atmospheric pressure was noted from which the true boiling point was calculated.

Measurement of the M. Pts. of the Metals

The spectroscopically pure metals (about 5 ml. of each) were melted in thick-walled test-tubes and a capillary tube, sealed at the bottom, was immersed centrally into the molten metal and held in place by a rubber bung. The thermocouple was inserted into the capillary at room temperature and the respective metal then heated to a few degrees above its melting point, the heat removed and the E.M.F. observed.

In the case of Indium supercooling was $<0.2^{\circ}$ ($<10\,\mu V$) and once crystallisation began the temperature rose and the DVM registered a constant E.M.F. for up to one minute. Lead and Zinc behaved similarly. Tin supercooled considerably (sometimes $>10^{\circ} = 550\,\mu V$) although after crystallisation started the temperature rose very quickly to a constant value, usually maintained for at least 15 seconds. However, there was the obvious danger that with such behaviour the true melting point might never be quite attained (although the latent heat is easily sufficient to reheat the metal)

so this point was taken several times, starting at between 1 and 50°C above the melting point thus causing various degrees of supercooling and agreement between the final temperatures attained was taken as proof of their correctness.

In the long term Zinc was found inconvenient because it tended to crack the glass tube on heating and cooling. It was also felt that the melting point of the Lead fell significantly after several heating cycles due perhaps to oxide (which formed visably) dissolving in the metal. However, once the general shape of the calibration curve for the particular batch of thermocouple wire was established measurements at the Pb and Zn points were discontinued. The other two points seemed perfectly consistant over nine months. Indium formed no visable oxide during the period although some tin oxide did form.

The calibration curve for a thermocouple was drawn in the following manner. The temperature (t_{ex}) corresponding to the E.M.F. obtained at a particular fixed point was read from the International Thermocouple Reference Tables[14] to the nearest 0.01°. Linear interpolation was used between adjacent degrees in the tables involving negligible error. If the true (defined) temperature of the fixed point was t_f then $\Delta t = t_{ex} - t_f$ was plotted versus t_{ex}. Δt was always negative, that is the thermocouples always indicated too low a temperature.

During the first week after their preparation the thermocouples' calibration curves changed considerably and needed checking prior to each experimental run. However, after 4 or 5 runs the calibration settled to an almost constant curve. Fig. (6) shows consecutive calibrations of the same thermocouple.

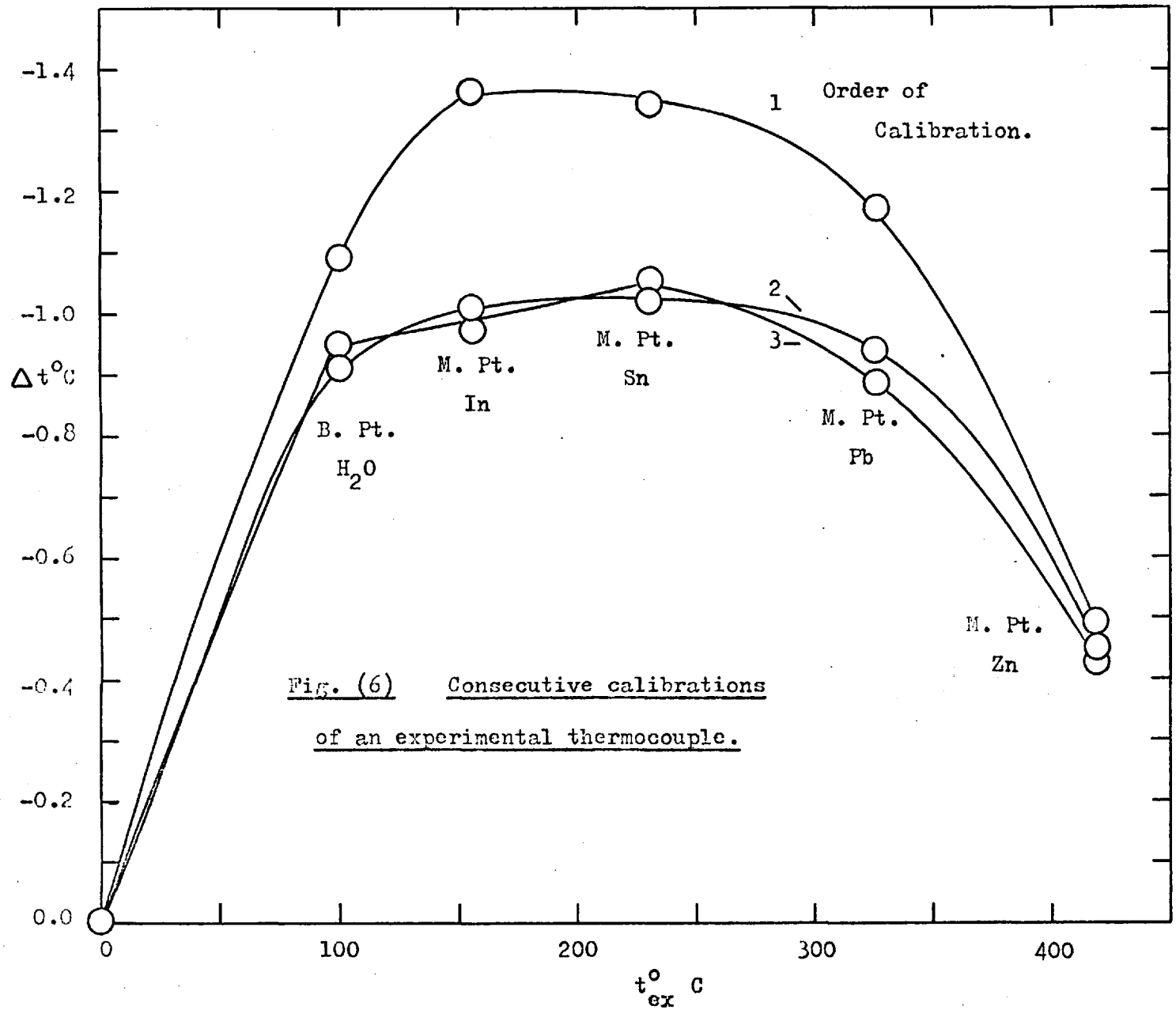


Fig. (6) Consecutive calibrations of an experimental thermocouple.

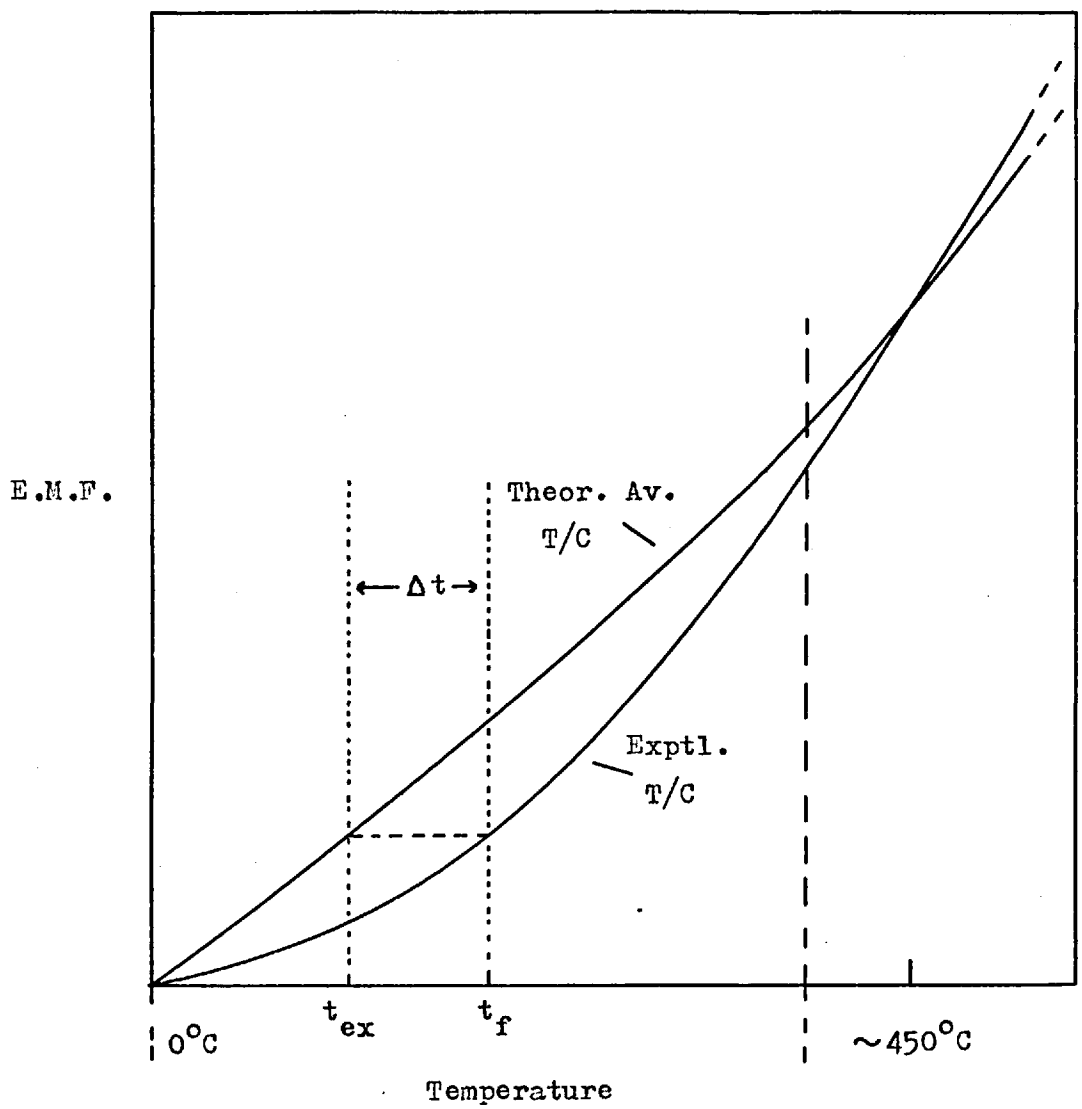


Fig. (7) Comparison of the E.M.F. versus t curves for theoretical average and experimental thermocouples.

The size of Δt (up to 1.5°) was large compared to platinum based thermocouples where values of perhaps 1° in 1000° are to be expected. The shape of the curve, its strong curvature and the obvious intention of Δt to change sign at somewhere above 450° were also surprising although they can be easily explained by comparing the E.M.F. versus t curves for an experimental thermocouple and the theoretical average one represented by the Reference Tables as shown in Fig. (7) (the curvature being greatly exaggerated). The dotted lines show the temperature range that is being considered in the present work. The relatively large divergence may be due to the thermocouple wires used being made to an old British Standard specification which differs slightly from that on which the new Tables are based. These Tables were used, however, because they quote the E.M.F. values to the nearest μV.

2.5 Silver-Silver Chloride Electrodes

Types and Preparation

There are three main methods of preparation of Ag-AgCl electrodes giving what are commonly called electrolytic, thermal-electrolytic and thermal electrodes.[17] The three procedures are:

i) Electrolytic

Smooth Ag is electroplated onto an inert metal substrate (usually platinum). This Ag layer is then chloridised by making it the anode in a cell containing either 1 M HCl or 0.05 M KCl.

ii) Thermal-electrolytic

An aqueous paste of Ag_2O is applied to a platinum wire spiral and the whole heated to 450°C at which temperature the oxide decomposes producing a porous sintered boule of metallic Ag. The process is repeated using a thinner paste to give a final, smooth Ag coating. This is then chloridised as above.

iii) Thermal

An aqueous paste of Ag_2O and $AgClO_3$ (or sometimes $AgClO_4$) is applied to a platinum spiral as before. The whole is heated to 650°C when both the oxide and chlorate (perchlorate) decompose, the latter forming AgCl which melts to produce a homogenous mass of Ag and AgCl. The process is repeated.

The decision as to which method of preparation to use (or even if it mattered) was not entirely obvious. It seems certain that at equilibrium $E^{\circ}_{Ag-AgCl}$ is identical for all three types (see below). However, each type has been recommended by various workers at the expense of the other two. Also all three have been used with success at above room temperature. However, it was finally decided to use the thermal type electrodes because, i) they are simply prepared and the starting materials easily purified and ii) they are homogenous and also the whole electrode has been effectively annealed during its preparation. This is an important point since Taniguchi and Janz[18] have suggested that thermal strain may exist in thermal-electrolytic electrodes possibly leading to erroneous values of $E^{\circ}_{Ag-AgCl}$. It is also certainly true that electrodeposition does not generally yield strain free phases ideal for thermodynamic

measurements. Moreover, there is the danger that the light, external coating of AgCl produced by chloridising in both the electrolytic type electrodes might flake or dissolve on being heated in an aqueous solutions.

Thermal Ag-AgCl electrodes were prepared as described above, supported on Pt spirals (about 5 mm. long) on the end of 3 cm. lengths of 0.3 mm. diameter Pt thermocouple wire. The $Ag_2O/AgClO_3$ paste was made from a mixture of the two solids containing 10 % by weight of the chlorate as recommended by Rule and La Mer.[19] Two or three coatings were given and after the final heating the electrodes were allowed to cool slowly in the oven. They were off-white in colour and glistened in bright light presumably due to small crystals of metallic silver.

Initially batches of six electrodes were prepared at one time and when cold immersed in 0.05 M KCl solution and their bias potentials measured. These were almost invariably within 0.05 mV of the mean and therefore subsequent batches of electrodes were taken straight from the oven and simply stored dry, in the dark until required at which time an arbitrary pair were chosen. Because of the reduction of AgCl by hydrogen only in a minority of cases could an electrode be used for more than one experimental run and usually a new pair was employed each time.

The Solubility of AgCl in Chloride Solutions

Raridon[20] has measured the solubility of AgCl in 0.01-3.06 m HCl solutions between 25 and 200°C. His data at 25° agreed closely with that in the literature giving AgCl solubility as a function of

NaCl concentration. Thus the solubility of AgCl in HCl is dependant on the chloride concentration and not on the pH which is, of course, only to be expected the increase in solubility being due to the formation of well established chloro complexes $AgCl_n^{1-n}$. It seemed reasonable therefore that interpolation of Raridon's data at higher temperatures would give a good guide to the solubility of AgCl in KCl-buffer solutions to be used in the present work.

At constant chloride concentration, Raridon's solubility data follows closely the relation

$$\log s = \frac{A}{T} + B \qquad -- (12)$$

where s is the AgCl molality and A and B are constants. Table (3a) shows the original data plus values at low HCl concentration at low temperatures and values at high HCl concentration at high temperatures (shown in parentheses) obtained by extrapolation of straight lines found by least squares fitting of relation (12). It can be seen that the solubility is increased greatly by both high chloride concentrations and high temperature, indeed at 200°C AgCl has become virtually a sparingly soluble salt, a 0.01 m chloride solution dissolving 0.16 $g.kg.^{-1}$

If the data is now considered at constant temperature it is found that it can be closely described by

$$\log s = a + b(\log m) + c(\log m)^2$$

where m is the chloride molality. Least square fits of this relation to the values in Table (3a) allows the solubilty of AgCl in KCl concentrations of interest to be estimated. Table (3b) gives

Table (3a)

Solubility of AgCl ($m.kg^{-1}$) in HCl Solutions

	HCl Molality				
t°C	0.01	0.10	0.50	1.49	3.06
25	$(6.11\ 10^{-7})$	$(3.15\ 10^{-6})$	$2.41\ 10^{-5}$	$1.58\ 10^{-4}$	$8.04\ 10^{-4}$
50	$(2.91\ 10^{-6})$	$1.30\ 10^{-5}$	$7.46\ 10^{-5}$	$4.43\ 10^{-4}$	$1.83\ 10^{-3}$
75	$(1.11\ 10^{-5})$	$4.17\ 10^{-5}$	$2.26\ 10^{-4}$	$1.07\ 10^{-3}$	$3.86\ 10^{-3}$
100	$3.59\ 10^{-5}$	$1.10\ 10^{-4}$	$5.18\ 10^{-4}$	$2.32\ 10^{-3}$	$7.12\ 10^{-3}$
125	$9.80\ 10^{-5}$	$2.62\ 10^{-4}$	$1.08\ 10^{-3}$	$4.78\ 10^{-3}$	$1.32\ 10^{-2}$
150	$2.38\ 10^{-4}$	$5.86\ 10^{-4}$	$2.18\ 10^{-3}$	$8.80\ 10^{-3}$	$(2.07\ 10^{-2})$
175	$4.80\ 10^{-4}$	$1.22\ 10^{-3}$	$4.95\ 10^{-3}$	$(1.47\ 10^{-2})$	$(3.19\ 10^{-2})$
200	$1.15\ 10^{-3}$	$2.51\ 10^{-3}$	$(7.50\ 10^{-3})$	$(2.38\ 10^{-2})$	$(4.72\ 10^{-2})$

Table (3b)

Solubility of AgCl (mg/150g) in HCl Solutions

	HCl Molality			
t°C	0.005	0.010	0.015	0.020
25	0.01	0.01	0.02	0.02
100	0.73	0.77	0.85	0.93
150	4.90	5.10	5.48	5.89
200	23.6	24.7	26.4	28.2

its solubility, in mg./150 g (the quantity of solution used in each run in the present work) in 0.005-0.020 m KCl.

Protection of the Ag-AgCl Electrodes

The increased solubility of AgCl in chloride solutions at elevated temperatures meant that there was a strong tendancy for AgCl to be leached from the Ag-AgCl electrodes, leading to spurious potentials. This tendancy could be greatly reduced by saturating the solution by the addition of about 50 mg. of solid AgCl and this was tried during initial runs with the KHphthalate buffer. However, AgCl is also reduced by hydrogen at elevated temperatures (see Appendix B) giving metallic silver and equal quantities of hydrogen and chloride ions. This effect was quite noticeable (by the formation of a dark stain of Ag around hydrogen bubbles stuck on the P.T.F.E. liner) when the only AgCl present was that leached from the Ag-AgCl electrodes. When excess, solid AgCl was added the effect became disastrous in the case of the phthalate buffer, the hydrogen ions produced by the reduction being sufficient to lower the pH at above 160°C (see Fig. (15)).

To overcome these difficulties it was decided to isolate each Ag-AgCl electrode from the bulk of the solution (in contact with the hydrogen electrodes) and allow only the essential mass transfer through a low porosity sinter. Such a sinter was, of course, unlikely to hinder hydrogen ion diffusion (which may anyway in water be regarded as a flow of electrons in the opposite direction) if significant AgCl reduction did take place, but it would act as an effective barrier to other ions, in particular

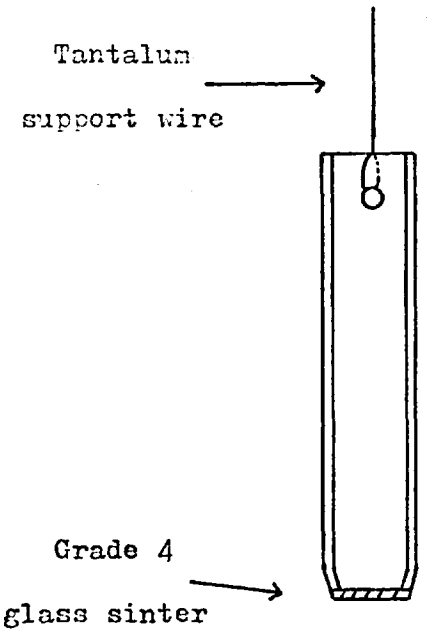


Fig. (8a)

Pyrex protective sheath for Ag-AgCl electrodes

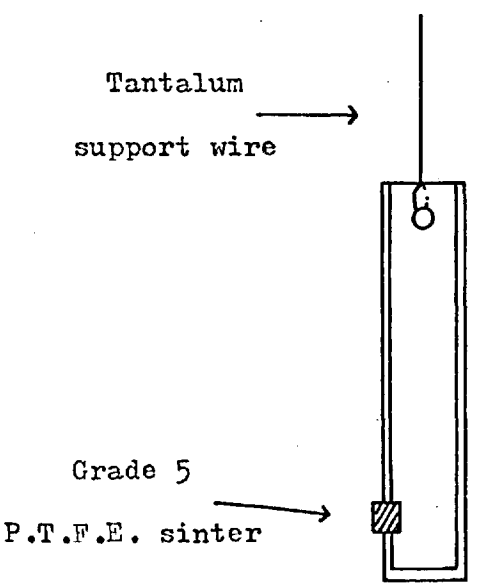


Fig. (8b)

P.T.F.E. protective sheath for Ag-AgCl electrodes

silver and chloride. Each Ag-AgCl electrode was therefore effectively in contact with only the 5 ml. of solution inside each sheath and the leaching of AgCl so reduced that addition of solid AgCl was no longer required. Although some reduction did take place (again detected by the brown stain on the inside of the sheaths) it was not enough to affect the pH of the phthalate solution.

The glass sheaths (see Fig. (8a)) were one half of pyrex filter tubes containing porosity 4 glass sinters. They were supported around the Ag-AgCl electrodes by pure tantalum wires through holes drilled as shown, the other ends of the wires being attached to small grub screws on the underside of the autoclave head. The stiffness of the wires was quite sufficient to keep the sheaths vertical.

These sheaths were found satisfactory for both oxalate and tartrate calibrations up to 170°C. However, on heating to 200°C they invariably cracked around the sinter and therefore similar sized sheaths were machined out of a rod of P.T.F.E. For these the sinter was a small disc (3 mm. diameter) cut from a sheet of porous P.T.F.E. Each disc was forced into a similar sized hole in the side of a sheath (see Fig. (8b)).

Although usable, these P.T.F.E. sheaths were not satisfactory. Firstly, considerable difficulties were encountered trying to wet the P.T.F.E. sinter, which was very hydrophobic. This could only by achieved by submerging it in the solution, evacuating to remove the air and then releasing the vacuum. Secondly, the sinter increased the internal resistance of the cell to such an extent that the vibron electrometer began to require a significant time

to reach its final reading. The earthing and screening of the potential measuring circuit had also to be improved. Thirdly, the highly hydrophobic character of the P.T.F.E. meant that hydrogen bubbles which formed as the solution was heated clung tenaciously to the sheath and if occasionally one formed around the P.T.F.E. sinter it effectively caused an infinite resistance in that cell's circuit making further measurements impossible. Finally, it has been mentioned before that heat transfer across water-P.T.F.E. surfaces seems particularly poor and thus compared to experimental runs using glass sheaths the cell's E.M.Fs. lagged badly behind the temperature. That is, the solution inside the sheaths took a long time to come to thermal equilibrium with the bulk of the solution. This effect was so bad at below 140°C as to make it impractical to use the P.T.F.E. sheaths below this temperature and therefore glass ones were always used under these conditions. At above this temperature there seemed to be a dramatic improvement and the P.T.F.E. sheaths could be employed.

Standard Potential of the Ag-AgCl Electrode

The standard potential of the Ag-AgCl electrode has been measured by many workers below 100°C. More important investigations have been made by Harned and Ehlers[21] between 0° and 60°C using the cell:

$$Pt(H_2)\,|\,HCl(m)\,|\,Ag\text{-}AgCl \qquad -- (13)$$

and by Harned and Paxton[22] between 0° and 50° using the cell:

Table (4)

$E^{o}_{Ag/AgCl}$ as a Function of Temperature

t°C	Harned & Ehlers[21]	Harned & Paxton[22]	Bates & Bower[23]	Izaki & Arai[26]	Greeley, et al.[27]	Ref.(26) Smoothed	Ref.(23) Smoothed	Ref.(27) Smoothed
0	0.23642	0.23652	0.23655	-	-	-	-	-
25	0.22246	0.22239	0.22234	0.2222	0.22233	0.2225	0.22225	0.22234
50	0.20444	0.20449	0.20449	0.2073	-	0.2044	0.20452	0.2048
60	0.19627	-	0.19649	-	0.1968	0.1964	0.19654	0.1968
90	-	-	0.16952	-	0.1696	0.1694	0.16958	0.1697
125	-	-	-	0.1319	0.1330	0.1325	(0.1324)	0.1329
150	-	-	-	0.1031	0.1032	0.1025	(0.1020)	0.1033
175	-	-	-	0.0691	0.0708	0.0697	(0.0685)	0.0707
200	-	-	-	-	0.0348	(0.0338)	(0.0319)	0.0348
225	-	-	-	-	-0.0051	(-0.0050)	(-0.0080)	-0.0051
250	-	-	-	-	-0.054	(-0.047)	(-0.051)	(-0.050)
275	-	-	-	-	-0.090	(-0.092)	(-0.097)	(-0.101)
300	-	-	-	-	-	(-0.139)	(-0.146)	(-0.158)

$$Pt(H_2)\,|\,0.01\ m\ HCl, SrCl_2(m)\,|\,Ag\text{-}AgCl$$

The most extensive investigation has been carried out by Bates and Bower[23] between 0° and 95°C involving nearly 700 measurements (81 at 25°C alone) using cell (13). Between 0° and 90°C they obtained the smoothed function,

$$E^{\circ}_{Ag\text{-}AgCl} = 0.23659 - 4.8564\ 10^{-4}\ t - 3.4205\ 10^{-6}\ t^2 + 5.869\ 10^{-9}\ t^3.$$

Some of the unsmoothed data from these three investigations are shown in Table (4). There is obviously quite good agreement although the sizes of the discrepancies are in some ways surprising. A critical comparison of these and other results is given by Bates including recalculation of older data with modern constants. Agreement was generally very good although the discrepancy between Bates' and Harned's and Ehlers' values could not be explained. Both sets of workers used thermal-electrolytic Ag-AgCl electrodes and Taniguchi and Janz[18] have attributed the differing values of $E^{\circ}_{Ag\text{-}AgCl}$ to thermal strain in this type of electrode.

Data above 100°C is less extensive. Lietze and Vaughen[24] measured the potential of the Ag-AgCl electrode in conjunction with the $Hg\text{-}Hg_2Cl_2$ electrode in 0.01-1.0 M HCl up to 263°C in a feasibility study. Roychoudhury and Bonilla[25] have studied cell (13) up to 250°C in 0.001 and 0.017 M HCl using electrolytic Ag-AgCl eletrodes. No values for $E^{\circ}_{Ag\text{-}AgCl}$ were given, however.

More recently Izaki and Arai[26] have measured $E^{\circ}_{Ag\text{-}AgCl}$ up to 175°C using cell (13) in 0.01 and 0.1 M HCl using electrolytic electrodes.

However, the most extensive investigation has been made by Greeley, et al,[27] who studied cell (13) up to 275°C using HCl concentrations ranging from 0.001 to 1.0 m. Their unsmoothed data, together with that of Izaki and Arai, are shown in Table (4). It can be seen that at 25°C agreement between Bates, Izaki and Greeley is very good and quite satisfactory up to 90°C. This is particularly relevant in that these three investigations used differently prepared Ag-AgCl electrodes, namely thermal-electrolytic, electrolytic and thermal respectively. Agreement between Izaki and Greeley is also good up to 175°C considering the less sophisticated nature of Izaki's investigation.

It is also useful to compare Greeley's results at higher temperatures with extrapolations of Bates' and Izaki's data. To do this Izaki's own smoothing function of his data,

$$E^{\circ}_{Ag-AgCl} = 0.23756 - 5.4386\ 10^{-4}\ t - 2.3750\ 10^{-6}\ t^2$$

and Greeley's fit of Bates' data

$$E^{\circ}_{Ag-AgCl} = 0.23683 - 5.2004\ 10^{-4}\ t - 2.5241\ 10^{-6}\ t^2$$

were used. (Bates' own cubic function seemed rather unsuited for extrapolation). The values, given in Table (4) in parentheses, show that there is satisfactory agreement, the greatest difference between Izaki and Greeley being 7 mV at 250°C (equivalent to 0.067 pH units) and that between Bates and Greeley being 7 mV at 275°C (0.064 pH units) although at all other temepratures the differences were always equivalent to less than 0.03 pH units.

Greeley has pointed out that the data of Roychoudhury disagrees

considerably with his own results (35 mV at 250°C) but suggests that the light AgCl coating used in the former investigation might well have dissolved in HCl at these temperatures. Roychoudhury also found that H_2 had a considerable effect on his Ag-AgCl eletrodes (although pressures of up to 40 atm were used) which Lietze[28] has suggested might be due to hydrogen sites forming on the electrode. Anderson[29] has found that finely divided Ag on a Pt electrode will give the hydrogen electrode reaction and in at least one run in the present work (0.05 m phthalate/0.005 m KCl) at 190°C a Ag-AgCl electrode was found to give a potential within 0.1 mV of a Pd black hydrogen electrode. Old Ag-AgCl electrodes also gave spurious potentials. However, Greeley has shown that with low H_2 pressures, i.e. 1-2 atm. and thermal Ag-AgCl electrodes reproducible and reversible potentials may be obtained. It seems, therefore, that only if the AgCl is leached or reduced by H_2, thus exhibiting an active Ag surface, will a spurious potential be observed due to the hydrogen electrode reaction on the Ag metal.

The values of $E^{\circ}_{Ag-AgCl}$ used in the present work were taken from Greeley who gives a smoothing function of his data between 25° and 200°,

$$E^{\circ}_{Ag-AgCl} = 0.23735 - 5.3783\ 10^{-4}\ t - 2.3728\ 10^{-6}\ t^2 \quad -- (14)$$

(The first term is quoted, in error, as 0.23755 in the original paper). However, because some temperatures greater than 200°C were used in the present work Greeley's crude data had to be resmoothed to include the value at 225°C. Unfortunately the

addition of the extra point made quadratic and cubic functions inadequate to fit the data with an accuracy comparable to (14) and the function:

$$E^{\circ}_{Ag-AgCl} = 0.23575 - 4.42722\ 10^{-4}\ t - 4.00232\ 10^{-6}\ t^2 + 1.05656\ 10^{-8}\ t^3 - 2.30103\ 10^{-11}\ t^4 \qquad (\sigma = 0.10\ mV)$$

was finally obtained. All values of $E^{\circ}_{Ag-AgCl}$ used in the present work were obtained from this function: some are given in the final column of Table (4).

2.6 Hydrogen Electrodes

Contrary to general knowledge, the hydrogen electrode is the most well-behaved and reproducible of all reference electrodes and although it is normally set up employing a platinised platinum electrode with hydrogen bubbling around neither of these conditions ~~are~~ is essential. Many metals, if activated, will catalyse the H^+/H_2 reaction and the only condition regarding H_2 (apart from its purity) is that it should be in equilibrium with both the liquid and gaseous phases and although bubbling obviously speeds up the attainment of this equilibrium it can also lead to supersaturation of the solution causing erroneous potentials.[30]

Although not essential, the experiences of many workers have shown that platinised platinum electrodes are perhaps the best and most active electrodes catalysing the H^+/H_2 reaction. Recipies for the platinisation have been faithfully copied over the years

without too much regard to their true suitability. Feltham and Spiro[31] have reviewed the previous work on platinisation and shown that although the addition of lead to the plating solution (as recommended by virtually all workers) is indeed beneficial, the amount required is actually much smaller than that normally employed. However, the present author still had some misgivings about the presence of lead in hydrogen electrodes working at 200°C because it might well be leached by the solution with unknown results.

In fact since the initial runs were carried out using the phthalate buffer solution platinum black hydrogen electrodes could not be used because they catalyse the reduction of phthalate by hydrogen to a cyclo-hexane dicarboxylic acid. This was detected by Hamer and Acree[32] who found, however, that the less active palladium black hydrogen eletrode could be used instead. These were, therefore, the initial electrodes used in the present work and despite them also eventually catalysing the reduction of phthalate at above 130°C were perfectly satisfactory as hydrogen electrodes. This being so, combined with the fact that no lead needs to be added to the palladium plating solution, they were also used (with total success) in both the oxalate and tartrate buffers. Platinum black electrodes were, in fact, never used and indeed their main advantage at room temperature over palladium black electrodes of reaching equilibrium quicker (palladium electrodes are certainly rather sluggish at 25°C) is considerably diminished at elevated temperature because of faster kinetics.

It will be seen below that the reduction of phthalate by hydrogen catalysed by the palladium black caused considerable

difficulties. A metal surface was required that was active enough to sustain the H^+/H_2 reaction but not the phthalate reduction. Consideration of the various platinum metals' blacks and other metal catalysts used for hydrogenation and dehydrogenation of organics suggested that most would be too reactive. An active, smooth metal surface seemed the most likely possibility and it was decided to try bright Iridium plating which has been recommended as a hydrogen electrode which is considerably less active than platinised platinum.[33,34] Smooth, bright Iridium was therefore electroplated onto the Pt foil substrate and found to be a satisfactory hydrogen electrode in the phthalate solutions up to 200°C causing only very slight reduction of the buffer.

As stated previously, continuous bubbling of H_2 around the electrode is not necessary and indeed would have been rather difficult to arrange in the closed system used. The solutions were therefore initially saturated at room temperature by bubbling through H_2 but once the autoclave had been totally sealed the equilibrium between the gaseous and liquid phases was maintained across the undisturbed liquid surface. Under these circumstances it seemed advisable to have the hydrogen electrodes as near to this surface as possible. Greeley[27] achieved this by using an ingenious silica float but such an arrangement seems unduly complicated. In the present work, strips of Pt foil, $\frac{1}{2}$ x 3 cm., were employed so as to allow for the change in height of the liquid surface due to the 16 % expansion of water that occurs between 25° and 200°C. These were spot welded to lengths of Pt thermocouple wire in the usual manner and hooked onto the Pt leads of the 'through-electrodes' so that the hydrogen electrodes would cut

the buffer solution's surface at all temperatures.

Palladium Electroplating

Hamer and Acree[32] have investigated four different palladium electroplating solutions, three of which contained lead. They found, however, that no great advantage was gained from lead addition (unlike in Pt black production) and as stated above it was felt that its presence was objectionable for the present work and therefore their plating solution without lead was used.

$PdCl_2$ was dissolved in water and reduced to metallic Pd by the addition of hydrazine. The metal was washed by decantation and after drying a weighed quantity was dissolved in the minimum quantity of aqua regia and the mixture evaporated to dryness on a water-bath. Concentrated HCl was added and the mass re-evaporated: this was repeated three times. The weight of the dark red solid that remained corresponded to $PdCl_2$. This was dissolved in hot, concentrated HCl (this is a very slow process) and the solution diluted with water to give a solution nominally 0.5 M H_2PdCl_4 (5.5 % Pd), in 0.1 M HCl.

Each $\frac{1}{2}$ x 3 cm. strip of Pt foil was plated for 5 minutes at 100 ma.cm.$^{-2}$ and brown-black, tenacious deposits of Pd black were formed.

During the electrodeposition Cl_2 was evolved at the carbon anode which inevitably oxidised some Pd(II) to Pd(IV) and after about fifty electrodes had been prepared the Pd black deposits quite suddenly became streaky (the Pd content of the solution had decreased negligibly) presumably because of loss of current

efficiency due to the formation of $PdCl_6^{=}$ ions. The solution had therefore to be re-prepared by evaporating to dryness, when Pd(IV) decomposes to Pd(II) and redissolving in hydrochloric acid. A Pd metal anode would, no doubt, avoid this difficulty.

Iridium Electroplating

Commercially, practical Ir electroplating is only possible from cyanide melts and no method of plating from aqueous solution has been used. Reid[35] has reviewed the literature prior to 1963. The most obvious choice of bath has been either an acid solution of a chloriridate (Ir(IV)) or a chloroiridite (Ir(III)). Perley[36] used a solution of chloroiridous acid which he prepared by dissolving H_2IrCl_6 in water, adding ethanol and boiling to form H_3IrCl_6. The preparation of a similar solution was attempted in the present work using K_2IrCl_6 as a starting material. Boiling with ethanol resulted in some black precipitate (presumably Ir metal) but after filtration some HCl was added to the solution and electroplating attempted using the conditions recommended by Perley. A 1 cm. square of Pt foil was cleaned by cathodically polarising in a Na_3PO_4 solution and a thin layer of gold electroplated using a standard cyanide bath. The Ir was then electroplated onto the gold at a current density of 1-2 ma.cm.$^{-2}$: a carbon anode was used. A bright Ir deposit was indeed obtained but plating was very slow (low current efficiency) and the Ir so thin that the gold always showed through the deposit. This method of Ir electroplating was not considered satisfactory.

Several other plating baths have been recommended. MacNamara[37]

has suggested any salt with the formula X_2IrY_6 where X = H^+, Na^+ or K^+ and Y = Cl^-, Br^- or I^- although chloroiridic acid is preferred. Conn[38] has used a bath containing $IrCl_3$ plus sulfamic acid (NH_2SO_3H) at 50-60°C. Skomoroski[39] has patented a similar recipe to be used at 50-75°C containing ammonium sulfamate in addition to the free acid. Ovendon[40] used a solution of ammonium fluoroborate, ammonium borate and iridium chloride and Ignatova and Vasserman[41] have used a mixture of ammonium fluoride and ammonium chloroiridite. Both these sets of workers plated at room temperature and their baths were unstable at higher temperatures. All workers recommend cathode current densities of 1-80 ma.cm.$^{-2}$

Tyrrell[42] has tested many of the previously recommended baths and also ones based on nitrate, nitrite, sulphate, hexahydroxyiridate and perchlorate but found that virtually all were more or less unsatisfactory due to instability or low current efficiency. The most promising was that based on Ir(IV) bromide in 0.1 M HBr in which current efficiences of up to ~45% were obtained. This recipe was used in the present work and found satisfactory.

Hydrated iridium dioxide was prepared by addition of 20 % KOH solution to K_2IrCl_6 followed by NaOCl solution to oxidise any Ir(III) to Ir(IV). The hydrated oxide formed as a dark blue precipitate which was separated by centrifuging (it was somewhat colloidal) washed with oxalic acid solution (to destroy hypochlorite), water and then dried for a short time at 80°C. Prolonged drying must be avoided otherwise dehydration occurs and the extremely unreactive anhydrous IrO_2 is formed. To prepare the plating bath 0.5 g of this solid was dissolved in 2 ml. of 48% HBr and made up to 50 ml with

water. The solution was initially yellowish-green but became purple on heating. Plating onto the Pt foil cathode was carried out at 70-75°C at a current density of 1 ma.cm.$^{-2}$ for 10 minutes: a carbon anode was used. The temperature is rather important in that if it is too low the current efficiency is greatly reduced, but at higher temperatures the bath decomposes through loss of HBr. Dark-grey, smooth deposits of Ir metal were obtained which were positively difficult to remove using emery paper although if higher current densities were employed the plate would sometimes flake off. Continual use of the bath did cause some decomposition due to loss of HBr and Br_2 formation at the anode, the solution turning blue. However, the addition of a small quantity of the concentrated HBr solution seemed to improve matters.

2.7 Reagents and Solutions

Hydrogen

Commercial (B.O.C.) high purity H_2 from a cylinder was used. The manufacturers quoted mean specification was $H_2 > 99.99\%$, $N_2 < 0.01\%$, $O_2 < 10$ v.p.m., $CO_2 < 10$ v.p.m., $CO < 5$ v.p.m., all other carbon compounds < 5 v.p.m. and H_2O about 0.15 g.m.$^{-3}$

Nitrogen is inert and of no consequence unless present in quantities which would significantly lower the partial pressure of H_2. This is also true for CO, hydrocarbons and CO_2 although for high pH buffers the latter would obviously become significant. O_2 is much more objectionable, however. A hydrogen electrode using H_2 which contains some O_2 will have a bias potential versus

an electrode using pure H_2 because the O_2 is reduced to H_2O at the former electrode, withdrawing electrons from it. Therefore in the present work a catalytic deoxygenator (Engelhard "Deoxo" Hydrogen purifier) followed by a CO_2 trap ("Sofnolite") were interposed between the cylinder and the experimental cells.

Silver Chlorate

$AgClO_3$ ws prepared by the method described in Inorganic Syntheses[43] which employs the double decomposition,

$$NaClO_3 + AgNO_3 = AgClO_3 + NaNO_3$$

in which $AgClO_3$ vis the least soluble salt and precipitates from solution on cooling in ice. One recrystallisation was reported to give a product 99.7 % $AgClO_3$. In this work G.P.R. $NaClO_3$ and AR. $AgNO_3$ were used and the product recrystallised from water three times.

Silver Oxide

Ag_2O precipitated from aqueous solutions has a strong tendancy to absorb electrolytes which must be removed when preparing Ag-AgCl electrodes. Bates[44] has found that approximately thirty manual washings were required before a filtrate with a constant conductance was obtained. Ag_2O (Lab. Reag.) was therefore leached with hot water in a Soxhlet apparatus for 2-3 hours (equivalent to 30-50 cycles) until the filtrate was colourless. The wet solid was dried at 110°C

Silver Chloride

AgCl was prepared by the addition of a slight excess of 1:1 AR. HCl solution to a solution of AR. $AgNO_3$. The precipitate was filtered, washed with water and purified by the method of Zimmerman.[45] The AgCl was dissolved in the minimum quantity of AR. .880 NH_3 solution which was then filtered and heated on the water-bath to drive off NH_3 until AgCl started to crystallise at which point heating was stopped and the solution allowed to cool in the dark. The filtered solid was washed with water, dilute HCl solution and finally water. Second and third crops were obtained from the ammoniacal mother liquor. The AgCl so prepared was mauve in colour.

Potassium Chloride

AR. KCl, dried at 150°C for 6 hours, was used. Pinching and Bates[46] have shown that various salts, in particular bromides, have a marked effect on the potential of Ag-AgCl electrodes. (The presence of iodide has a much less pronounced effect than bromide and this has been explained as being due to the fact that AgCl and AgBr form solid solutions whereas AgCl and AgI do not[17]). KCl is often a source of trace quantities of bromide which, if present in quantities 0.005 mole %, must be removed. The batch of KCl used in the present work contained 35 p.p.m. Br+I (assayed as Br by Hopkin and Williams) which is equivalent to 0.0033 mole % Br. The KCl was not therefore purified further.

Potassium Tetroxalate Dihydrate.

$KH_3(Ox)_2.2H_2O$ has a rather uncertain water content and may not be dried at above 60°C without some decomposition of the hydrate.[47] and therefore the purity of a sample was determined. Weighed samples of the AR. solid were titrated versus 0.05 M NaOH (standardised versus solid potassium hydrogen phthalate) using phenolphthalein as indicator. An average purity of 98.49 % was obtained. On drying at 50°C for 2 hours this rose to 99.64±0.2 %. Further drying at this temperature after crushing the sample gave a product of purity 99.60±0.2 % which was bottled and kept in a desiccator. The necessary adjustment for this assay was made when making up the tetroxalate buffer solutions.

Potassium Hydrogen Tartrate

The AR. solid straight from the bottle was employed.

Potassium Hydrogen Phthalate

The AR. solid is at least 99.9 % pure after drying. A crushed sample was therefore dried at 120°C for three hours.

Potassium Dihydrogen Phosphate and Disodium Hydrogen Phosphate

The AR. solids dried at 110° and 120° respectively were used.

Calcium Hydroxide

A sample was prepared as recommended by Bates.[48] Crushed, low-alkali grade calcium carbonate was leached with hot water in a Soxhlet apparatus and then slowly decomposes at 1000°C. On cooling

the CaO was added to water and its conversion to the hydroxide completed by boiling. The $Ca(OH)_2$ was filtered and dried.

Solutions

The solutions were prepared by weight. The correction for the buoyancy of air (d = 0.0012 $g.ml.^{-1}$) and stainless steel balance weights (d = 8.0 $g.ml.^{-1}$) was calculated from[49]

$$W_v = W_a(1 + 0.0012(\frac{1}{d} - \frac{1}{8}))$$

in which W_v and W_a are the weights of the substance in vacuum and air respectively and d is its density.[50] In the case of the tartrate buffer, a saturated solution of potassium hydrogen tartrate was prepared by keeping the solid in contact with the solution for 2 hours (with occasional shaking) in a thermostatically controlled water-bath at 25 $\pm$ 0.2°C. The required KCl was then dissolved in this solution (0.0341 m KHTartrate; d = 1.0036 $g.ml.^{-1}$)[51]

Water Evaporation

i) As the solutions were heated in the autoclave water evaporated into the vapour phase thus causing an increase in the molalities of the buffer substance and KCl. The gas space in the measurement pot containing a P.T.F.E. liner, 150 ml. of solution, electrodes etc. was approximately 110 ml. and since the density of saturated water vapour is 7.86 $g.l.^{-1}$ at 200°C contained about 0.87 g H_2O.at this temperature. The evaporation of this quantity of water from the solution would lead to an increase of 0.6 % in the buffer and KCl molalities. Such a change would have

a negligible effect on the hydrogen ion concentration (because of buffer action) but the increase of m_{KCl} by a factor of 1.006 is equivalent to a decrease of 0.003 units in $p(a_H\gamma_{Cl})$ (see equation (8)). This is not totally insignificant and the effect would certainly have to be taken into account at higher temperatures however, no correction was made for it in the present work because measurements at 200°C were performed only on the phthalate buffer and the rather large experimental errors from other sources made the effect negligible in this case. At lower temperatures the correction becomes rapidly insignificant.

ii) To remove air from the experimental system and saturate the buffer solution prior to each run H_2 was bubbled through the buffer for about 2 hours. To avoid any evaporation of the solution a pre-saturator was employed which was conveniently the other autoclave pot containing an identical solution through which the H_2 bubbled via a glass sinter. A check on the efficiency of this device was made. The apparatus was set up (as in Fig. (2) but without electrodes etc.) with each pot containing equal volumes of a solution of $KH_3(Ox)_2$ (about 0.05m; the strength was accurately determined by titration versus 0.1 M NaOH using phenolphthalein). H_2 was bubbled through these solutions consecutively for 1 hour at about 6-7 bubbles per second. The concentrations of the solutions were then redetermined and expressed as a percentage of the original concentrations. The experiment was carried out at 70°C and at room temperature and the results shown in Table (5).

Table (5)

Temperature	Saturator	Test
70°	104.2 %	102.5 %
R.T.	100.1 %	100.4 %

It can be seen that at 70°C significant evaporation did occur from the saturating solution and that the device was not efficient enough to prevent evaporation also occurring from the test solution. At room temperature the effects are much smaller, within experimental error for the titrations and would be insignificant at the slower rate of H_2 bubbling (<3 per second) actually used prior to experimental runs. However, the experiment did show that using this device the autoclave had to be at room temperature and that artificial cooling would be essential between runs on consecutive days.

2.8 Experimental Procedure.

The same experimental procedure was used for all buffer solutions, (see Fig. (2)).

Approximately 130 g of buffer/KCl solution were placed in both P.T.F.E. lined autoclave pots. The autoclave head was conveniently supported on a frame so that the Ag-AgCl electrodes could be hooked onto the Pt wire spirals of their respective through-electrodes. The glass or P.T.F.E. protective sheaths were filled with the solution and suspended around these electrodes. The hydrogen electrodes (prepared about 2 hours previously and allowed to stand in distilled water to remove any entrained plating solution) were washed with the buffer solution and hooked onto their respective Pt wire spirals. The thermo-well sheath, P.T.F.E. tubes and sintered glass bubbler etc. were fixed into position and the whole head carefully lowered onto the autoclave body and all bolts and pressure unions tightened. The thermocouple hot junction was threaded down the thermo-well and the leads from the potential measuring circuit plugged into the sockets of the four through-electrodes.

Initially valves B, C and D were open and valve A closed. H_2 was delivered from the cylinder (via a pressure reduction valve) at around 80 p.s.i. Valve A was carefully opened to allow a steady stream of gas through the system. The rate could be observed as the gas passed through a bubbler (containing n-dibutyl phthalate) beyond valve D (not shown in Fig. (2)) and was adjusted to 2-3 bubbles per second. During initial experiments the bias potential between the two hydrogen electrodes was

monitored on the recorder and found to quickly rise to up to 500 mV when H_2 was first introduced, presumably due to general heterogeneity in the buffer solution around the two electrodes, but then slowly decrease to <0.3 mV within $1\frac{1}{2}$-2 hours as the solution became saturated with H_2. Therefore in all subsequent experiments H_2 was passed through the system for about 2 hours. (In fact the bias potential did not always decrease to zero during this time and was sometimes still 10 mV or higher, however, this was no doubt due to one of the hydrogen electrodes being particularly sluggish since the two electrodes always agreed closely when the first measurements were subsequently made at an elevated temperature).

Valve D was then closed and the H_2 allowed to pressurise the system to 30-40 p.s.i. gauge pressure. Valves A and B were then closed and any leaks could be spotted. The autoclave was normally left over-night in this condition.

The power to the heaters was turned on in the early hours of the morning with the aid of a time-switch and the autoclave generally came to thermal equilibrium at its first set temperature in about 4 hours.

Before the first measurements were taken the potential of one of the pairs of hydrogen and Ag-AgCl electrodes was monitored for 20 minutes to check that it was stable. If so, the vibron potential, back-off potential and thermoelectric potential were read from the DVM and the pressure on the gauge noted. The measuring circuit was then switched to the other pair of electrodes and further measurements taken. The atmospheric pressure was then read from the Hg barometer. The temperature controller was

set to the next temperature and further measurements taken at equilibrium. About 2 hours were required between each set temperature although this time decreased at higher temperatures. Measurements at up to 7 set temperatures could be made on one day.

After the final measurement the power was turned off and the autoclave allowed to cool over-night. On the following morning the buffer solutions were removed from the measurement and saturator pots and their pH compared to that of the original solution, using a glass electrode, to check if any decomposition or reduction had taken place.

3. ANALYSIS OF EXPERIMENTAL DATA

3.1 The Hydrogen Gas Activity

The hydrogen gas activity that appears in equation (8) was basically calculated from the relation,

$$a_{H_2} = P_g^{corr.} + P_{atm.} - P^{v}_{H_2O} \qquad -- (15)$$

in which $P_g^{corr.}$ is the corrected gauge pressure, $P_{atm.}$ the atmospheric pressure (read from a Hg barometer) and $P^{v}_{H_2O}$ is the saturated water vapour pressure at the respective temperature. There were, however, a number of small effects that needed to be considered.

Vapour Pressure of the Solutions.

At the higher temperatures the hydrogen partial pressure becomes small (<25 %) compared to the total pressure, due to the increased vapour pressure of water. Therefore, it is under these conditions that the difference between the vapour pressure of a solution and that of pure water may become significant. There are two effects to be considered.

i) The Activity of Water in the Solution is Significantly Less that 1 due to the Solute

If ϕ is the osmotic coefficient of a solution then

$$\ln a^{s}_{H_2O} = - \frac{vmM\phi}{1000} \qquad -- (16)$$

where m is the solute molality, M the molecular weight of water and v is the number of ions (or particles) produced by dissociation of the solute (i.e. v = 2 for a strong 1:1 electrolyte). Generally the activity of a substance is the ratio of its fugacity to its fugacity in the standard state and therefore in this case the activity of the water vapour above the solution is $a^s_{H_2O} = f^s_{H_2O}/f^v_{H_2O}$, where $f^s_{H_2O}$ and $f^v_{H_2O}$ are the fugacities of water in the solution and pure state respectively. Assuming that the fugacity coefficients (see below) are equal, this reduces to $a^s_{H_2O} = P^s_{H_2O}/P^v_{H_2O}$, the respective vapour pressures. Equation (16) now becomes,

$$\ln (P^s_{H_2O}/P^v_{H_2O}) = - \frac{vmM\phi}{1000} \qquad -- (17)$$

Because $P^s_{H_2O}/P^v_{H_2O}$ is very close to, but less than one, equation (17) may be simplified by using the expansion,[52]

$$\ln (1-x) = -x - \frac{x^2}{2} - \frac{x^3}{3} - \ldots\ldots\ldots \qquad (x<1)$$

Putting $P^s_{H_2O}/P^v_{H_2O} = (1-x)$ and ignoring x^2 and higher powers gives

$$P^s_{H_2O} = P^v_{H_2O} (1 - \frac{vmM\phi}{1000})$$

Osmotic coefficients of aqueous salt solutions at elevated temperatures are, as is to be expected, few and far between. However, Greeley, et al.[53] have measured the osmotic coefficient of HCl in 0.01-1.0 m solutions up to 275°C. Some of their values ϕ (up to 0.2 m HCl) together with the corresponding values of

Table (6)

Osmotic Coefficients, Water Activities etc. in HCl Solutions

m_{HCl}	t°C	90°	125°	200°	250°
	ϕ	0.965	0.961	0.951	0.94
0.01	a_{H_2O}	0.9997	0.9997	0.9997	0.9997
	ΔP (p.s.i.)	0.00	0.01	0.07	0.17
	ϕ	0.941	0.933	0.916	0.88
0.05	a_{H_2O}	0.9983	0.9983	0.9983	0.9984
	ΔP (p.s.i.)	0.02	0.06	0.38	0.92
	ϕ	0.933	0.923	0.901	0.85
0.10	a_{H_2O}	0.9966	0.9967	0.9968	0.9969
	ΔP (p.s.i.)	0.03	0.11	0.72	1.79
	ϕ	0.932	0.920	0.892	0.84
0.20	a_{H_2O}	0.9933	0.9934	0.9936	0.9939
	ΔP (p.s.i.)	0.07	0.22	1.44	3.52

$a^{s}_{H_2O}$ and $\Delta P = P^{s}_{H_2O} - P^{v}_{H_2O}$ are given in Table (6). It can be seen that the values of ϕ change slowly with temperature and it is only the greatly increased values of $P^{v}_{H_2O}$ that cause ΔP to become significant at the higher temperatures. The effect is still small at 200°C, however, and because the product (vm) for the buffer solutions used in the present work was always < 0.1 and in the absence of any data for ϕ for similar solutions at elevated temperatures the effect was ignored. Any error in so doing will be manifest as a hydrogen activity calculated from equation (15) which is slightly too low leading to a slightly high value of $p(a_{H}\gamma_{Cl})$, although the effect is probably never greater than 0.002 pH units.

ii) <u>The Activity of Water Vapour is Increased due to Hydrogen</u>

The presence of a gas above a liquid generally causes an increase in the vapour's fugacity. The effect in the present work is small: 4 atm. of H_2 above water at 200°C would cause an increase in the water fugacity of approximately 0.5 p.s.i. and is negligible at below 160°. However, the correction is easy to apply and was incorporated for completeness.

It may be shown that the fugacity of a volatile component in the vapour phase above its liquid in the presence of a second gaseous component (assumed insoluble in the liquid) is given at constant temperature , assuming perfect mixing, by[54]

$$\frac{\partial(\ln f)}{\partial P} = \frac{\overline{V}_i}{RT}$$

where $\overline{V}_i$ is the partial molal volume of the liquid phase (equal to the molal volume of the pure liquid component). Integration of this equation between $f^{s'}_{H_2O}$, P_T (for a solution plus hydrogen) and $f^{s}_{H_2O}$,

$P^{s}_{H_2O}$ (for the pure solution alone) yields,

$$\ln (f^{s'}_{H_2O}/f^{s}_{H_2O}) = \frac{\overline{V}_i}{RT}(P_T - P^{s}_{H_2O}) \qquad -- (18)$$

in which $\overline{V}_i$ rightly refers to the solution but will be assumed equal to that of water. If the fugacity coefficients are equal then equation (18) becomes,

$$\ln (P^{s'}_{H_2O}/P^{s}_{H_2O}) = \frac{\overline{V}_i}{RT}(P_T - P^{s}_{H_2O})$$

Because $P^{s'}_{H_2O}/P^{s}_{H_2O}$ is close to, but greater than one, once again the inconvenient logarithmic term may be removed by employing this time the expansion,[52]

$$\ln x = (x-1) - \frac{(x-1)^2}{2} + \frac{(x-1)^3}{3} - \ldots$$

$$(0<x\leq 2)$$

Putting $P^{s'}_{H_2O}/P^{s}_{H_2O} = x$ and neglecting $(x-1)^2$ and higher powers yields,

$$P^{s'}_{H_2O} = P^{s}_{H_2O}\left(1 + \frac{\overline{V}_i}{RT}(P_T - P^{s}_{H_2O})\right)$$

which gives the vapour pressure of the solution in the presence of hydrogen as a function of the total pressure and the vapour pressure of the solution alone (assumed equal to the vapour pressure of water at the same temperature).

Saturated Water Vapour Pressure

The values of the saturated water vapour pressure were taken from the Steam Tables[55] in the form of a smoothed function relating the reduced pressure to the reduced temperature:

$$B_k(\theta) = \exp\left[\frac{\frac{1}{\theta}\sum_{v=1}^{5} k_v(1-\theta)^v}{1 + k_6(1-\theta) + k_7(1-\theta)^2} - \frac{(1-\theta)}{k_8(1-\theta)^2 + k_9}\right]$$

in which $B_k(\theta)$ is the reduced pressure, $P^v_{H_2O}/P_C$ and θ is the reduced temperature T/T_C. For this equation the critical values, P_C and T_C are defined as 22.12 MPa and 647.3 K respectively and

$k_1 = -7.691\ 234\ 564$ $\qquad$ $k_6 = 4.167\ 117\ 320$

$k_2 = -2.608\ 023\ 696\ 10^1$ $\qquad$ $k_7 = 2.097\ 506\ 760\ 10^1$

$k_3 = -1.681\ 706\ 546\ 10^2$ $\qquad$ $k_8 = 10^9$

$k_4 = 6.423\ 285\ 504\ 10^1$ $\qquad$ $k_9 = 6$

$k_5 = -1.189\ 646\ 225\ 10^2$

A computer programme was written to produce from this function the saturated vapour pressure of water, to 0.01 p.s.i., at 0.1° intervals from 0 to 300°C. Linear interpolation of the pressure between adjacent temperatures was used involving negligible error.

Fugacity Coefficient of Hydrogen

The activity of a gas is properly the ratio of two fugacities, f/f°, where f° is its fugacity in the standard state, normally

1 atm., and therefore the activity becomes equal to its fugacity. At pressures near to 1 atmosphere or less the fugacities of most gases may be taken as equal to their pressures. This implies perfect gas behaviour in that the fugacity of a real gas may be interpreted as its pressure, supposing it to be a perfect gas, with the same chemical potential. At higher pressures, or in the presence of another component molecular interactions can be expected to cause deviations from the perfect gas laws and therefore the fugacity of a gas becomes significantly different from its pressure. This divergence is conveniently described by the gas' fugacity coefficient, f/P.

In the present work it was thought necessary to make some estimate of the fugacity coefficient of H_2 in H_2-H_2O mixtures, to find the magnitude of the error involved in taking the H_2 fugacity as equal to the H_2 partial pressure as defined by equation (15).

When dealing with mixtures of gases various assumptions have been made in the past,[56] e.g. Dalton's Law that pressures are additive at constant volume, the partial pressure being defined as $P_i = x_i P_m$. This applies to perfect gas mixtures only and is normally in considerable error. A better assumption is that of Amagat: volumes are additive at constant pressure. This has been shown to be equivalent to Lewis' and Randall's Rule applicable to ideal gas mixtures, $f_i = x_i f_i^o$, where f_i^o is the fugacity of pure component, i, at the same pressure as the mixture. However, this also is generally not applicable especially when considering a mixture of very different gases.

A method was therefore used in the present work involving the virial equations of state of the two gaseous components at

constant total pressure. The errors involved in the method derive solely from the curtailing of the virial equations after the second term and from the estimation of the various first virial coefficients. The method has been used by Needes[57] to estimate fugacity coefficients of H_2 in H_2-H_2O-NH_3 mixtures and his data has been used in this calculation. It will be seen that the method is relatively lengthy (even more so if further values of the virial coefficients, at different temperatures, had had to have been calculated) so one calculation was carried out in detail at 200°C with a representative H_2 pressure.

The original virial equation of state of Kammerlingh Onnes is,

$$\frac{PV}{RT} = 1 + \frac{B}{V} + \frac{C}{V^2} + \frac{D}{V^2} + \cdots\cdots$$

which on inversion to a power series in P becomes[58,59]

$$\frac{PV}{RT} = 1 + \frac{BP}{RT} + \frac{(C-B^2)P^2}{(RT)^2} + \cdots\cdots$$

Substitution into Lewis' (partial) definition of gas fugacity,

$$\frac{\partial(\ln f)}{\partial P} = \frac{V}{RT}$$

and integrating gives

$$\ln (f/P) = \frac{BP}{RT} + \frac{(C-B^2)P^2}{(RT)^2} + \cdots\cdots$$

Ignoring P^2 and higher powers, this becomes

$$RT \ln f = RT \ln P + BP \qquad \text{— (19)}$$

The first virial coefficient, B, may be interpreted as a measure of the interaction between two molecules in the gas.

The free energy of mixing ΔG_m of a gas mixture with two components is given by[60]

$$\Delta G_m = RT \ln f_m^o - RT \sum_i^2 x_i \ln f_i^o + RT \sum_i^2 x_i \ln x_i$$

in which x_i is the mole fraction of component i and f_m^o and f_i^o are the fugacities of the mixture and pure components respectively, all at a total pressure of P_m. Substitution for these fugacities from equation (19) gives

$$\Delta G_m = B_m P_m - \sum_i^2 x_i B_i P_i + RT \sum_i^2 x_i \ln x_i \qquad \text{-- (20)}$$

where B_m and B_i are the constants in the virial equations of state of the mixture and pure components respectively. It can be shown[56] that B_m is a function of the components' mole fractions and for two components becomes

$$B_m = x_1^2 B_1 + x_2^2 B_2 + 2x_1 x_2 B_{12}$$

where B_{12} is the "interaction constant" between the unlike pairs of molecules. Substitution of B_m into equation (20) and recalling that $\Sigma x_i = 1$ gives

$$\Delta G_m = RT\sum_i^2 x_i \ln x_i + x_1 x_2 P_m \Delta B \qquad \text{-- (21)}$$

where $\Delta B = 2B_{12} - B_1 - B_2$.

The partial free energy of mixing of one component is given by[60]

$$\Delta \bar{G}_i = \Delta G_m + (1-x_i)\cdot\frac{\partial G_m}{\partial x_i}$$

and therefore substituting for ΔG_m from (21) and differentiating gives

$$\Delta \bar{G}_1 = RT\ln x_1 + x_2^2 P_m \Delta B \qquad \text{-- (22a)}$$

$$\Delta G_2 = RT\ln x_2 + x_1^2 P_m \Delta B \qquad \text{-- (22b)}$$

$\Delta\bar{G}_i$ is the change in free energy per mole on transfering pure component i, at P_m, to the mixture also at P_m. Therefore

$$\Delta \bar{G}_i = RT\ln f_i - RT\ln f_i^o$$

which combined with equations (22a) and (22b) gives

$$RT\ln f_1 = RT\ln f_1^o + RT\ln x_1 + x_2^2 P_m \Delta B \qquad \text{-- (23a)}$$

$$RT\ln f_2 = RT\ln f_2^o + RT\ln x_2 + x_1^2 P_m \Delta B \qquad \text{-- (23b)}$$

(It may be noticed that these two equations reduce to the Lewis and Randall Rule when $\Delta B = 0$. That this condition is far from true for a H_2-H_2O mixture may be seen from the value of ΔB given

below.)

Values of B_{H_2}, B_{H_2O} and B_{H_2,H_2O} for temperatures between 190° and 230°C have been calculated by Needes using the Lennard-Jones and Stockmeyer Potentials. (See Needes[57] p 265 et seq. and Hirschfelder, et al.[61] especially ch. 3; ch 4, pp 419-426; p 1110, 1119, 1147-1149). Needes has shown (ibid. p 67) that using his values of B_{H_2} in equation (19) yields fugacity coefficients for pure H_2 at 210°C and up to 70 atm. in good agreement with those calculated from the empirical equation of state of Shaw and Wones[62] fitted to known experimental data. (The constant, C_3, appearing in this equation is quoted wrongly as a function of temperature by both Shaw and Wones and by Needes. The correct function is $C_3 = 300(\exp(-0.0011901T - 5.941))$ which may be checked from graphical data in the original paper. The particular values of C_3 at different temperatures quoted in both references are, however, correct).

The H_2-H_2O system may now be solved for fugacities and pressures as follows. For water, from equation (19)

$$RT\ln f^{\circ}_{H_2O} = RT\ln P_m + B_{H_2O}P_m \qquad -- (24)$$

and equations (23)

$$RT\ln f_{H_2O} = RT\ln f^{\circ}_{H_2O} + RT\ln x_{H_2O} + x^2_{H_2} P_m \Delta B \qquad -- (25)$$

By comparison to equation (18) relating the fugacities of a saturated vapour with and without another gaseous component

present,

$$RT\ln f_{H_2O} - RT\ln f^{v}_{H_2O} = \bar{V}(P_m - P^{v}_{H_2O}) \qquad -- (26)$$

and from equation (19) for pure water,

$$RT\ln f^{v}_{H_2O} = RT\ln P_{H_2O} + B_{H_2O}P^{v}_{H_2O} \qquad -- (27)$$

in which $f^{v}_{H_2O}$ and $P^{v}_{H_2O}$ are the fugacity and pressure of pure water vapour.

Equations (24), (25), (26) and (27) may be solved simultaneously for P_m which becomes an implicit function of B_{H_2O}, ΔB, x_{H_2O}, $\bar{V}$ etc. If a value for x_{H_2O} is now chosen a method of successive approximations (e.g. Newton's Method) quickly gives P_m. Substitution of P_m with B_{H_2}, B_{H_2O} or B_m into equation (19) gives $f^{o}_{H_2}$, $f^{o}_{H_2O}$ and f^{o}_{m} respectively and substitution of $f^{o}_{H_2}$ and $f^{o}_{H_2O}$, P_m, ΔB etc. into equations (23a) and (23b) gives f_{H_2} and f_{H_2O}, the fugacities of the two components in the mixture. Finally, substitution of these values, together with B_{H_2} or B_{H_2O} into equation (19) yields, again after successive approximations, two new values of P_{H_2} and P_{H_2O}, the pressures of H_2 and H_2O in the mixture (not their partial pressure as defined by Dalton's Law). The whole procedure is then repeated until constant values are obtained. The fugacity coefficients (f_{H_2}/P_{H_2}) and (f_{H_2O}/P_{H_2O}) may then be calculated.

The data at 200°C used in the calculation is shown in Table (7) (Values in parentheses are taken from the list of first virial coefficients in Kaye and Laby[63] and are seen to be in excellant agreement with those of Needes actually used in the calculation).

Table (7)

Pressures, Fugacities and Fugacity Coefficients in a H_2-H_2O Mixture at 200°C

$B_{H_2} = 1.47949\ 10^{-2}\ (1.6\ 10^{-2})\ 1.m.^{-1}$ $\quad B_{H_2O} = -1.92303\ 10^{-1}\ (-1.96\ 10^{-1})\ 1.m.^{-1}$

$B_{H_2,H_2O} = -4.1634\ 10^{-4}\ 1.m.^{-1}$ $\quad \Delta B = 1.766754\ 10^{-1}\ 1.m.^{-1}$

$P^v_{H_2O} = 15.346$ atm. $\quad \bar{V}_{H_2O} = 2.0835\ 1.m.^{-1}$

$x_{H_2} = 0.2$ $\quad x_{H_2O} = 0.8$

	In Mixture at P_m			Pure Component at P_m	
	Pressure atm.	Fugacity atm.	Fugacity Coefficient	Fugacity atm.	Fugacity Coefficient
H_2	4.1660	4.1726	1.0016	19.7078	1.0075
H_2O	15.3833	14.2547	0.9266	17.7551	0.9077
Mixture	19.5614 ($=P_m$)	18.3895	0.9401	-	-

The results in Table (7) show that the fugacity coefficient of H_2 in the mixture differs only slightly from unity and by an amount equivalent to 0.03 mV or 0.0003 pH units at 200°C. This is completely negligible compared to experimental errors in the present work.

Greeley, et al.[27] have also made an estimate of the fugacity of hydrogen at 200°C in saturated water vapour. Assuming a H_2 pressure of 1.6 atm. they calculated a fugacity of 1.642 atm. i.e. a fugacity coefficient of 1.0263. Precise details of the calculations were not given, although values of B_i and ΔB were calculated from the van der Waals constants a and b of the components from,

$$B_i = b_i - \frac{a_i}{RT}$$

$$\Delta B = (a_1^{\frac{1}{2}} - a_2^{\frac{1}{2}})^2/RT$$

From these equations, using values of a and b for H_2 and H_2O from Kaye and Laby, $B_{H_2} = 2.03\ 10^{-2}$ l.m.$^{-1}$, $B_{H_2O} = -1.10\ 10^{-1}$ l.m.$^{-1}$ and $\Delta B = 0.0875$ l.m.$^{-1}$ which are not too different from those used above. It was stated that equation (22) was used in the calculation, but it seems unlikely that the whole system was solved simultaneously as in the present work. Their value for the fugacity coefficient is, however, undoubtedly too high. At constant pressure an increase in the mole fraction of H_2O obviously decreases the fugacity coefficient of hydrogen and even for pure H_2 a value of 1.0263 would require a pressure of about 68 atm. In fact, Greeley assumed a value of unity for his work.

3.2 The Dielectric Constant of Water: the Debye-Huckel Constants

To calculate the ionic strengths and pH_S of the buffers it was conventionally assumed that single ion activity coefficients may be expressed by

$$\log \gamma = \frac{-A.Z^2 I^{\frac{1}{2}}}{1 + BaI^{\frac{1}{2}}}$$

On the molal scale (i.e. I is a function of molalities) the Debye-Huckel constants A and B are given by(64)

$$A = \frac{1}{\ln 10}\left[\frac{2\pi e^6 N}{1000k^3}\right]^{\frac{1}{2}}\left[\frac{d}{D^3T^3}\right]^{\frac{1}{2}}$$

$$B = \left[\frac{8\pi e^2 N}{1000k}\right]^{\frac{1}{2}}\left[\frac{d}{DT}\right]^{\frac{1}{2}}$$

Apart from these constants' direct temperature dependence both d, the density and D, the dielectric constant of water are themselves functions of temperature. Values of d were taken from Steam Tables(55) in the form of its reciprocal, specific volume. The most recent determination of D over the required temperature range seems to be that of Akerlof and Oshry(65) who quote the function,

$$D = \frac{5321}{T'} + 233.76 - 0.9297\,T' + 1.417\,10^{-3}\,T'^2 - 8.292\,10^{-7}\,T'^3$$

where $T' = t + 273.1$: $t = 0\text{-}370^{\circ}C$.

Table (8)

The Dielectric Constant of Water

	Malmberg & Maryott	Akerlof & Oshry
t°C	D	D
0	87.74	88.14
20	80.10	80.27
40	73.15	73.13
60	66.81	66.63
80	61.03	60.72
100	55.72	55.34
120	(50.83)	50.43
140	(46.28)	45.94
160	(42.01)	41.82
180	(37.95)	38.03
200	(34.04)	34.52
220	(30.20)	31.24
240	(26.36)	28.14

Table (9)

The Debye-Huckel Constants

$t^{\circ}C$	A $(mole.^{-\frac{1}{2}}kg.^{\frac{1}{2}})$	$10^{-8}B$ $(cm.^{-1}mole.^{-\frac{1}{2}}kg.^{\frac{1}{2}})$
95	0.5944	0.3415
100	0.6020	0.3426
105	0.6099	0.3436
110	0.6179	0.3447
115	0.6262	0.3457
120	0.6348	0.3468
125	0.6436	0.3479
130	0.6526	0.3490
135	0.6619	0.3501
140	0.6715	0.3512
145	0.6814	0.3524
150	0.6916	0.3535
155	0.7021	0.3547
160	0.7129	0.3559
165	0.7240	0.3571
170	0.7355	0.3583
175	0.7473	0.3595
180	0.7596	0.3608
185	0.7723	0.3620
190	0.7854	0.3633
195	0.7989	0.3646
200	0.8130	0.3659

In a more recent determination between 0 and 100°C Malmberg and Maryott[66] gave

$$D = 87.740 - 0.40008\,t + 9.398\,10^{-4}\,t^2 - 1.410\,10^{-6}\,t^3$$

which Bates used for his values of A and B.[51] A comparison of the two determinations of D is shown in Table (8) in which Malmberg and Maryott's function is extrapolated to 240°C. It can be seen that the extrapolated values are in remarkable agreement with those of Akerlof and Oshry up to 200°, the deviations between the two determinations being only slightly higher between 100–200°C than between 0–100°C. The values of Akerlof and Oshry, between 100 and 200°C could therefore be used with confidence and the values of the constants A and B, at 5° intervals, derived from them are given in Table (9).

3.3 General Analysis of $p(a_{H\gamma_{Cl}})$ Data

Statistical

For each buffer solution and chloride concentration several values of $p(a_{H\gamma_{Cl}})$ were generally obtained at each set temperature. However, despite these temperatures being nominally the same from one experimental run to the next the actual temperatures of the solutions at which the measurements were made usually differed slightly and by more than the likely error in the temperature measurement. It was not possible, therefore, to simply average the respective values of $p(a_{H\gamma_{Cl}})$ at each set temperature for one type of solution to obtain a mean. To overcome this difficulty all the $p(a_{H\gamma_{Cl}})$ data for similar solutions were smoothed as a function of temperature.

A suitable function for this was

$$p(a_{H\gamma_{Cl}}) = \frac{A}{T} + B + CT + DT^2 + \ldots\ldots$$

and by rearranging to give

$$T.p(a_{H\gamma_{Cl}}) = A + BT + CT^2 + DT^3 + \ldots$$

a standard computer program (CERN E202) could be used allowing least squares fitting of $T.p(a_{H\gamma_{Cl}})$ onto polynomials in T.

When performing this, however, considerable care had to be taken to avoid overfitting. For instance, for the 0.05 m $KH_3(Ox)_2$ solutions containing 0.015m KCl, fifteen values of $p(a_{H\gamma_{Cl}})$ were obtained allowing a fit to polynomials up to T^{15} although such a procedure would have been obviously ludicrous

since basically only four independent nominal set temperatures had been used. Therefore, to decide the best smoothing function in each case the statistical F ratio test was applied.(67)

The F ratio, as normally defined, is the ratio of the variances of two independent random samples with sizes n_1 and n_2 drawn from the same larger population which is normally distributed. Because these two variances are estimates of the same quantity, namely the variance of the total population, their ratio should be close to one, although it may be expected to differ somewhat depending on the sizes of the samples. The F distribution gives the probability of obtaining specific values of this ratio, as a function of (n_1-1) and (n_2-1), the respective degrees of freedom.

The F test is applied to the present problem as follows. If the $T.p(a_H\gamma_{Cl})$ data for one type of solution is fitted successively to polynomials in T of maximum degrees (k-1) and k and if the sums of the squares of the deviations of the data about these curves are R_{k-1} and R_k respectively, then

$$R_{k-1} - R_k = D_k$$

where D_k is a function of the data and always positive.(67) An F ratio may now be calculated from

$$F = \frac{D_k}{R_k/(n-k-1)}$$

or in terms of the respective variances of the data about the two curves,

Table (10)

F Ratio Test Applied to $T.p(a_H \gamma_{Cl})$ Data for Sat. KHTartrate, m_{KCl} Solutions

Max. Degree of Polynomial k	Degrees of Freedom (n-k-1)	$F^{95\%}_{1,(n-k-1)}$	F Ratio m_{KCl} = 0.015	0.010	0.005
0	6	6.0	$>10^8$	$>10^8$	$>10^7$
1	5	6.6	$>10^6$	$>10^5$	$>10^5$
2	4	7.7	$>10^3$	346.	33.3
3	3	10.1	111.	89.8	61.8
4	2	18.5	21.5	0.2	0.3
5	1	161.5	12.4	0.9	17.0
6	0	∞	12.2	32.4	8.4

$$F = (n-1)\left(\frac{\sigma^2_{k-1}}{\sigma^2_k} - 1\right) + 1$$

and follows an $F_{1,(n-k-1)}$ distribution. If this calculated ratio is greater than the value of $F_{1,(n-k-1)}$ in the standard F distribution at percentage level, P, then there is a probability of P/100 that the polynomial of degree k is giving a significantly better fit to the data than that of degree (k-1).

Table (10) shows how this test was applied to the data for KHTartrate solutions. Columns 4, 5 and 6 contain the F ratios obtained on fitting polynomials of increasing maximum degree (k) to the $p(a_{H\gamma_{Cl}})$ data for different m_{KCl} and column 3 contains the $F_{1,(n-k-1)}$ point at the 95 % level in the standard F distribution. (n = 7 since measurements were taken at 7 independent nominal set temperatures.) It can be seen that for m_{KCl} = 0.005 and 0.01 the experimental F ratios are insignificant after k = 3 and for m_{KCl} = 0.015 is only just significant at k = 4. Therefore smoothing functions with k = 3 were chosen to describe the data, corresponding to

$$p(a_{H\gamma_{Cl}})(T)_{s,m_i} = \frac{A}{T} + B + CT + DT^2 + \ldots.$$

where $p(a_{H\gamma_{Cl}})(T)_{s,m_i}$ are the smoothed values of $p(a_{H\gamma_{Cl}})$ as a function of temperature (T) at a chloride concentration of m_i.

The Standard Error of the $p(a_{H\gamma_{Cl}})$ data about this curve was then obtained from

$$\sigma_D = \sqrt{\frac{\sum_{j}^{N} (p(a_H\gamma_{Cl})(T_j)_{s,m_i} - p(a_H\gamma_{Cl})_{T_j})^2}{(N-k-1)}}$$

in which N is the total number of data points (not independent set temperatures) and remembering that the maximum degree of T in the smoothing function for $p(a_H\gamma_{Cl})$ is (k-1).

Calculation of $p(a_H\gamma_{Cl})^\circ$

It will be recalled from Section (1.5) that $p(a_H\gamma_{Cl})^\circ$ is the value of $p(a_H\gamma_{Cl})$ in the buffer solution at zero chloride concentration. Thus to obtain $p(a_H\gamma_{Cl})^\circ$ it is necessary to plot $p(a_H\gamma_{Cl})$ versus some function of m_{Cl} and extrapolate to $m_{Cl} = 0$ at each temperature. Obvious possible functions are m_{Cl}, $\sqrt{m_{Cl}}$, m_{Cl}/I etc.

Hamer and Acree[68] have plotted $p(a_H\gamma_{Cl})$ for 0.05 m KHphthalate solutions containing KCl versus m_{Cl} (0.001-0.05 m) and obtained good straight lines that could be easily extrapolated, at temperatures from 0-60°C. Bower, et al.[69] have plotted $p(a_H\gamma_{Cl})$ for 0.05 m $KH_3(Ox)_2$ solutions versus m_{Cl} and also m_{Cl}/I (the fractional contribution of KCl to the ionic strength) for m_{KCl} = 0.005, 0.01 and 0.015 m KCl and obtained straight lines in both cases which on extrapolation to $m_{Cl} = 0$ gave similar values of $p(a_H\gamma_{Cl})^\circ$ within experimental error. Generally Bates and co-workers have plotted $p(a_H\gamma_{Cl})$ versus m_{Cl} and extrapolated the least squares best straight line to $m_{Cl} = 0$ and this method was used in the present work since the accuracy of the data could not justify any more sophisticated

procedure. Thus

$$p(a_{H\gamma_{Cl}})(T)_{s,m_{Cl}} = a(T).m_{Cl} + p(a_{H\gamma_{Cl}})(T)^{\circ} \quad -- (28)$$

defines $p(a_{H\gamma_{Cl}})(T)^{\circ}$ as the intercept at $m_{Cl} = 0$ of the best straight line of gradient $a(T)$ obtained on plotting $p(a_{H\gamma_{Cl}})(T)_{s,m_{Cl}}$ versus m_{Cl} at each temperature. Least Squares gives,

$$p(a_{H\gamma_{Cl}})(T)^{\circ} = \frac{\sum_i^3 m_i^2 \sum_i^3 p(a_{H\gamma_{Cl}})(T)_{s,m_i} - \sum_i^3 m_i \sum_i^3 m_i . p(a_{H\gamma_{Cl}})(T)_{s,m_i}}{3\sum_i^3 m_i^2 - (\sum_i^3 m_i)^2}$$

$$a(T) = \frac{3\sum_i^3 m_i . p(a_{H\gamma_{Cl}})(T)_{s,m_i} - \sum_i^3 m_i \sum_i^3 p(a_{H\gamma_{Cl}})(T)_{s,m_i}}{3\sum_i^3 m_i^2 - (\sum_i^3 m_i)^2}$$

For the oxalate and tartrate buffers $m_i = 0.005$, 0.010 and 0.015 giving,

$$p(a_{H\gamma_{Cl}})(T)^{\circ} = \frac{7}{3}\sum_i^3 p(a_{H\gamma_{Cl}})(T)_{s,m_i} - 200\sum_i^3 m_i . p(a_{H\gamma_{Cl}})(T)_{s,m_i}$$

$$a(T) = 20000\sum_i^3 m_i . p(a_{H\gamma_{Cl}})(T)_{s,m_i} - 200\sum_i^3 p(a_{H\gamma_{Cl}})(T)_{s,m_i}$$

and for the phthalate buffer $m_i = 0.010$, 0.015 and 0.020 giving,

$$p(a_{H\gamma_{Cl}})(T)^{\circ} = \frac{29}{6}\sum_i^3 p(a_{H\gamma_{Cl}})(T)_{s,m_i} - 300\sum_i^3 m_i . p(a_{H\gamma_{Cl}})(T)_{s,m_i}$$

$$a(T) = 20000\sum_{i}^{3} m_i \cdot p(a_{H\gamma Cl})(T)_{s,m_i} - 300\sum_{i}^{3} p(a_{H\gamma Cl})(T)_{s,m_i}$$

Coefficients of like powers of T are added algebraically and therefore a(T) and $p(a_{H\gamma Cl})(T)^{\circ}$ become functions of T similar to $p(a_{H\gamma Cl})(T)_{s,m_{Cl}}$.

At constant temperature, the standard error, σ_p, of the $p(a_{H\gamma Cl})(T)_{s,m_i}$ data about the best straight line (28) is given by,

$$\sigma_p = \sum_{i}^{3} (p(a_{H\gamma Cl})(T)_{s,m_i} - a(T).m_i - p(a_{H\gamma Cl})(T)^{\circ})^2$$

(N-k-1 = 1 for this line). The standard error of the intercept, i.e. $p(a_{H\gamma Cl})(T)^{\circ}$, is

$$\sigma_p \cdot \sqrt{\left(\frac{1}{3} + \frac{\bar{m}^2}{\sum_{i}^{3}(m_i - \bar{m})^2}\right)}$$

and is therefore $1.528\sigma_p$ for the oxalate and tartrate buffers and $2.198\sigma_p$ for the phthalate buffer.

4. RESULTS

4.1 Stability of Standard Buffer Solutions

The U.S. National Bureau of Standards recommends five primary and two secondary pH_S Buffer Standards calibrated up to 95°C.[51] Their compositions and pH_S values at 25°C are given in Table (11). (It is to be understood that the distinction between the primary (B-F) and secondary (A and G) standards refers only to the fact that with a glass electrode-reference electrode assembly, liquid junction potentials are not very successfully smoothed out between the buffer and unknown solution during practical pH measurement at $11.5 < pH_S < 2.5$; in all other respects, e.g. accuracy, all seven standards are comparable).

Initially to test the stability of these standard buffers at elevated temperatures, 10 ml. of each solution were sealed (under air) into small pyrex ampoules (cf. Appendix C) and heated in an autoclave to 200°C for $2\frac{1}{2}$ hours. On cooling the phials were cut open and the pH_S of the solutions measured versus their original values using a glass electrode. The results are given in Table (12).

It is obvious that both A (tetroxalate) and B (tartrate) decomposed extensively. C (phthalate) and D (phosphate) seemed unaffected and although E (phosphate) showed an increase of 0.033 pH units this must have been due to something other than decomposition (e.g. glass dissolution) since the solution is qualitatively identical to D. Solution F (borate) showed a significant decrease of 0.11 pH units. This might again be due

Table (11)

N.B.S. Seven Standard Buffer Solutions

Buffer	Substance	Molality	$pH_S(25^\circ C)$
A	$KH_3(Ox)_2.2H_2O$	0.05	1.679
B	KHTartrate	Sat. at 25°C	3.557
C	KHPhthalate	0.05	4.008
D	KH_2PO_4 Na_2HPO_4	0.025 0.025	6.865
E	KH_2PO_4 Na_2HPO_4	0.008695 0.03043	7.413
F	$Na_2B_4O_7.10H_2O$	0.01	9.180
G	$Ca(OH)_2$	Sat. at 25°C 0.0203	12.454

Table (12)

Stability of Buffer Solutions at 200°C

pH_S(20°C)

		Before (Defined)	After	Remarks
A	Tetroxalate	1.674	> 4.46	Gas bubbles in phial; probably CO_2.
B	Tartrate	3.564	3.787	Very faint alcohol or aldehyde smell.
C	Phthalate	4.000	3.998	-
D	Phosphates	6.879	6.882	-
E	Phosphates	7.429	7.462	-
F	Borate	9.228	9.118	-
G	$Ca(OH)_2$	12.627	< 9.314	Precipitate in phial.

to glass attack or alternatively to a frozen elevated temperature equilibrium, involving polymerised borate species. However, Mesmer, et al.[70] have shown that in borate solutions (0.05 m B) at 200°C less than 10 % of the boron exists as complex borates such as $B_2(OH)_7^-$ and $B_3(OH)_{10}^-$ and that the majority exists as $B(OH)_3$ and $B(OH)_4^-$. Moreover, Manov, et al.[71] and Owen[72] have shown that borax ($Na_2B_4O_7$) reacts quickly in dilute solution to produce these latter mononuclear species in equilibrium amounts. It seems, therefore, that a frozen equilibrium is unlikely to be formed.

The precipitation of $Ca(OH)_2$ from solution G was expected since the hydroxides solubility has an inverse temperature dependence.

From these results it seemed that standards C, D, E and F could probably be used as satisfactory buffers at elevated temperatures and that although A and B decomposed before 200°C it was suspected that they might still be useful up to 150°C or higher and therefore their calibration was worth attempting.

4.2 0.05 m Potassium Tetroxalate

It was initially suspected that this solution would be stable up to 160-180°C but unfortunately it was found that extensive decomposition took place at 130°C. A definite kink in the $p(a_{H\gamma_{Cl}})_{m_{Cl}}$ versus T curves occurred at around this temperature and the data became much more scattered. Therefore only values of $p(a_{H\gamma_{Cl}})_{m_{Cl}}$ at temperatures < 125°C were considered.

The F ratio test indicated that functions with k = 2, equivalent to,

$$p(a_{H\gamma_{Cl}})_{m_{Cl}} = \frac{A}{T} + B + CT$$

were adequate to describe the data and the experimental and smoothed values of $p(a_{H\gamma_{Cl}})_{m_{Cl}}$ at the experimental temperatures are given in Table (13). The scatter of the data about the smoothed $p(a_{H\gamma_{Cl}})_{m_{Cl}}$ versus T curves is shown in Figs. (9a-c). The coefficients of the smoothing functions and the standard error, σ_D, of the data about them, plus the derived coefficients of the $p(a_{H\gamma_{Cl}})(T)^\circ$ and a(T) functions are given in Table (14). Values of $p(a_{H\gamma_{Cl}})(T)_{s,m_{Cl}}$, a(T) and $p(a_{H\gamma_{Cl}})(T)^\circ$ derived from these functions at 5° intervals between 95 and 120°C are given in Table (15). The equivalent plots of $p(a_{H\gamma_{Cl}})(T)_{s,m_{Cl}}$ versus m_{Cl}, at constant temperature, are shown in Fig. (10). Also given in Table (15) are the Standard Errors, $(1.528\sigma_p)$ of $p(a_{H\gamma_{Cl}})^\circ$ at each temperature (where σ_p is the Standard Error of the three values of $p(a_{H\gamma_{Cl}})_{s,m_{Cl}}$ about each respective best straight line shown in Fig. (10)).

Table (13)

Experimental and Smoothed Values of $p(a_H\gamma_{Cl})$ in 0.05 m Potassium Tetroxalate Solutions

Run No. 0423 m_{Cl} = 0.015

t^oC	T^oK	$p(a_H\gamma_{Cl})$ Exptl	Smthd
92.76	365.91	1.902	1.905
92.76	365.91	1.897	1.905
102.66	375.81	1.942	1.931
102.68	375.83	1.933	1.931
112.66	385.81	1.957	1.962
112.66	385.81	1.948	1.962
122.60	395.75	1.993	1.995
122.64	395.79	1.988	1.995

Run No. 0501 m_{Cl} = 0.015

93.09	366.24	1.908	1.906
93.11	366.26	1.908	1.906
102.74	375.89	1.934	1.932
102.75	375.90	1.933	1.932
112.85	386.00	1.964	1.962
112.85	386.00	1.965	1.962
123.27	396.42	2.008	1.998
123.23	396.38	2.001	1.998

Table (13) (cont.)

Run No. 0426 m_{Cl} = 0.010

$t^{o}C$	$T^{o}K$	$p(a_{H}\gamma_{Cl})$ Exptl	$p(a_{H}\gamma_{Cl})$ Smthd
92.43	365.58	1.899	1.893
92.45	365.60	1.900	1.893
102.81	375.96	1.924	1.924
102.79	375.94	1.923	1.923
112.87	386.02	1.951	1.956
112.87	386.02	1.949	1.956
123.11	396.26	2.000	1.993

Run No. 0503 m_{Cl} = 0.010

92.85	366.00	1.884	1.894
92.85	366.00	1.885	1.894
102.38	375.53	1.936	1.922
102.42	375.57	1.922	1.922
112.40	385.55	1.961	1.955
112.40	385.55	1.950	1.955
122.10	395.25	1.997	1.989
122.15	395.30	1.978	1.989

Table (13) (cont.)

Run No. 0429 m_{Cl} = 0.005

$t^{\circ}C$	$T^{\circ}K$	$p(a_{H}\gamma_{Cl})$ Exptl	$p(a_{H}\gamma_{Cl})$ Smthd
92.93	366.08	1.895	1.895
92.93	366.08	1.896	1.895
102.79	375.94	1.918	1.920
102.79	375.94	1.919	1.920
112.85	386.00	1.951	1.949
112.85	386.00	1.950	1.949
121.85	395.88	1.978	1.979
121.87	395.90	1.978	1.979

Table (14)

Coefficients of the Data Smoothing Functions and the Standard Errors of the Data about the Curves for 0.05 m Potassium Tetroxalate Solutions

$$f(T) = \frac{A}{T} + B + CT$$

	$p(a_H\gamma_{Cl})_{0.015}$	$p(a_H\gamma_{Cl})_{0.010}$	$p(a_H\gamma_{Cl})_{0.005}$	$p(a_H\gamma_{Cl})^\circ$	a
A	9.44466062 E 2	8.17592427 E 2	6.09063394 E 2	4.54971293 E 2	3.35402668 E 4
B	-4.17425474 E 0	-3.60034481 E 0	-2.33568161 E 0	-1.53152058 E 0	-1.83857314 E 2
C	9.55923636 E -3	8.90830409 E -3	7.01156531 E -3	5.94536419 E -3	2.54767106 E -1
σ_D	0.00683	0.00832	0.00161	-	-

Table (15)

Values of $p(a_H\gamma_{Cl})(T)_{s,m_{Cl}}$, $a(T)$, $p(a_H\gamma_{Cl})(T)^\circ$ and Standard Error

for 0.05 m Potassium Tetroxalate Solutions

		$p(a_H\gamma_{Cl})(T)_{s,m_{Cl}}$					
$t^\circ C$	m_{Cl} =	0.015	0.010	0.005	$a(T)$	$p(a_H\gamma_{Cl})(T)^\circ$	$1.528\sigma_p$
95		1.910	1.900	1.900	1.04	1.893	0.006
100		1.924	1.915	1.913	1.09	1.906	0.004
105		1.938	1.930	1.926	1.18	1.920	0.003
110		1.953	1.947	1.940	1.29	1.934	0.001
115		1.969	1.964	1.955	1.44	1.948	0.003
120		1.986	1.982	1.970	1.62	1.963	0.005

Table (16)

Effect of 'ionic radius,' a, (equation (30)) on the Ionic Strength, I, and log γ^{o}_{Cl} in 0.05 m Potassium Tetroxalate Solution

	I			- log γ^{o}_{Cl}		
$t^{o}C$	a = 2.0 Å	4.0 Å	6.0 Å	a = 2.0 Å	4.0 Å	6.0 Å
95	0.0740	0.0719	0.0705	0.115	0.114	0.113
100	0.0734	0.0713	0.0700	0.116	0.115	0.114
105	0.0728	0.0708	0.0694	0.117	0.116	0.115
110	0.0722	0.0702	0.0689	0.118	0.117	0.116
115	0.0716	0.0697	0.0684	0.120	0.118	0.118
120	0.0710	0.0691	0.0678	0.121	0.120	0.119

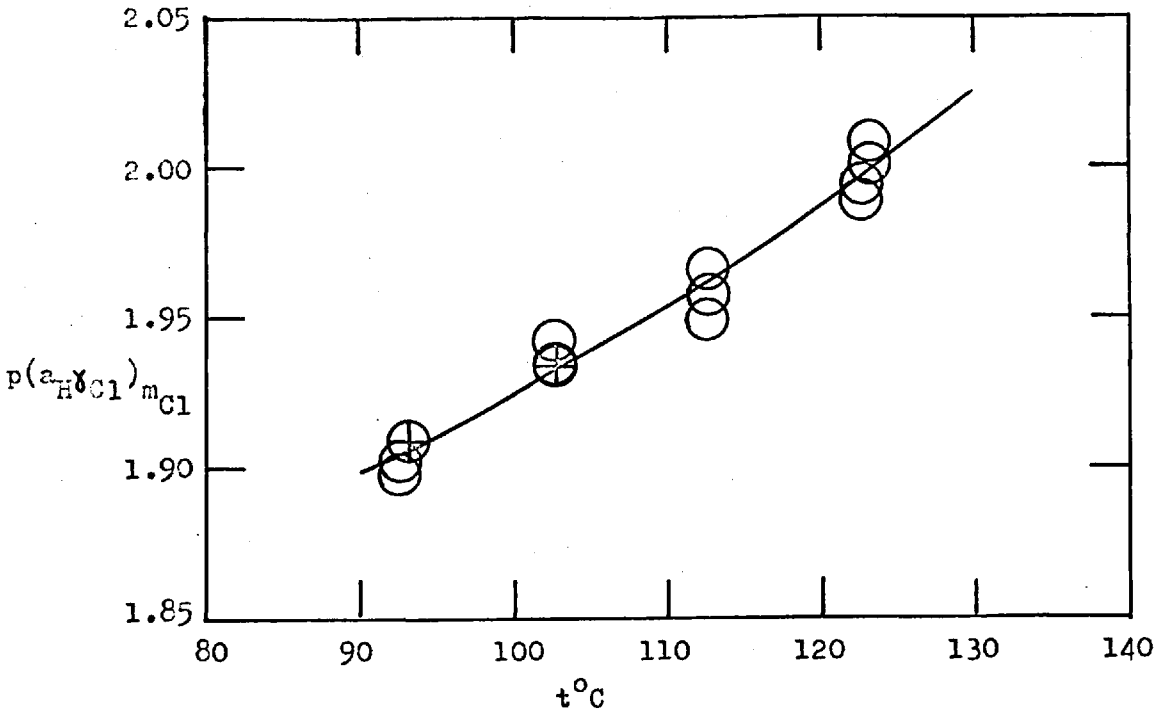


Fig. (9a) Experimental $p(a_H\gamma_{Cl})_{m_{Cl}}$ data about smoothing curve for 0.05 m $KH_3(Ox)_2$/0.015 m KCl solution.

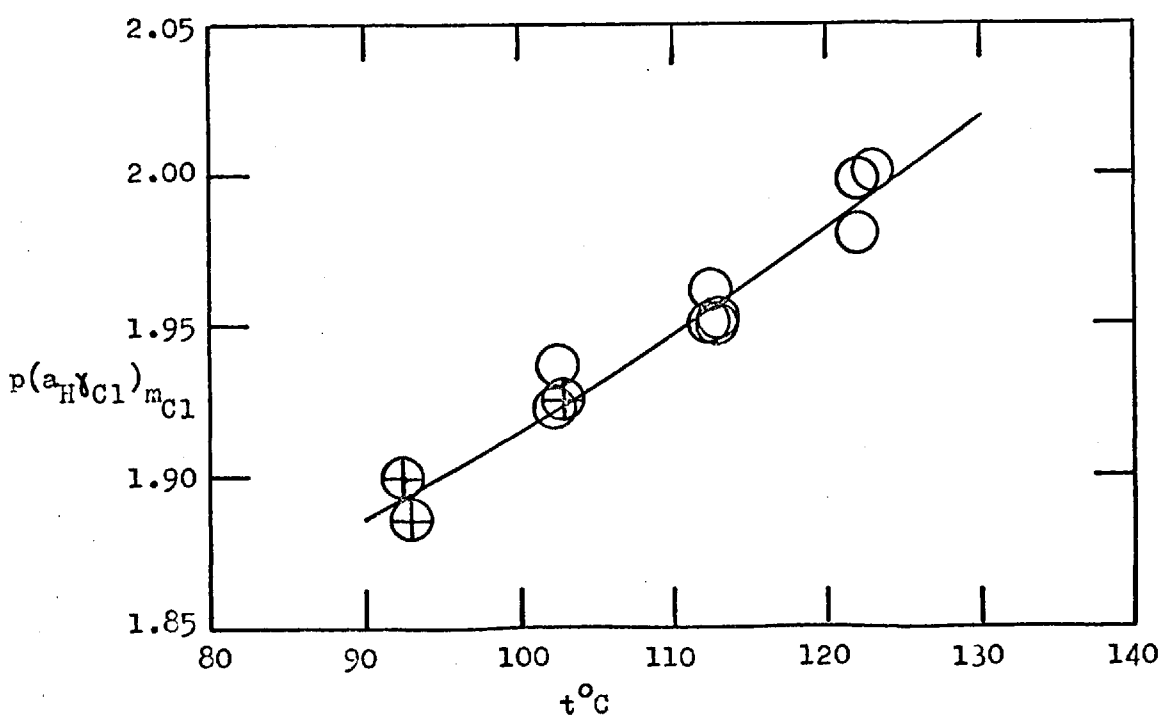


Fig. (9b) Experimental $p(a_H\gamma_{Cl})_{m_{Cl}}$ data about smoothing curve for 0.05 m $KH_3(Ox)_2$/0.010 m KCl solution.

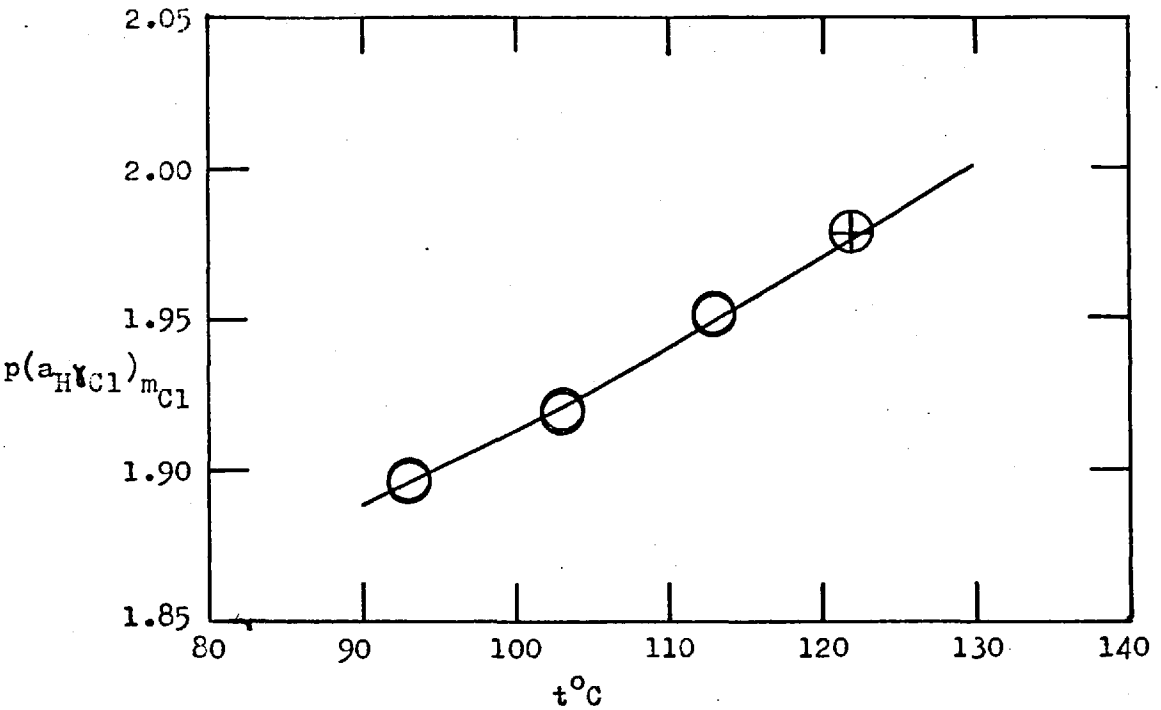


Fig. (9c) Experimental $p(a_{H}\gamma_{Cl})_{m_{Cl}}$ data about smoothing curve for 0.05 m $KH_3(Ox)_2$/0.005 m KCl solution.

⊕ in Figs. (9a-c), (12a-c), (15), (16) and (17a-c) refer to two identical data points.

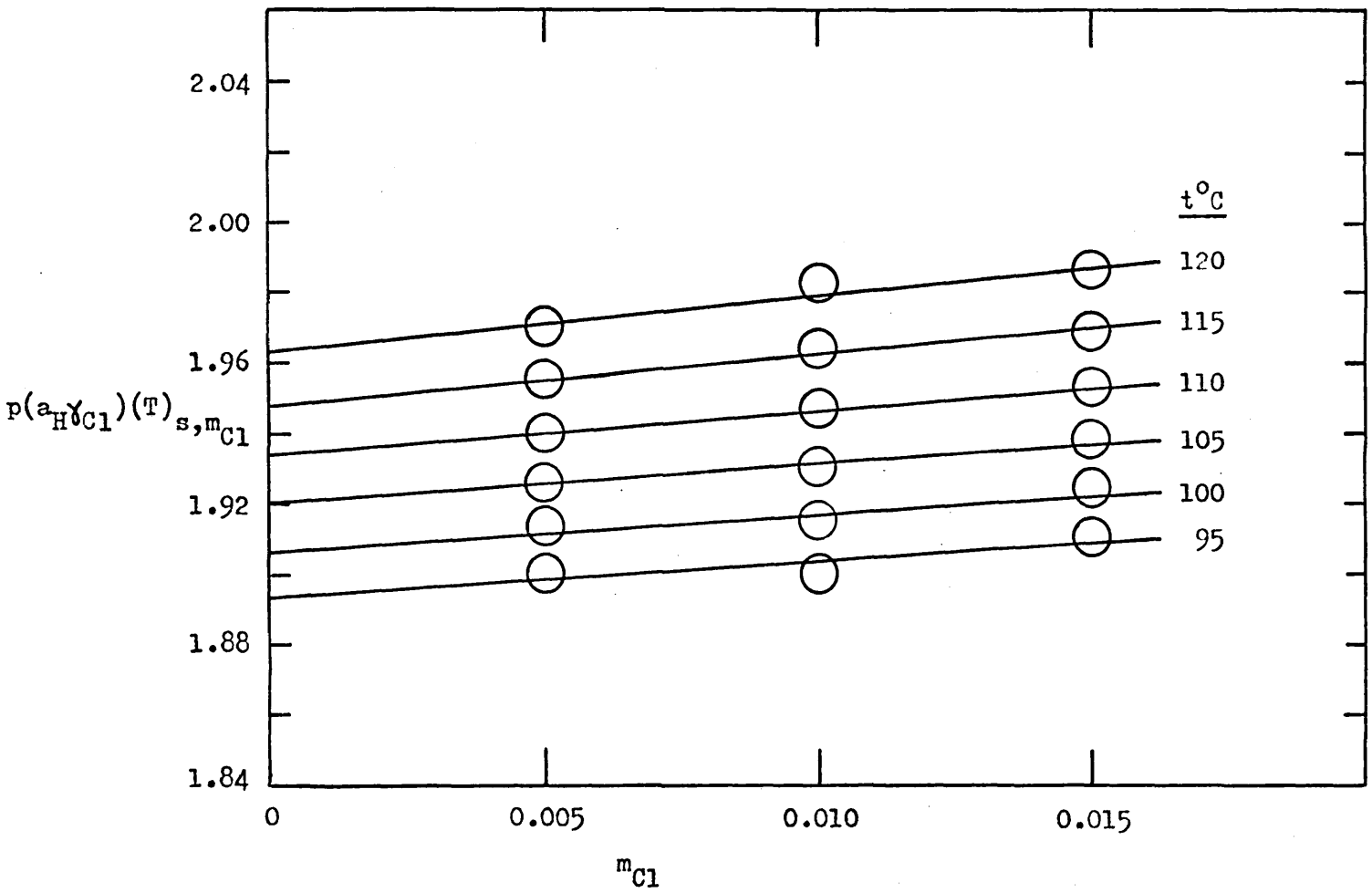


Fig. (10) Extrapolation of $p(a_H\gamma_{Cl})(T)_{s,m_{Cl}}$ to $m_{Cl} = 0$ for 0.05 m $KH_3(Ox)_2$ solution.

Ionic Strength

To calculate the ionic strength of the 0.05 m Potassium Tetroxalate solution (containing no KCl) the method of Bower, et al.[69] was employed. Formally, the ionic strength is given by,

$$I = \tfrac{1}{2}(m_K + m_H + m_{OH} + m_{HOx} + 4m_{Ox}),$$

however, m_{OH} is negligible at the low pH and may be neglected. Moreover, extrapolation of Pinching's values of the second dissociation constant of oxalic acid between 0 and 50°C[73] to 95-120°C show it to be 0.95-1.7 10^{-5} and therefore m_{Ox} may also be ignored.

It is assumed that when $KH_3(Ox)_2$ dissolves in water to give a solution of molality, m*, then the dissociation,

$$H_2Ox = H^+ + HOx^-$$

is partial and

$$KHOx = K^+ + HOx^-$$

complete, and therefore

$$m_K = m^*$$

$$m_{HOx} = m_K + m_H$$

$$= m^* + m_H$$

and the ionic strength becomes,

$$I = m^* + m_H \qquad \text{— (29)}$$

For the sake of this calculation it is assumed that,

$$\log \gamma_H = \log \gamma_{Cl} = \frac{-A.I^{\frac{1}{2}}}{1 + BaI^{\frac{1}{2}}}$$

therefore,

$$-\log m_H = p(a_H\gamma_{Cl})^\circ + \log \gamma_H \cdot \gamma_{Cl}$$

$$= p(a_H\gamma_{Cl})^\circ - \frac{2A.I^{\frac{1}{2}}}{1 + BaI^{\frac{1}{2}}} \quad -- (30)$$

At each temperature, by letting $-\log m_H = p(a_H\gamma_{Cl})^\circ$ a first approximation for m_H was obtained which on substitution with m* (=0.05) into equation (29) gave a first value for I. Substitution of this, plus $p(a_H\gamma_{Cl})^\circ$ etc. into (30) gave a second approximation for m_H leading to a better estimate of I from (29). Three to four reiterations of this procedure gave a constant value of I.

The value chosen for a, (nominally an 'effective ionic radius') in (30) is not very critical. Pinching [73] has used 5.0 Å in a similar Debye-Huckel expression, to extrapolate pK_2 (the second dissociation constant of oxalic acid) to zero ionic strength. However, this choice was really just a matter of convenience enabling a linear plot to be obtained. Table (16) shows the values of I obtained in the present work, at each temperature, using a = 2.0, 4.0 and 6.0 Å. There is generally a difference of 4.5 % between the largest and smallest values at each temperature.

γ°_{Cl} in the Solution

γ°_{Cl} was calculated by substitution of I into equation (11)

$$\log \gamma^{\circ}_{Cl} = \frac{-AI^{\frac{1}{2}}}{1 + 1.5I^{\frac{1}{2}}} \qquad -- (11)$$

Values so obtained are shown in Table (16). It can be seen that using a = 2.0 or 6.0 $\mathring{A}$ leads to a difference of only 0.002 units in log γ°_{Cl} and therefore the values with a = 4.0 $\mathring{A}$ were chosen. Substitution of these, together with $p(a_H\gamma_{Cl})^{\circ}$ into equation (10) leads to the final values of pH_S for the 0.05 m Potassium Tetroxalate solution given in Table (17).

Table (17)

$t^{\circ}C$	pH_S
95	1.779
100	1.792
105	1.804
110	1.817
115	1.830
120	1.843

These values are plotted and compared with those of Bates[51] which are derived from the two previous investigations of Bower, et al.[69] and Bower and Bates[74] in Fig. (11).

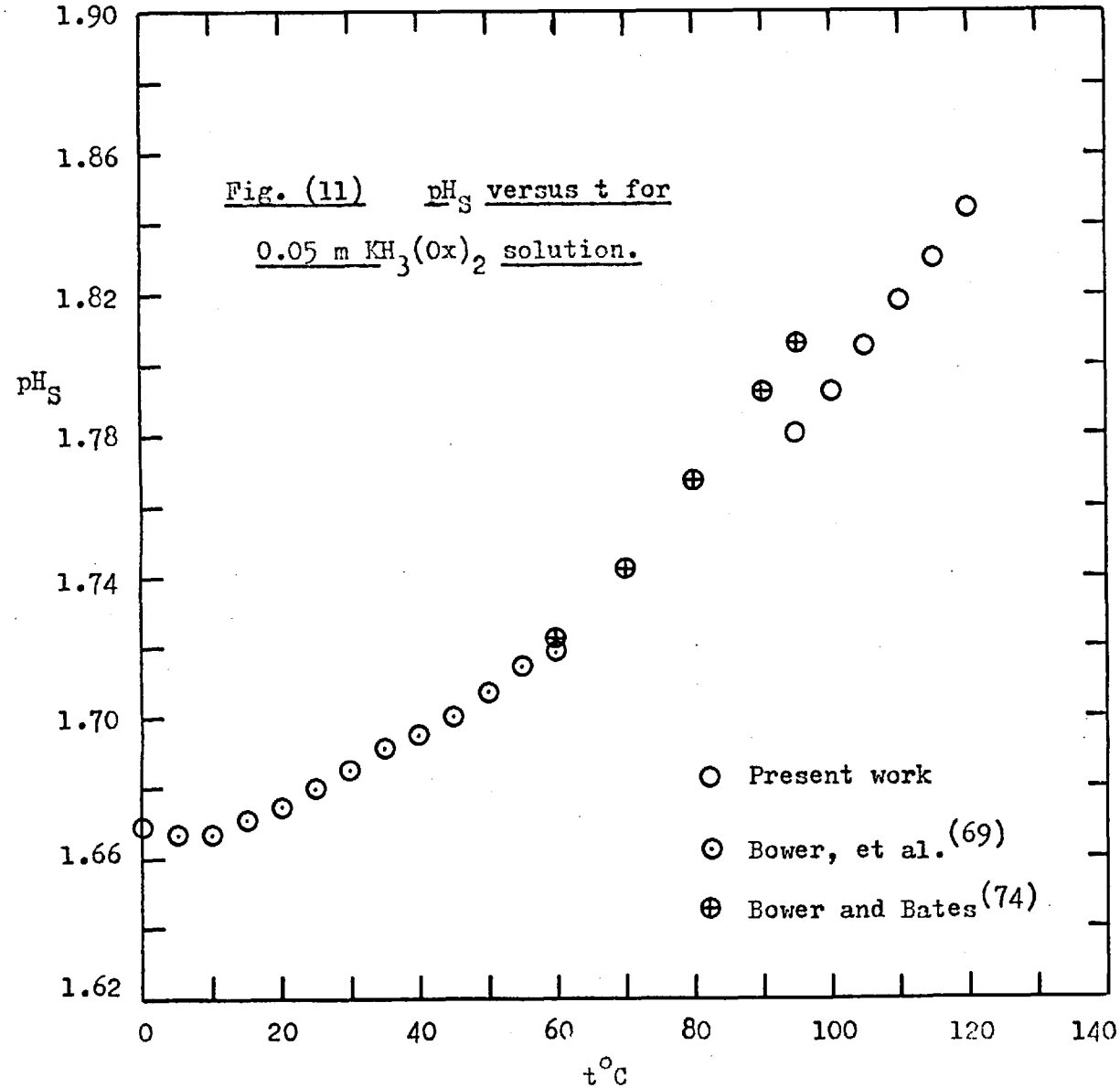


Fig. (11) pH_S versus t for 0.05 m $KH_3(Ox)_2$ solution.

4.3 Saturated (at 25°C: 0.0341 m) Potassium Hydrogen Tartrate

Le Peintre[11] gives a pH value for this solution at 150°C but not at 175°C suggesting that decomposition takes place at below the latter temperature. In the present work it was found that the final pH (at room temperature) of solutions heated to 180°C was up to 0.2 units higher than that of the original solution. However, the pH of solutions heated to 160-162°C seemed unchanged. Thus decomposition is presumed to start at between 165-175°C and the few $p(a_H\gamma_{Cl})$ values measured at ≥170°C (m_{Cl} = 0.015) were significantly higher than an extrapolation of the smoothing function obtained from the data at ≤162°C.

The Ag-AgCl electrodes behaved quite well in this solution and any reduction by H_2 was not great enough to cause a significant lowering of the pH.

Smoothing functions with k = 3, equivalent to

$$p(a_H\gamma_{Cl})_{m_{Cl}} = \frac{A}{T} + B + CT + DT^2$$

were found adequate to describe the data (see Table (10)). The results are given in Tables (18), (19) and (20) and the respective plots in Figs. (12a-c) and (13) similar to those for the Potassium Tetroxalate solution.

Table (18)

Experimental and Smoothed Values of $p(a_{H\delta Cl})$ in Saturated Potassium Hydrogen Tartrate Solutions

Run No. 0515 m_{Cl} = 0.015

$t^{\circ}C$	$T^{\circ}K$	$p(a_{H\delta Cl})$ Exptl	Smthd
97.59	370.74	3.743	3.750
97.59	370.74	3.744	3.750
121.95	395.10	3.841	3.848
121.86	395.01	3.844	3.847
142.49	415.64	3.961	3.953
142.52	415.67	3.954	3.954
151.85	425.00	3.997	4.001
151.85	425.00	3.994	4.001
161.66	434.81	4.052	4.048
161.69	434.84	4.045	4.048

Run No. 0520 m_{Cl} = 0.015

113.03	386.18	3.805	3.806
113.03	386.18	3.805	3.806
132.73	405.88	3.901	3.902
132.73	405.88	3.889	3.902

Table (18) (cont.)

Run No. 0606 m_{Cl} = 0.015

$t^{\circ}C$	$T^{\circ}K$	$p(a_{H}\gamma_{Cl})$ Exptl	Smthd
97.58	370.73	3.754	3.750
97.58	370.73	3.756	3.750
112.00	385.15	3.807	3.802
112.00	385.15	3.809	3.802
122.23	395.38	3.852	3.849
122.25	395.40	3.852	3.849
131.41	404.56	3.898	3.895
131.46	404.61	3.895	3.896
141.69	414.84	3.947	3.949
141.69	414.84	3.953	3.949
150.94	424.09	4.003	3.997
150.98	424.13	4.004	3.997
161.55	434.70	4.045	4.048
161.59	434.74	4.049	4.048

Run No. 0522 m_{Cl} = 0.010

97.54	370.69	3.748	3.754
97.56	370.71	3.746	3.754
123.00	396.15	3.841	3.845
123.00	396.15	3.837	3.845
142.31	415.46	3.924	3.931
161.39	434.54	4.000	4.006

Table (18) (cont.)

Run No. 0524	m_{Cl} = 0.010		
		$p(a_{H}\gamma_{Cl})$	
$t^{\circ}C$	$T^{\circ}K$	Exptl	Smthd
132.31	405.46	3.892	3.887
141.96	415.11	3.927	3.930
151.71	424.86	3.973	3.970
161.89	434.04	4.006	4.007
Run No. 0527	m_{Cl} = 0.010		
97.74	370.89	3.760	3.755
97.74	370.89	3.763	3.755
122.68	395.83	3.854	3.844
122.70	395.85	3.845	3.844
141.87	415.02	3.937	3.929
Run No. 0530	m_{Cl} = 0.010		
97.74	370.89	3.753	3.755
97.74	370.89	3.758	3.755
112.68	385.83	3.801	3.802
112.70	385.85	3.802	3.802
141.96	415.11	3.927	3.930
142.01	415.16	3.929	3.930
161.34	434.49	4.009	4.006
161.37	434.52	4.009	4.006

Table (18) (cont.)

Run No. 0605 m_{Cl} = 0.005

$t^{\circ}C$	$T^{\circ}K$	$p(a_{H\gamma Cl})$ Exptl	$p(a_{H\gamma Cl})$ Smthd
97.91	371.06	3.757	3.760
97.91	371.06	3.763	3.760
112.18	385.33	3.803	3.807
112.20	385.35	3.806	3.807
122.56	395.71	3.850	3.847
122.58	395.73	3.848	3.847
132.21	405.36	3.890	3.884
132.22	405.37	3.883	3.884
142.34	415.49	3.906	3.918
142.34	415.49	3.918	3.918
151.61	424.76	3.946	3.941
151.63	424.78	3.943	3.941
161.00	434.15	3.961	3.954
161.00	434.15	3.946	3.954

Table (19)

Coefficients of the Data Smoothing Functions and the Standard Errors of the Data about the Curves for Saturated Potassium Hydrogen Tartrate Solutions

$$f(T) = \frac{A}{T} + B + CT + DT^2$$

	$p(a_H\gamma_{Cl})_{0.015}$	$p(a_H\gamma_{Cl})_{0.010}$	$p(a_H\gamma_{Cl})_{0.005}$	$p(a_H\gamma_{Cl})^o$	a
A	1.25344302 E 4	1.42536020 E 4	1.77956254 E 4	2.01224144 E 4	-5.2611952 E 5
B	-8.97039980 E 1	-1.03389479 E 2	-1.33246794 E 2	-1.52322887 E 2	4.3542796 E 3
C	2.27785749 E -1	2.64543502 E -1	3.48037521 E -1	4.00374029 E -1	-1.20251772 E 1
D	-1.80464486 E -4	-2.13748850 E -4	-2.91209878 E -4	-3.39219797 E -4	1.10745392 E -2
σ_D	0.00491	0.00564	0.00607	-	-

Table (20)

Values of $p(a_{H\gamma Cl})(T)_{s,m_{Cl}}$, $a(T)$, $p(a_{H\gamma Cl})(T)^{\circ}$ and Standard Error

for Saturated Potassium Hydrogen Tartrate Solutions

		$p(a_{H\gamma Cl})(T)_{s,m_{Cl}}$					
$t^{\circ}C$	m_{Cl} =	0.015	0.010	0.005	$a(T)$	$p(a_{H\gamma Cl})(T)^{\circ}$	$1.528\sigma_p$
100		3.757	3.760	3.765	-0.83	3.769	0.001
105		3.774	3.775	3.781	-0.71	3.784	0.003
110		3.793	3.792	3.799	-0.52	3.800	0.005
115		3.815	3.811	3.817	-0.25	3.817	0.006
120		3.838	3.832	3.837	+0.12	3.835	0.007
125		3.863	3.854	3.857	0.62	3.852	0.008
130		3.888	3.876	3.876	1.25	3.868	0.008

Table (20) (cont.)

$p(a_{H\gamma Cl})(T)_{s,m_{Cl}}$

$t^{\circ}C$	m_{Cl} = 0.015	0.010	0.005	a(T)	$p(a_{H\gamma Cl})(T)^{\circ}$	$1.528\sigma_p$
135	3.914	3.899	3.894	2.04	3.882	0.006
140	3.940	3.921	3.910	2.99	3.894	0.005
145	3.966	3.943	3.925	4.12	3.904	0.003
150	3.992	3.964	3.938	5.45	3.910	0.001
155	4.017	3.983	3.947	6.98	3.913	0.002
160	4.041	4.001	3.953	8.73	3.911	0.005

Table (21)

Effect of 'ionic radius,' a, (equations (30), (38) and (39)) on the

Ionic Strength, I and log γ^{o}_{Cl} in Saturated Potassium Hydrogen Tartrate Solutions

	I			$-\log \gamma^{o}_{Cl}$		
$t^{o}C$	a = 2.0 A°	4.0 A°	6.0 A°	a = 2.0 A°	4.0 A°	6.0 A°
100	0.0400	0.0399	0.0398	0.093	0.093	0.092
120	0.0398	0.0397	0.0396	0.097	0.097	0.097
140	0.0396	0.0395	0.0394	0.103	0.103	0.103
160	0.0394	0.0393	0.0392	0.109	0.109	0.109

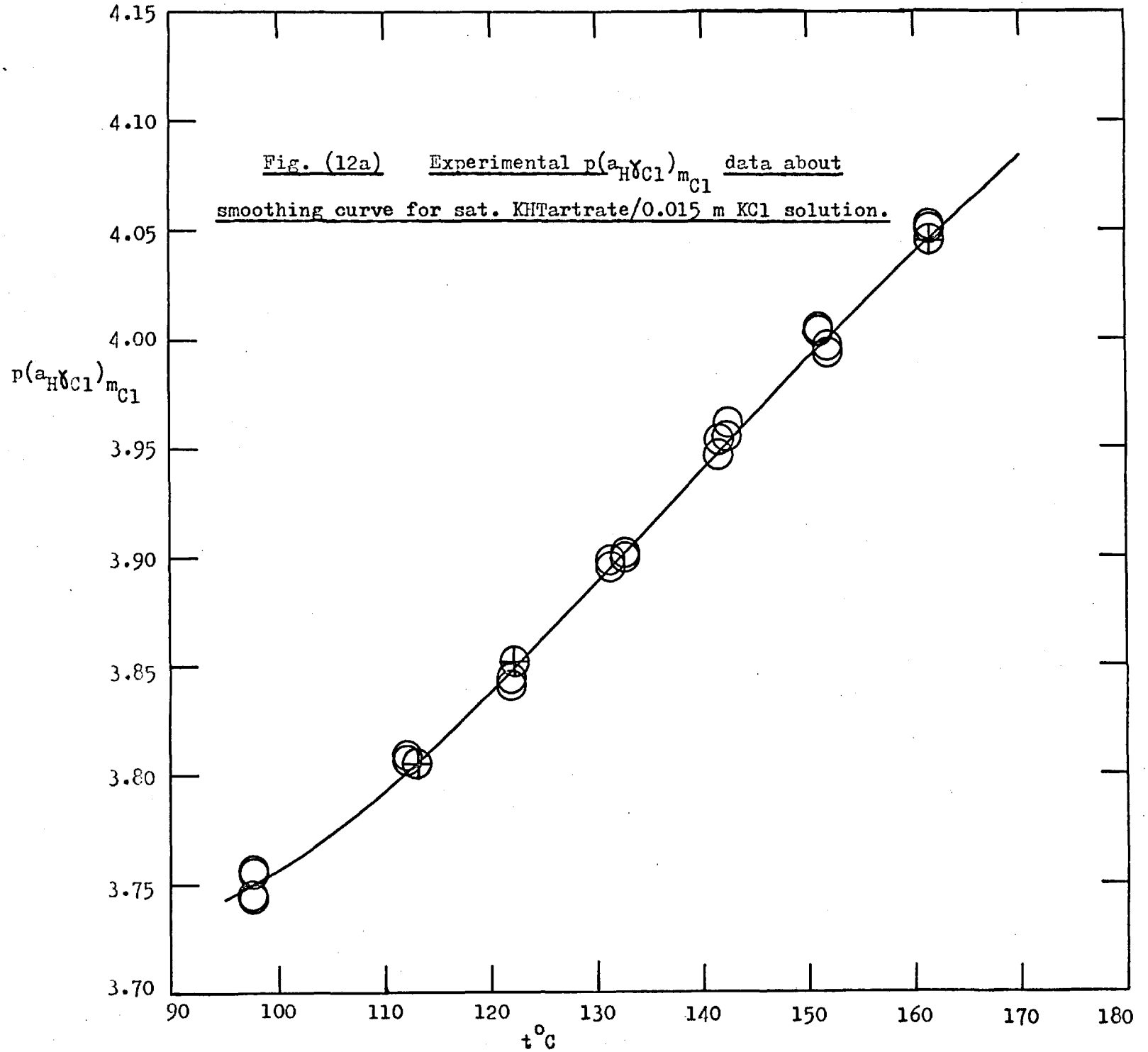


Fig. (12a) Experimental $p(a_{H\gamma Cl})_{m_{Cl}}$ data about smoothing curve for sat. KHTartrate/0.015 m KCl solution.

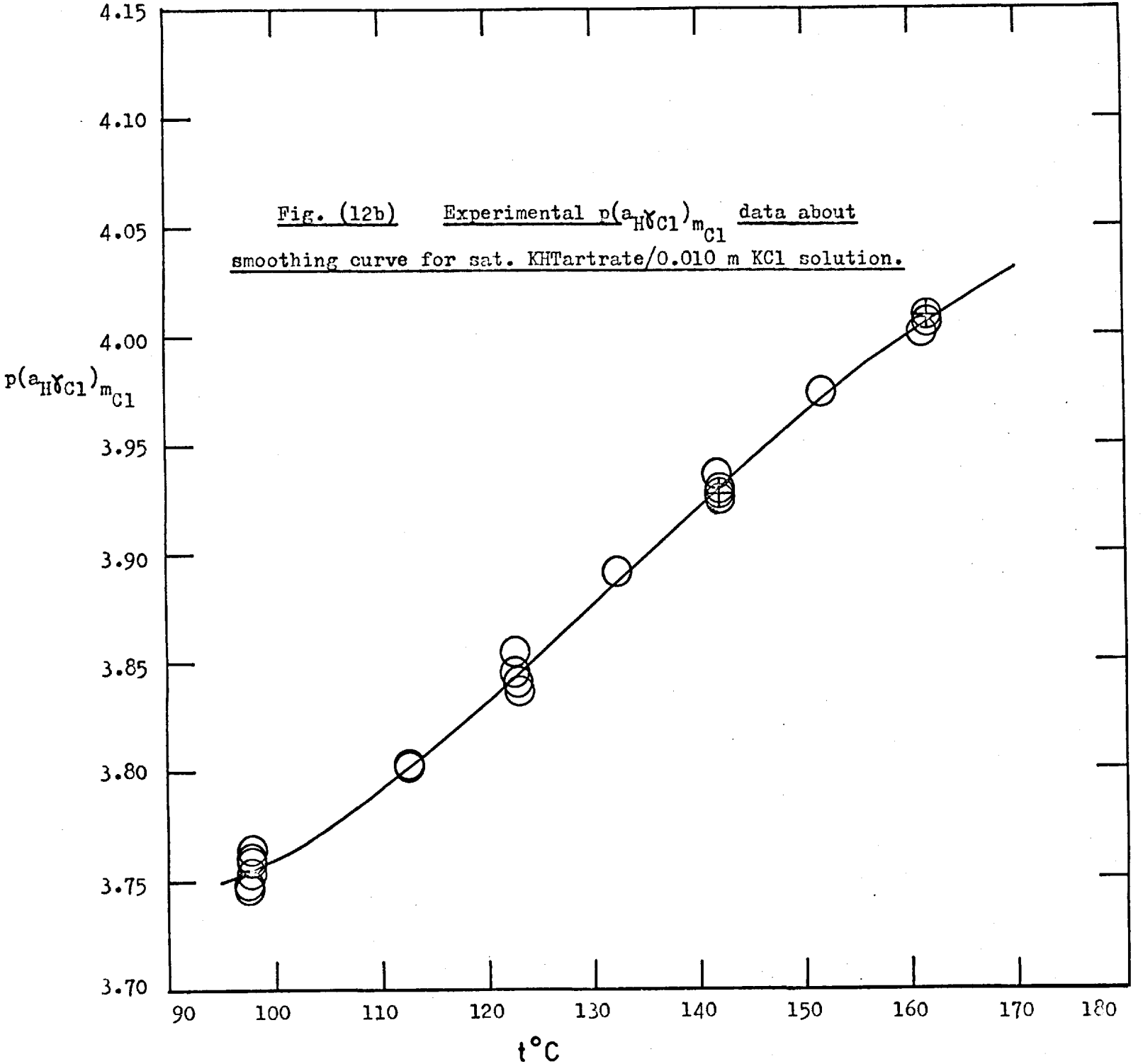


Fig. (12b) Experimental $p(a_{H}\gamma_{Cl})_{m_{Cl}}$ data about smoothing curve for sat. KHTartrate/0.010 m KCl solution.

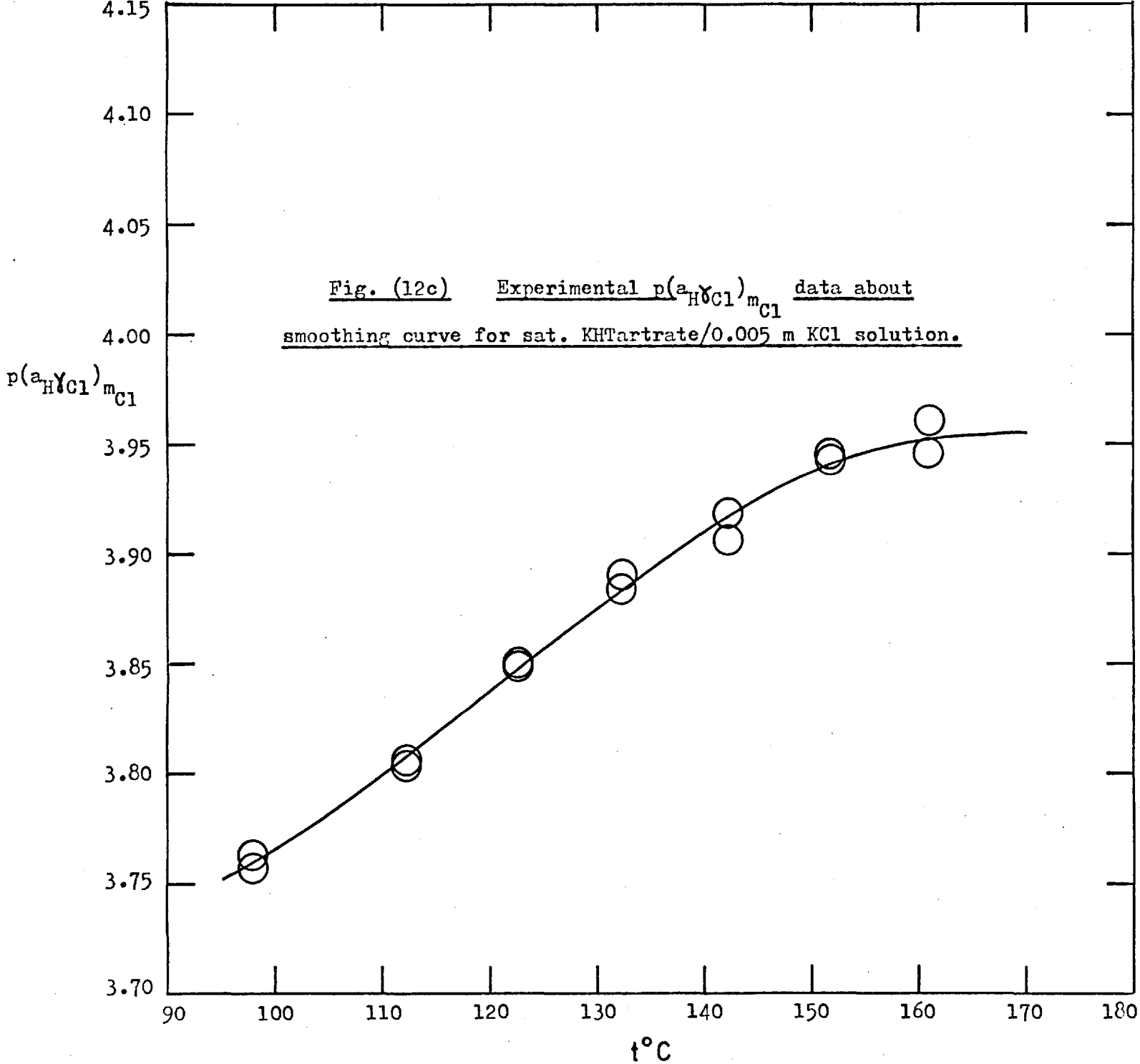


Fig. (12c) Experimental $p(a_{H\gamma Cl})_{m_{Cl}}$ data about smoothing curve for sat. KHTartrate/0.005 m KCl solution.

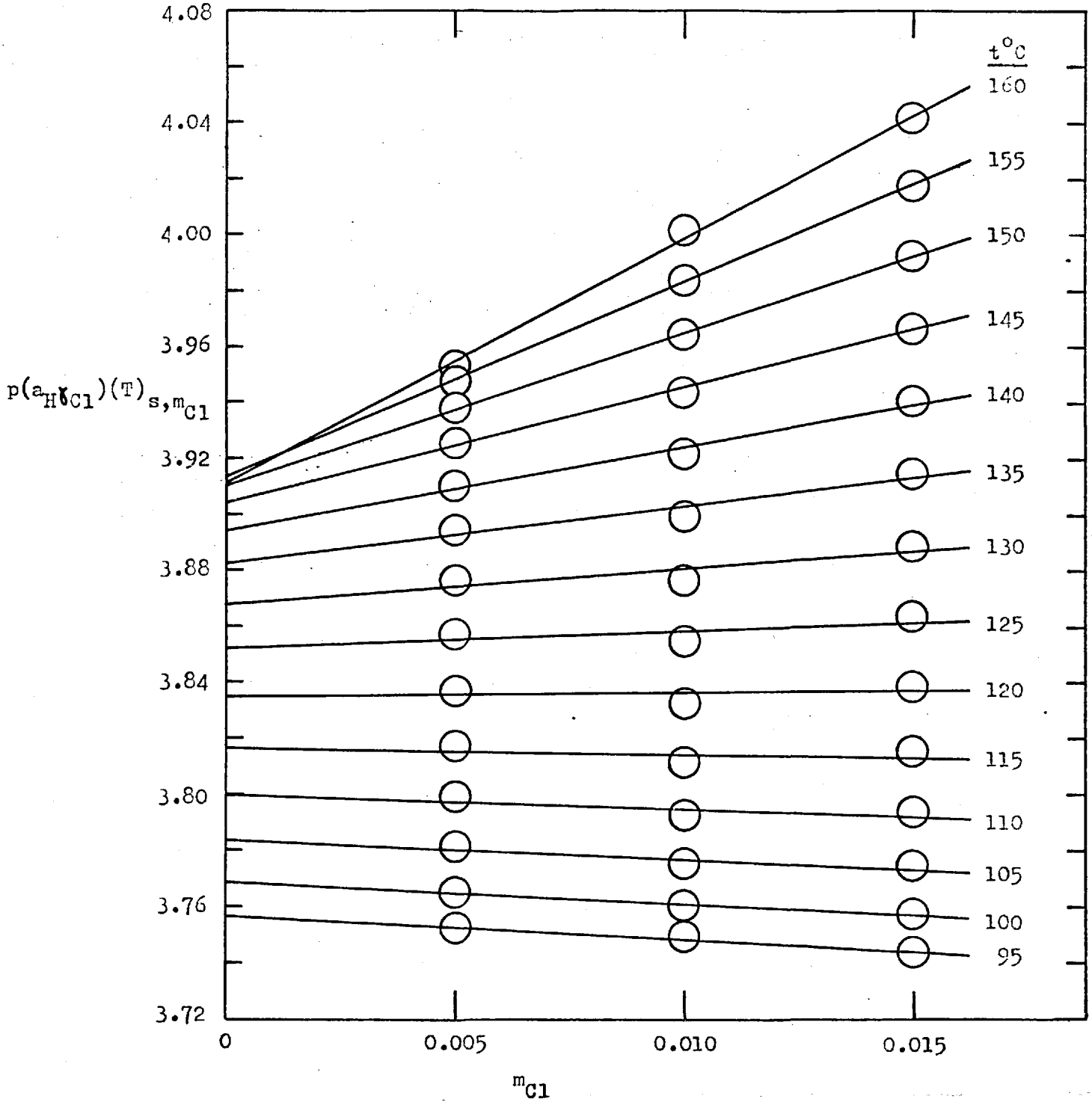


Fig. (13) Extrapolation of $p(a_H\gamma_{Cl})(T)_{s,m_{Cl}}$ to $m_{Cl} = 0$ for saturated (25°C) KHTartrate solution.

Ionic Strength

To calculate the ionic strength the method of Bates, et al,[75] was employed which is similar, in broad outline, to that used for the tetroxalate solution but complicated by the fact that the dissociation constants of tartaric acid are quite small and of similar magnitude (at 25°C, $K_1 = 9.2\ 10^{-4}$ and $K_2 = 4.3\ 10^{-5}$).

It is assumed that in a solution of Potassium Hydrogen Tartrate (KHT) of molality, m*, the dissociation,

$$KHT = K^+ + HT^- \qquad (30)$$

is complete, but that,

$$H_2T = H^+ + HT^- \qquad -- (31)$$

$$HT^- = H^+ + T^= \qquad -- (32)$$

are only partial.

From mass balances in solution

$$m^* = m_K$$

$$m^* = m_{H_2T} + m_{HT} + m_T \qquad -- (33)$$

and from reactions (31) and (32) (ignoring any contribution from water dissociation)

$$m_H = m_T - m_{H_2T} \qquad -- (34)$$

Elimination of m_{H_2T} from between (33) and (34) yields,

$$m_T = \tfrac{1}{2}(m^* - m_{HT} + m_H) \qquad -- (35)$$

Therefore, assuming m_{OH} to be negligible at the pH of the solution, the ionic strength becomes,

$$I = \tfrac{1}{2}(m_K + m_H + m_{HT} + 4m_T)$$

$$= \tfrac{1}{2}(3m^* - m_{HT} + 3m_H) \qquad -- (36)$$

Molality equilibrium constants are now defined for reactions (31) and (32)

$$k_1 = \frac{m_H \cdot m_{HT}}{m_{H_2T}}$$

and $$k_2 = \frac{m_H \cdot m_T}{m_{HT}}$$

and therefore $$\frac{k_2}{k_1} = \frac{m_{H_2T} \cdot m_T}{(m_{HT})^2} \qquad -- (37)$$

Elimination of m_T from between (33) and (34) gives,

$$m_{H_2T} = \tfrac{1}{2}(m^* - m_{HT} - m_H)$$

which on substituting, together with (35), into (37), and noting that $m_H \ll m_{HT}$, yields,

$$\frac{k_2}{k_1} = \left[\frac{m^* - m_{HT}}{2m_{HT}}\right]^2$$

or $$m_{HT} = m^*/(1 + \sqrt{4k_2/k_1})$$

which on substitution into (36) gives,

$$I = m^*(1 + 0.5x) + 1.5m_H \quad \text{— (38)}$$

in which $$x = \frac{\sqrt{4k_2/k_1}}{1 + \sqrt{4k_2/k_1}}$$

The ratio of the molality equilibrium constants is related to the ratio of the thermodynamic equilibrium constants, K_2/K_1 by,

$$\frac{k_2}{k_1} = \frac{K_2 \cdot \gamma_{HT}^2}{K_1 \cdot \gamma_{H_2T} \cdot \gamma_T}$$

The activity coefficients of neutral species in solution are generally taken as unity.[76] (For example, extrapolation of data for sucrose solutions[77] shows that at 0.01 m, γ = 1.0017 and in the present work m_{H_2T} was always ~0.01 m). Also it is assumed that

$$4\log \gamma_{HT} = \log \gamma_T = \frac{-AI^{\frac{1}{2}}}{1 + BaI^{\frac{1}{2}}}$$

and therefore,

$$\log \frac{k_2}{k_1} = \log \frac{K_2}{K_1} + \frac{2AI^{\frac{1}{2}}}{1 + BaI^{\frac{1}{2}}} \quad \text{— (39)}$$

The thermodynamic equilibrium constants were obtained by extrapolating the functions obtained by Bates and Canham [78]

between 0° and $50^{\circ}C$,

$$pK_1 = \frac{1525.59}{T} - 6.6558 + 0.015336\ T$$

$$pK_2 = \frac{1765.35}{T} - 7.3015 + 0.019276\ T$$

The ionic strength was then obtained by substituting the respective value of $p(a_H\gamma_{Cl})^{\circ}$ at each temperature into equation (30) and solving simultaneously with equations (38) and (39) by reiteration.

The calculation was performed using three values for the ionic radius parameter, a, and the results, together with the derived values of $\log \gamma^{\circ}_{Cl}$ (from equation (11)), are given in Table (21) at four different temperatures. It can be seen that I is relatively insensitive to the value of a and that to three figures, $\log \gamma^{\circ}_{Cl}$ is virtually independent of it. Also I is little affected by temperature (Bates, et al.[75] calculated a value of 0.040 at $25^{\circ}C$) and that the change in $\log \gamma^{\circ}_{Cl}$ is virtually entirely due to the temperature dependence of the Debye-Huckel parameter, A. These values, combined with those of $p(a_H\gamma_{Cl})^{\circ}$ in Table (20) lead to the final values of pH_S for the Saturated ($25^{\circ}C$) Potassium Hydrogen Tartrate solution given in Table (22).

These values, together with those of Bates[51] derived from the investigations of Bates, et al.[75] and Bower and Bates[74] are plotted in Fig. (14).

Table (22)

pH_S in Sat. (25°C) KHTartrate Solution

t°C	pH_S
100	3.676
105	3.690
110	3.705
115	3.721
120	3.738
125	3.753
130	3.768
135	3.781
140	3.791
145	3.800
150	3.804
155	3.806
160	3.802

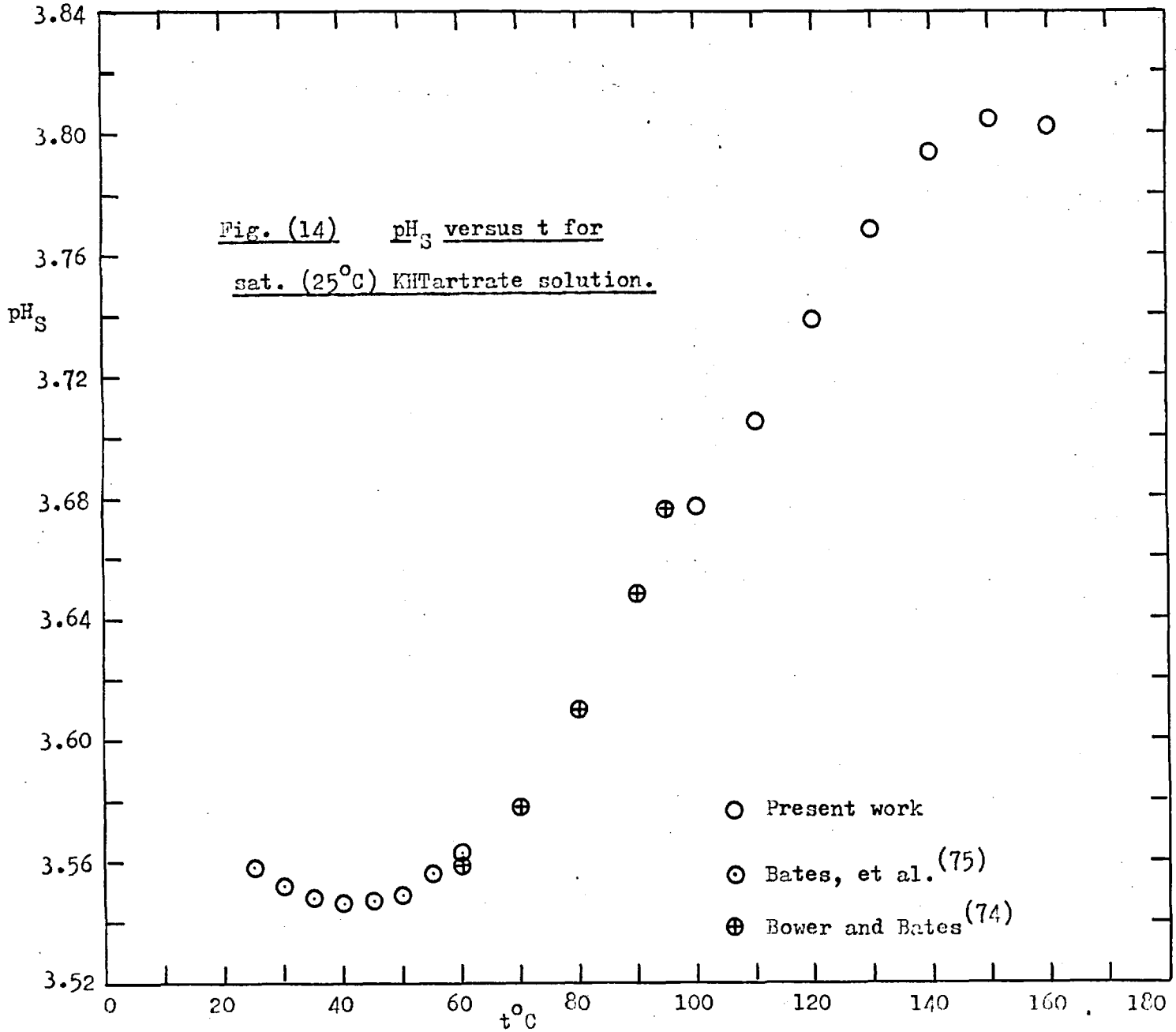


Fig. (14) pH_S versus t for sat. (25°C) KHTartrate solution.

4.4 0.05 m Potassium Hydrogen Phthalate

It has been demonstrated in Section 4.1 that aqueous KHPhthalate solution is stable in air to at least 200°C and may be expected to remain so to considerably higher temperatures. (Solid phthalic acid loses water at 200-230°C forming phthalic anhydride, which is very stable and distils unchanged at 284°C. However, presumably this dehydration would not occur in solution and therefore it seems likely that this buffer is stable to around 300°C). Because of this thermal stability this buffer was used in the very first experimental runs, in which Pd black hydrogen electrodes and unprotected Ag-AgCl electrodes were employed. However, this initial choice of solution proved particularly unfortunate since hydrogen reduction of AgCl and phthalate took place simultaneously leading to results which, although erroneous, were often remarkably consistant from one run to the next.

Firstly it was noticed that the final pH, after cooling, of the experimental solutions was significantly lower (>0.2 units) than that of the original solution. This effect was obviously due to extensive reduction of AgCl (producing HCl, see Appendix B) and led to the design and use of the pyrex/P.T.F.E. protective sheaths around the Ag-AgCl electrodes (see Section 2.5) which were employed in all further runs (including those for the oxalate and tartrate buffers). Subsequent $p(a_{H}\gamma_{Cl})$ data, at temperatures >140°C were indeed different from those previously obtained, but the final pH of the solutions was now rather higher (~0.1 units) than that of the original solution. Since saturated carboxylic acids are generally weaker than the corresponding unsaturated

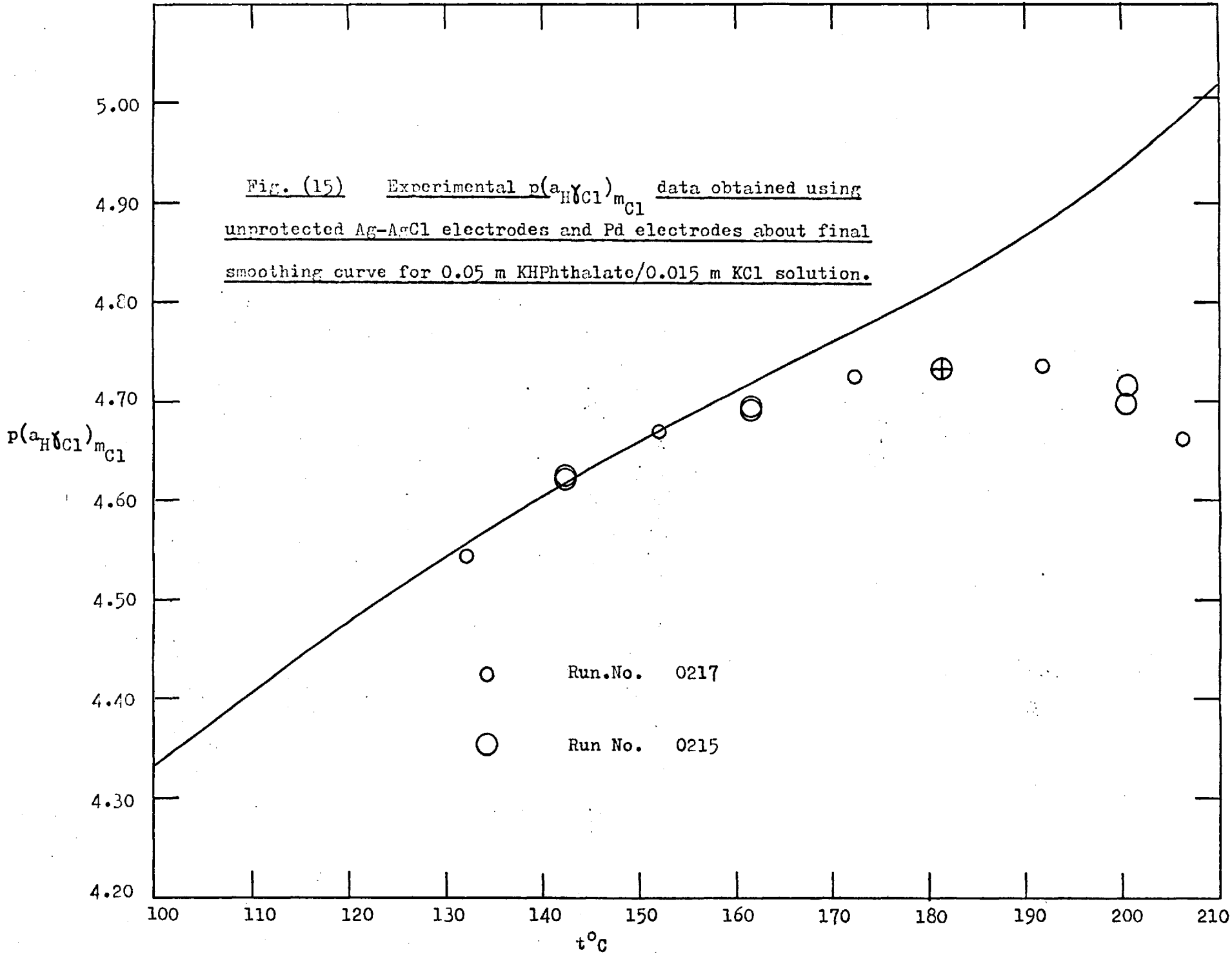
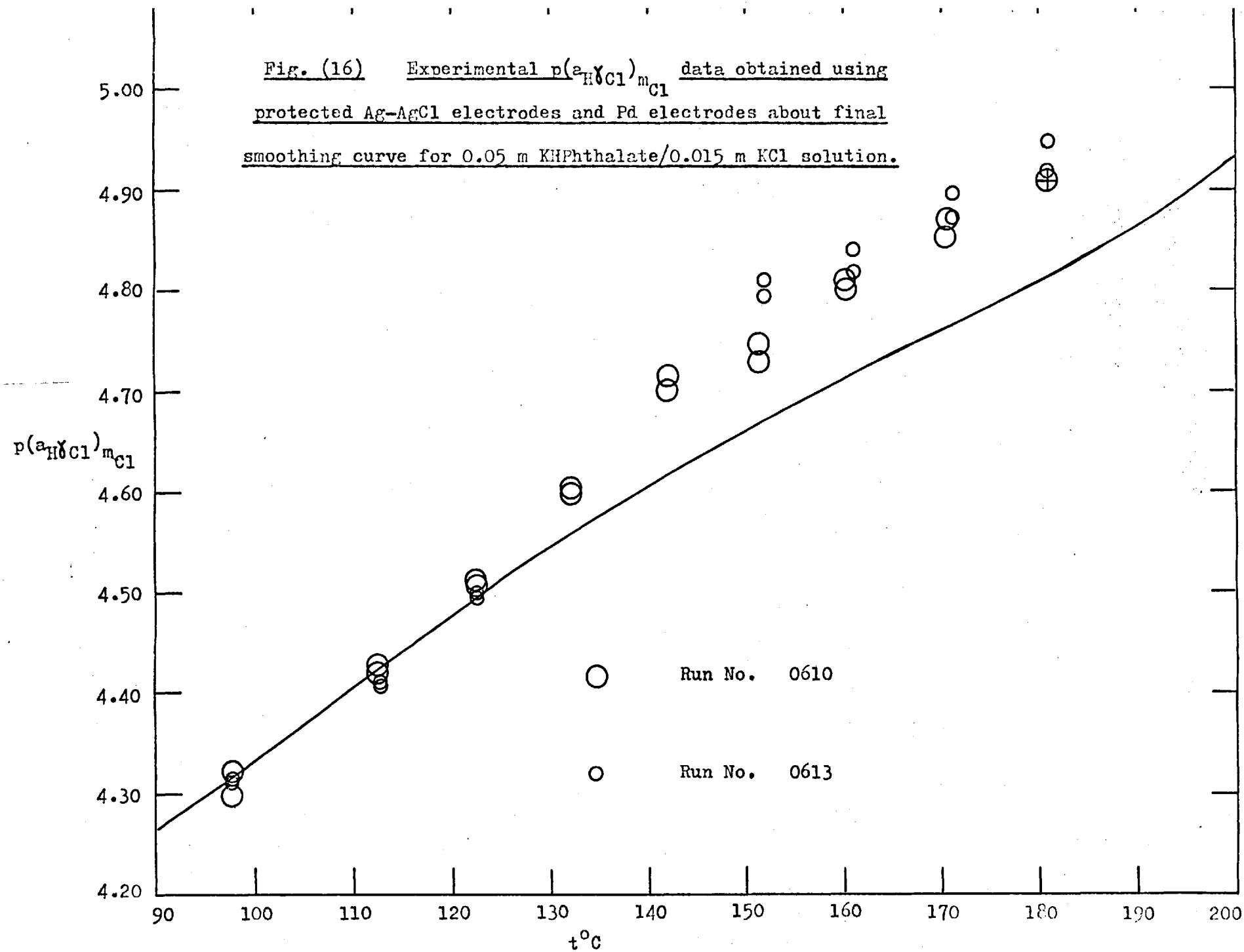


Fig. (15) Experimental $p(a_H\gamma_{Cl})_{m_{Cl}}$ data obtained using unprotected Ag-AgCl electrodes and Pd electrodes about final smoothing curve for 0.05 m KHPhthalate/0.015 m KCl solution.

Fig. (16) Experimental $p(a_{H\gamma Cl})_{m_{Cl}}$ data obtained using protected Ag-AgCl electrodes and Pd electrodes about final smoothing curve for 0.05 m KHPhthalate/0.015 m KCl solution.



compounds, due to the greater 'electron attraction power' of any unsaturated group (in this case the delocalised system of the phthalate ion as compared to the saturated c-hexane ring) this result strongly suggested that hydrogen reduction of phthalate to some c-hexane dicarboxylic acid was occurring, probably catalysed by the Pd black of the hydrogen electrodes. As stated in Section 2.6, Hamer and Acree[32] originally used Pd black electrodes because this very reaction is catalysed by Pt black at room temperature and although Bower and Bates[74] have used Pd electrodes in phthalate solutions up to 95°C it seems that at slightly higher temperatures these too become unusable. To prove this point, 150 ml. of 0.05 m KHPhthalate solution were heated under 60 p.s.i. H_2 pressure with 0.1 g of 10% Pd on Carbon catalyst to 200°C for 1 hour. At room temperature, the final pH of this solution was 0.4 units higher than that of the original solution, whereas when the experiment was repeated, but with no catalyst present, no significant change in pH was observed. These facts led to the use of smooth, Ir hydrogen electrodes (Section 2.6) in all subsequent runs for the phthalate buffer. These electrodes were not totally inert as a hydrogenation catalyst but they did greatly reduce the effect and the final pH of experimental solutions was rarely greater than 0.03 units higher than that of the original solution.

These two effects, relative to the final results obtained for the solution containing 0.015 m KCl are shown in Figs. (15) and (16). In Fig. (15) are shown $p(a_{H}\gamma_{Cl})$ data obtained from two runs using unprotected Ag-AgCl electrodes versus Pd black electrodes together with the final smoothing curve (see below) from data mostly derived from runs using protected Ag-AgCl electrodes and

smooth Ir hydrogen electrodes. It can be seen that extensive AgCl reduction occurs at temperatures >140°C but that there is nevertheless good agreement between the two runs.

Fig. (16) shows data from two runs in which protected Ag-AgCl electrodes versus Pd electrodes were used, together with the same smoothing function and clearly indicates that significant phthalate reduction is occurring at >120°C. Comparison of these two figures shows that at higher temperatures AgCl reduction was great enough as to completely counteract the effect of phthalate reduction, but that between 120° and 140° combination of both effects seems to fortuitously have given results close to the true values.

Despite the protective sheaths around the Ag-AgCl electrodes it was found that AgCl reduction was so extensive in a 0.05 m KHPhthalate/0.005 m KCl solution that reproducible results could not be obtained in this case and therefore measurements were made with m_{Cl} = 0.010, 0.015 and 0.020.

The F ratio test showed that functions with k = 4, equivalent to,

$$p(a_H\gamma_{Cl})_{m_{Cl}} = \frac{A}{T} + B + CT + DT^2 + ET^3$$

were adequate to describe the data. The results are given in Tables (23), (24) and (25) and the corresponding plots in Figs. (17a-c) and (18).

Table (23)

Experimental and Smoothed Values of $p(a_{H}\gamma_{Cl})$ in 0.05 m Potassium Hydrogen Phthalate Solutions

Run No. 0809 m_{Cl} = 0.020

$t^{\circ}C$	$T^{\circ}K$	$p(a_{H}\gamma_{Cl})$ Exptl	Smthd
97.47	370.62	4.329	4.329
97.47	370.62	4.326	4.329
112.35	385.50	4.429	4.427
112.35	385.50	4.426	4.427
122.18	395.33	4.484	4.479
122.18	395.33	4.478	4.479
132.03	405.18	4.524	4.527
141.25	414.40	4.569	4.573

Run No. 0821 m_{Cl} = 0.020

97.81	370.96	4.339	4.332
97.81	370.96	4.335	4.332
112.56	385.71	4.416	4.428
112.56	385.71	4.420	4.428
123.01	396.16	4.476	4.483
123.03	396.18	4.486	4.483
132.38	405.53	4.533	4.529
132.40	405.55	4.551	4.529
141.63	414.78	4.586	4.575
141.65	414.80	4.594	4.515

Table (23) (cont.)

Run No. 0823 m_{Cl} = 0.020

$t^{\circ}C$	$T^{\circ}K$	$p(a_H\gamma_{Cl})$ Exptl	$p(a_H\gamma_{Cl})$ Smthd
142.12	415.27	4.575	4.577
142.10	415.25	4.568	4.577
161.22	434.37	4.680	4.683
161.22	434.37	4.675	4.683
180.78	453.93	4.804	4.805
180.80	453.95	4.793	4.805
200.68	473.83	4.924	4.928
200.73	473.88	4.919	4.928

Run No. 0828 m_{Cl} = 0.020

141.87	415.02	4.589	4.576
141.87	415.02	4.569	4.576
161.26	434.41	4.696	4.683
161.26	434.41	4.678	4.683
180.87	454.02	4.825	4.806
180.87	454.02	4.805	4.806
200.57	473.72	4.948	4.927
200.59	473.74	4.917	4.927

Table (23) (cont.)

Run No. 0904	m_{Cl} = 0.020		
		$p(a_{HCl}\gamma_{Cl})$	
$t^{\circ}C$	$T^{\circ}K$	Exptl	Smthd
141.27	414.42	4.557	4.573
141.28	414.43	4.566	4.573
160.87	434.02	4.668	4.681
160.87	434.02	4.675	4.681
179.79	452.94	4.806	4.799
200.30	473.45	4.905	4.925
200.32	473.47	4.945	4.926
Run No. 0127	m_{Cl} = 0.015		
101.65	374.80	4.335	4.345
Run No. 0213	m_{Cl} = 0.015		
102.64	375.79	4.346	4.352
102.68	375.83	4.346	4.352
122.76	395.91	4.503	4.496
122.78	395.93	4.505	4.496
142.28	415.43	4.631	4.618
142.30	415.45	4.627	4.618
161.63	434.78	4.730	4.718
161.64	434.79	4.723	4.718

Table (23) (cont.)

Run No. 0215	m_{Cl} = 0.015		
		$p(a_{H\gamma_{Cl}})$	
$t^{\circ}C$	$T^{\circ}K$	Exptl	Smthd
142.22	415.37	4.621	4.618
142.23	415.38	4.625	4.618
Run No. 0217	m_{Cl} = 0.015		
132.02	405.17	4.543	4.557
132.05	405.20	4.543	4.557
152.18	425.33	4.668	4.671
152.14	425.29	4.668	4.671
Run No. 0220	m_{Cl} = 0.015		
93.00	366.15	4.294	4.284
93.00	366.15	4.288	4.284
112.30	385.85	4.428	4.425
112.74	385.89	4.430	4.425
132.03	405.18	4.578	4.557
132.02	405.17	4.575	4.557
151.98	425.13	4.694	4.670
151.98	425.13	4.690	4.670

Table (23) (cont.)

Run No. 0610	m_{Cl} = 0.015		
		$p(a_H \gamma_{Cl})$	
t^oC	T^oK	Exptl	Smthd
97.63	370.78	4.321	4.316
97.64	370.79	4.298	4.316
112.37	385.52	4.426	4.422
112.39	385.54	4.416	4.422
122.35	395.50	4.512	4.493
122.35	395.50	4.506	4.493
132.02	405.17	4.597	4.557
132.02	405.17	4.604	4.557
Run No. 0613	m_{Cl} = 0.015		
97.66	370.81	4.312	4.316
97.66	370.81	4.314	4.316
112.59	385.74	4.406	4.424
112.59	385.74	4.410	4.424
122.38	395.38	4.500	4.493
122.40	395.55	4.496	4.493
Run No. 0708	m_{Cl} = 0.015		
97.88	371.03	4.330	4.318
160.99	434.14	4.705	4.715
180.83	453.98	4.832	4.813
190.01	463.16	4.872	4.865

Table (23) (cont.)

Run No. 0710 m_{Cl} = 0.015

$t^{\circ}C$	$T^{\circ}K$	$p(a_H\gamma_{Cl})$ Exptl	$p(a_H\gamma_{Cl})$ Smthd
97.57	370.72	4.337	4.316
131.92	405.07	4.536	4.556
131.92	405.07	4.536	4.556
141.96	415.11	4.592	4.616
141.96	415.11	4.599	4.616
151.37	424.52	4.679	4.667
151.37	424.52	4.676	4.667
170.65	443.80	4.783	4.762

Run No. 0729 m_{Cl} = 0.015

97.77	370.92	4.320	4.317
97.77	370.92	4.300	4.317
112.72	385.87	4.424	4.425
112.73	385.88	4.422	4.425
132.54	405.69	4.532	4.560
132.52	405.67	4.529	4.560
152.21	425.36	4.642	4.671
152.25	425.40	4.648	4.672
171.44	444.59	4.758	4.766
171.44	444.59	4.753	4.766
190.31	463.46	4.861	4.867
190.31	463.46	4.859	4.867

Table (23) (cont.)

Run No. 0828	m_{Cl} = 0.015		
		$p(a_{H}\gamma_{Cl})$	
$t^{o}C$	$T^{o}K$	Exptl	Smthd
141.68	414.83	4.590	4.614
161.19	434.34	4.705	4.716
180.62	453.77	4.807	4.812
Run No. 0201	m_{Cl} = 0.010		
103.00	376.15	4.361	4.376
103.00	376.15	4.353	4.376
113.24	386.39	4.444	4.435
113.10	386.25	4.445	4.435
123.75	396.90	4.505	4.488
123.64	396.79	4.505	4.487
Run No. 0712	m_{Cl} = 0.010		
97.34	370.49	4.355	4.337
97.36	370.51	4.351	4.337
122.23	395.38	4.476	4.480
122.25	395.40	4.476	4.480
141.92	415.07	4.562	4.577
141.92	415.07	4.566	4.577
164.07	437.22	4.685	4.695
164.03	437.18	4.690	4.695
180.34	453.49	4.780	4.780

Table (23) (cont.)

$t^{\circ}C$	$T^{\circ}K$	$p(a_{H}\gamma_{Cl})$ Exptl	$p(a_{H}\gamma_{Cl})$ Smthd
180.34	453.49	4.775	4.780
199.61	472.76	4.833	4.848
199.54	472.69	4.841	4.848
Run No. 0717	m_{Cl} = 0.010		
97.41	370.56	4.326	4.337
112.18	385.33	4.454	4.430
132.03	405.18	4.553	4.528
Run No. 0731	m_{Cl} = 0.010		
122.75	395.90	4.462	4.483
122.75	395.90	4.462	4.483
132.28	405.43	4.516	4.529
132.30	405.45	4.509	4.529
170.68	443.83	4.729	4.731
Run No. 0802	m_{Cl} = 0.010		
150.94	424.09	4.647	4.624
150.94	424.09	4.645	4.624
180.34	453.49	4.790	4.780
180.36	453.51	4.772	4.780
196.78	469.93	4.858	4.842
196.92	470.07	4.837	4.842

Table (23) (cont.)

Run No. 0805	m_{Cl} = 0.010		
		$p(a_H\gamma_{Cl})$	
t^oC	T^oK	Exptl	Smthd
150.97	424.12	4.641	4.624
150.97	424.12	4.605	4.624
179.31	452.46	4.780	4.775
198.63	471.77	4.854	4.846
Run No. 0807	m_{Cl} = 0.010		
97.19	370.34	4.334	4.335
97.19	370.34	4.331	4.335
112.66	385.81	4.435	4.432
112.66	385.81	4.428	4.432
122.59	395.74	4.481	4.482
122.57	395.72	4.479	4.482
132.14	405.29	4.537	4.528
132.14	405.29	4.525	4.528
141.97	415.12	4.593	4.577
141.97	415.12	4.565	4.577
Run No. 0902	m_{Cl} = 0.010		
141.41	414.56	4.577	4.574
141.41	414.56	4.571	4.574
160.67	433.82	4.666	4.676
199.65	472.80	4.852	4.848

Table (24)

Coefficients of the Data Smoothing Functions and the Standard Errors of the Data about the Curves for 0.05 m Potassium Hydrogen Phthalate Solutions

$$f(T) = \frac{A}{T} + B + CT + DT^2 + ET^3$$

	$p(a_{H\gamma Cl})_{0.020}$	$p(a_{H\gamma Cl})_{0.015}$	$p(a_{H\gamma Cl})_{0.010}$	$p(a_{H\gamma Cl})^{\circ}$	a
A	-8.13389152 E 4	6.94251241 E 4	-1.03341863 E 5	-7.14229732 E 4	2.20029479 E 6
B	7.68892293 E 2	-6.83348182 E 2	9.96725385 E 2	7.02506137 E 2	-2.27833092 E 4
C	-2.69439766 E 0	2.53083133 E 0	-3.57606049 E 0	-2.56903652 E 0	8.81662827 E 1
D	4.21114257 E -3	-4.11216747 E -3	5.72298008 E -3	4.20840799 E -3	-1.51183751 E -1
E	-2.45417483 E -6	2.49879297 E -6	-3.42376151 E -6	-2.58076114 E -6	9.6958668 E -5
σ_D	0.01106	0.01666	0.01376	-	-

Table (25)

Values of $p(a_H\gamma_{Cl})(T)_{s,m_{Cl}}$, $a(T)$, $p(a_H\gamma_{Cl})(T)^\circ$ and Standard Error

for 0.05 m Potassium Hydrogen Phthalate Solutions

		$p(a_H\gamma_{Cl})(T)_{s,m_{Cl}}$					
$t^\circ C$	m_{Cl} =	0.020	0.015	0.010	$a(T)$	$p(a_H\gamma_{Cl})(T)^\circ$	$2.198\sigma_p$
100		4.349	4.333	4.356	-0.73	4.357	0.035
105		4.383	4.369	4.389	-0.55	4.388	0.031
110		4.414	4.405	4.418	-0.40	4.418	0.020
115		4.442	4.441	4.444	-0.27	4.447	0.004
120		4.468	4.477	4.469	-0.18	4.474	0.015
125		4.493	4.511	4.494	-0.12	4.501	0.031
130		4.517	4.544	4.518	-0.08	4.527	0.048
135		4.541	4.575	4.542	-0.07	4.554	0.060
140		4.566	4.605	4.567	-0.05	4.580	0.069
145		4.592	4.633	4.592	-0.03	4.606	0.074

Table (25) (cont.)

		$p(a_{H\gamma_{Cl}})(T)_{s,m_{Cl}}$					
$t^{o}C$	m_{Cl} =	0.020	0.015	0.010	a(T)	$p(a_{H\gamma_{Cl}})(T)^{o}$	$2.198\sigma_{p}$
150		4.619	4.660	4.619	+0.02	4.632	0.074
155		4.647	4.686	4.645	0.12	4.657	0.072
160		4.676	4.710	4.673	0.29	4.682	0.064
165		4.706	4.735	4.700	0.55	4.705	0.057
170		4.736	4.759	4.727	0.94	4.727	0.049
175		4.768	4.783	4.753	1.47	4.746	0.040
180		4.800	4.809	4.778	2.18	4.763	0.036
185		4.832	4.836	4.801	3.11	4.776	0.035
190		4.864	4.865	4.821	4.29	4.785	0.040
195		4.894	4.897	4.837	5.75	4.790	0.057
200		4.924	4.933	4.848	7.53	4.789	0.084

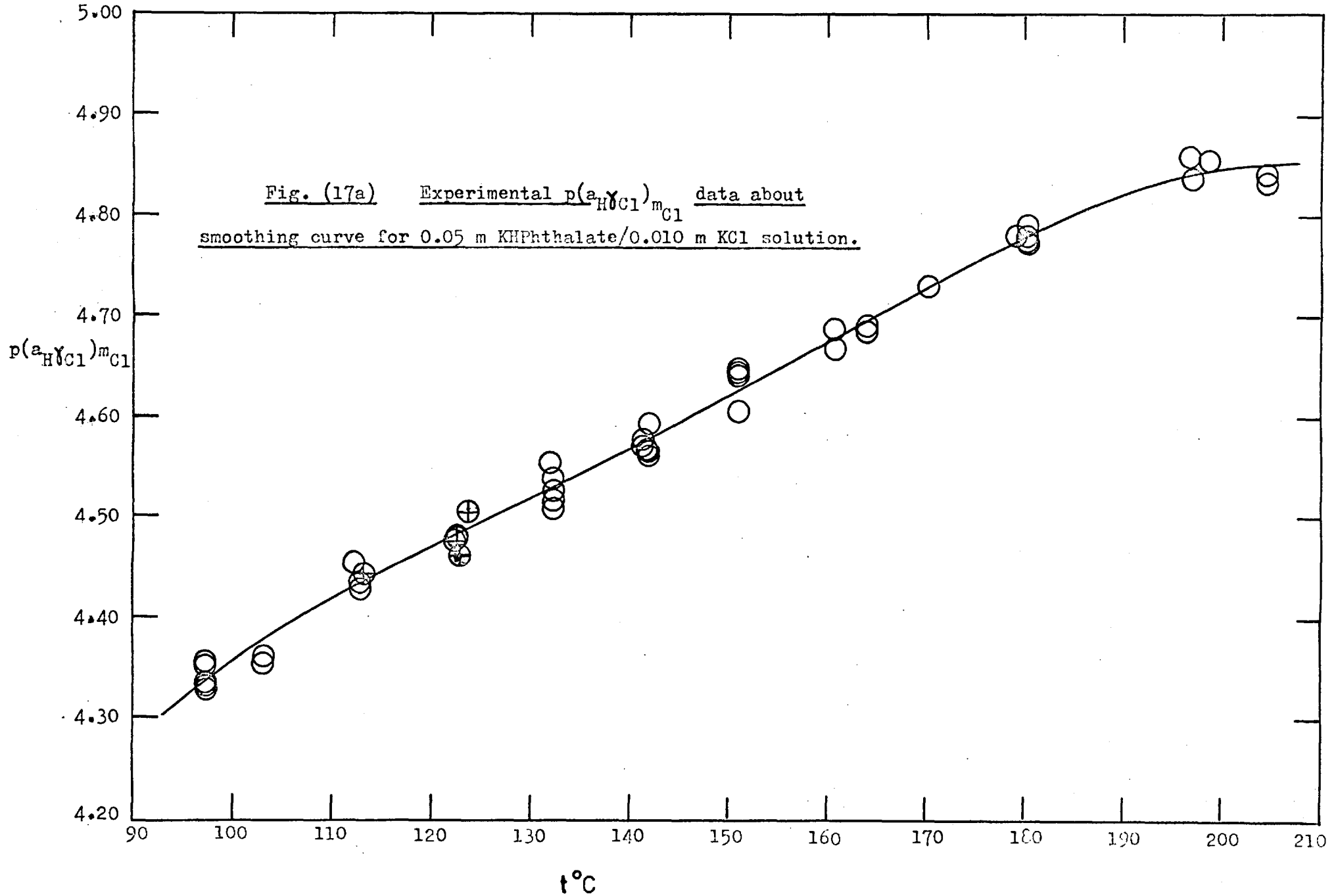


Fig. (17a) Experimental $p(a_{H\gamma Cl})_{m_{Cl}}$ data about smoothing curve for 0.05 m KHPhthalate/0.010 m KCl solution.

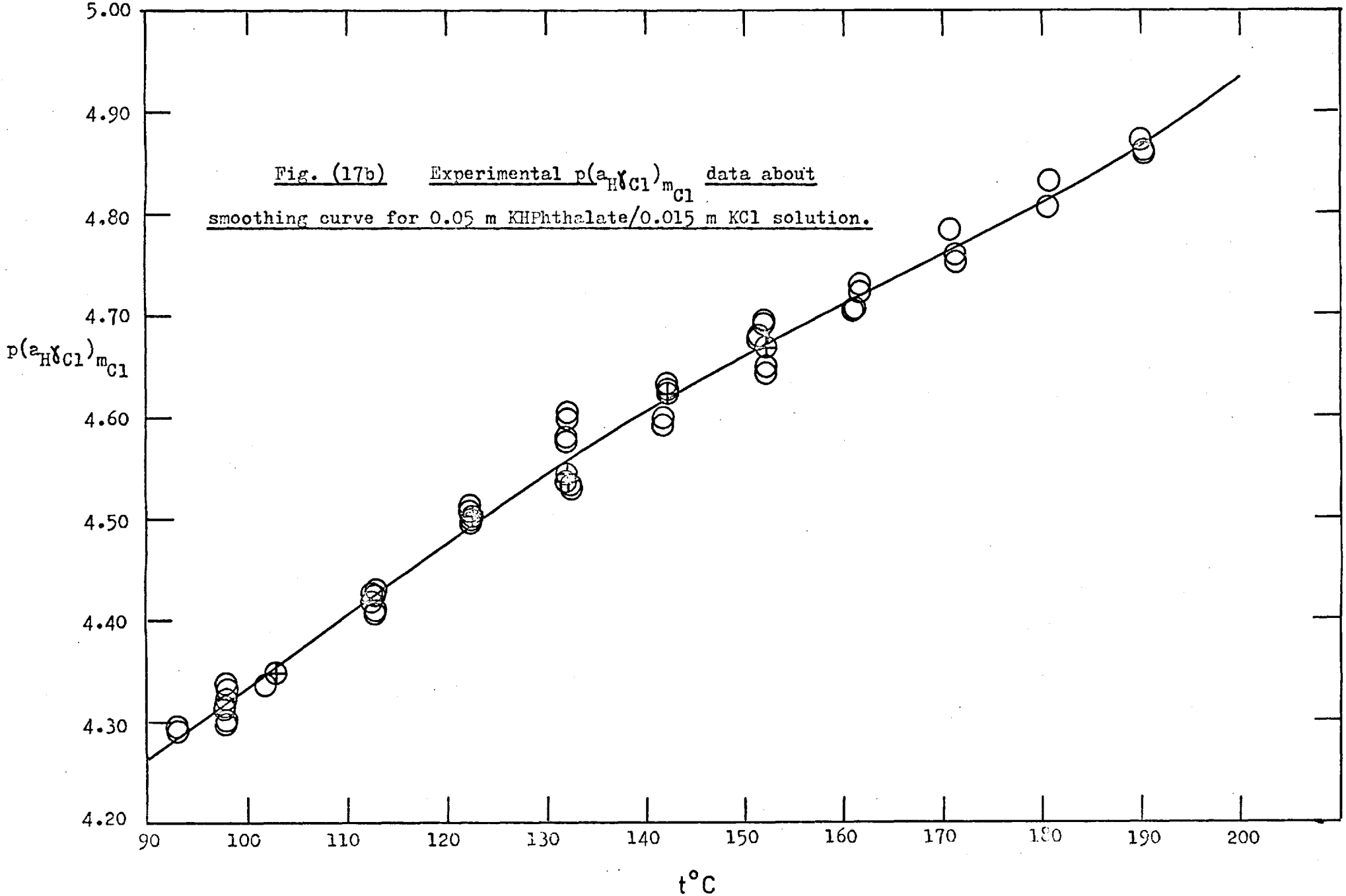


Fig. (17b) Experimental $p(a_H\gamma_{Cl})_{m_{Cl}}$ data about smoothing curve for 0.05 m KHPhthalate/0.015 m KCl solution.

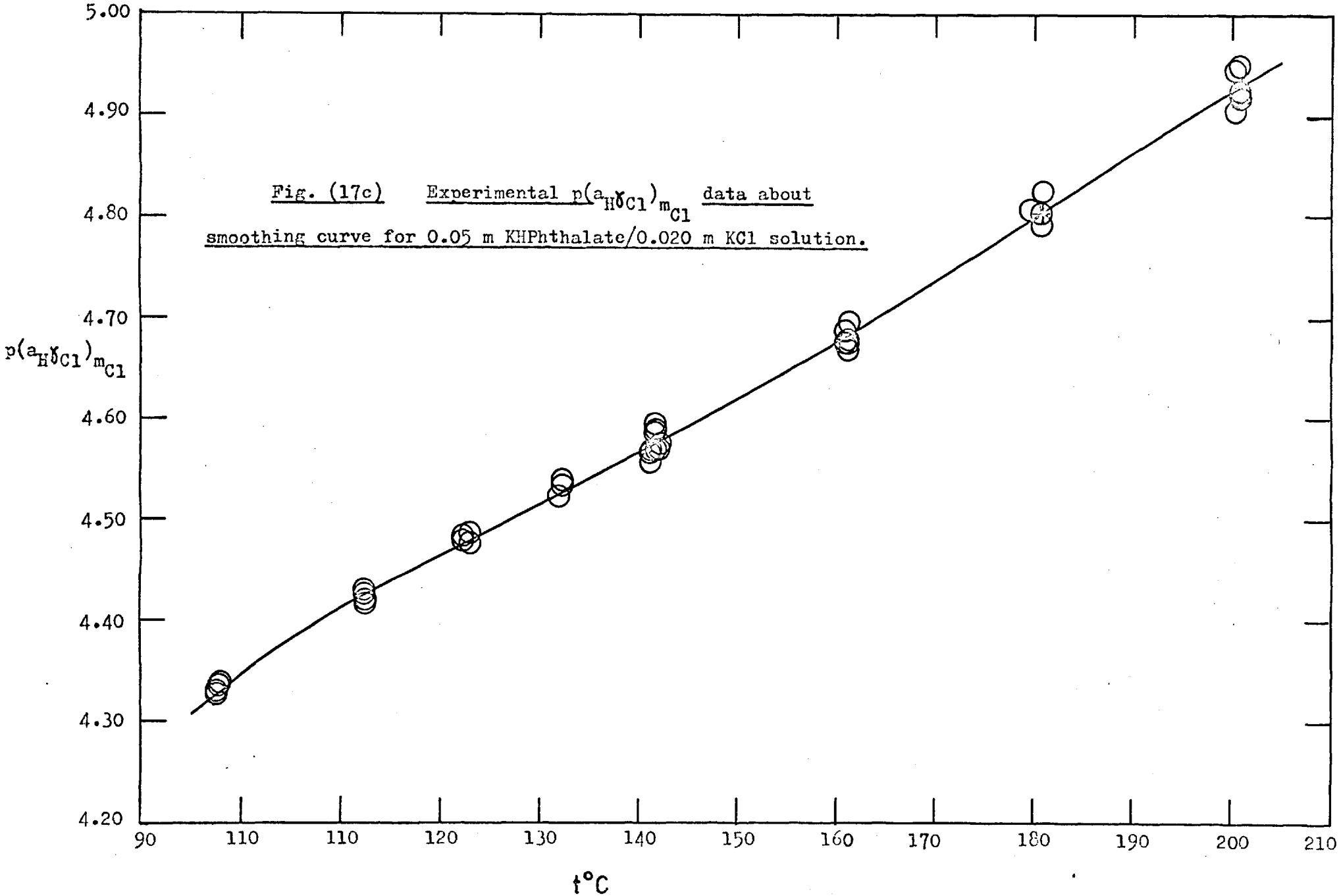


Fig. (17c) Experimental $p(a_{H\gamma Cl})_{m_{Cl}}$ data about smoothing curve for 0.05 m KHPhthalate/0.020 m KCl solution.

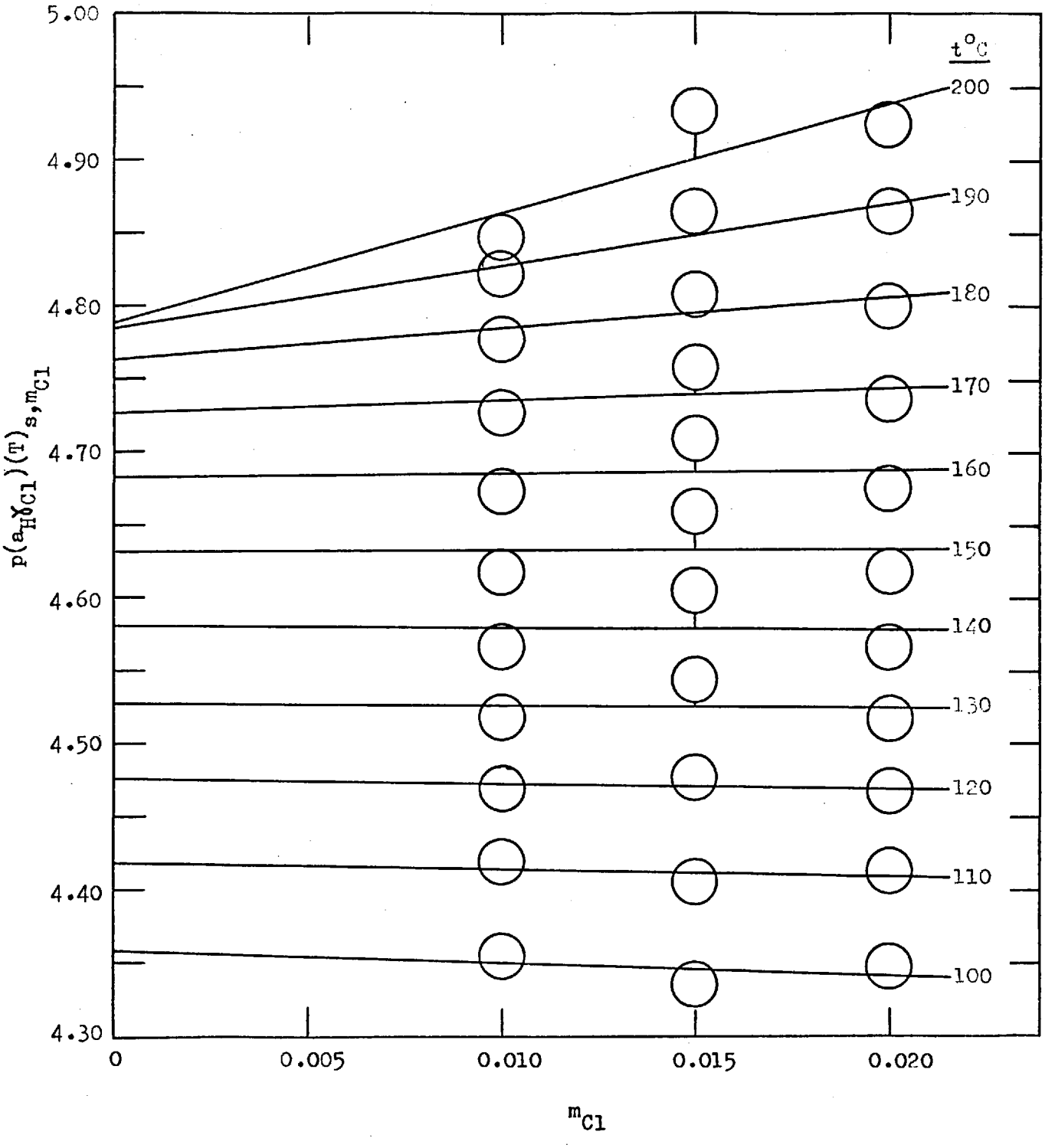


Fig. (18) Extrapolation of $p(a_H\gamma_{Cl})^{(T)}_{s,m_{Cl}}$ to $m_{Cl} = 0$ for 0.05 m KHPhthalate solution.

Ionic Strength

The ionic strength of a solution of KHPhthalate (KHPh) is given by (ignoring m_{OH})

$$I = \tfrac{1}{2}(m_K + m_H + m_{HPh} + 4m_{Ph}) \qquad \text{— (40)}$$

The values of m_H, m_{HPh}, m_{Ph} (and m_{H_2Ph}) in 0.001-0.2 m KHPhthalate solutions between 0° and 60°C have been obtained by Hamer, et al.[79] from detailed calculations using the first and second dissociation constants of o-phthalic acid[76,80] and by assuming that the activity coefficients of H^+, Cl^-, HPh^- and $Ph^=$ are given by,

$$\log \gamma_i = \frac{-AZ_i^2 I^{\frac{1}{2}}}{1 + 3.76BI^{\frac{1}{2}}} - \beta_i m_i$$

in which β_i is a constant (dependent on temperature) for each ion. The value of 3.76 ($\pm$0.07) Å for the ionic radius parameter was chosen by Hamer and Acree[80] in order to make pK_2 (for phthalic acid) a linear function of the ionic strength. It was also these authors who showed that the extra term ($\beta_i m_i$) in the Debye-Huckel expression was necessary in order to adequately describe the dependence of activity coefficients and pH on the ionic strength of phthalate solutions. They determined values of β_i for the various ions from 0° to 60°C, e.g. at 25°C, $\beta_{Cl^-} = -0.10$, $\beta_{HPh^-} = -0.023$ and $\beta_{Ph^=} = -0.38$.

Substitution of m_H, etc in 0.05 m KHPhthalate solution, into equation (40) gives the values for I shown in Table (26). They go through a maximum at 30°C and then decrease with increasing

Table (26)

Ionic Strength of 0.05 m KHPhthalate Solution

$t^{\circ}C$	I	$t^{\circ}C$	I
0	0.05318	35	0.05337
5	0.05324	40	0.05336
10	0.05329	45	0.05333
15	0.05332	50	0.05329
20	0.05335	55	0.05325
25	0.05337	60	0.05321
30	0.05337	-	-

temperature. However the change is very small, only 0.00004 units between 50-55° and 55-60° and extrapolation on this basis gives at 100°C, 0.05289 and at 200°C, 0.05209. An average value of 0.05250 was therefore assumed across this temperature range which on substitution into equation (11) gives log γ°_{Cl}. These values combined with those of $p(a_H\gamma_{Cl})^{\circ}$ from Table (25) give the final values of pH_S for the 0.05 m Potassium Hydrogen Phthalate solution shown in Table (27).

These values, together with those of Bates[51] derived from the investigations of Hamer and Acree[80] and Bower and Bates[74] are plotted in Fig. (19).

Table (27)

pH_S in 0.05 m KHPhthalate Solution

$t^{\circ}C$	pH_S
100	4.254
105	4.284
110	4.313
115	4.340
120	4.366
125	4.391
130	4.416
135	4.441
140	4.465
145	4.490
150	4.514
155	4.537
160	4.560
165	4.582
170	4.602
175	4.619
180	4.633
185	4.645
190	4.651
195	4.654
200	4.651

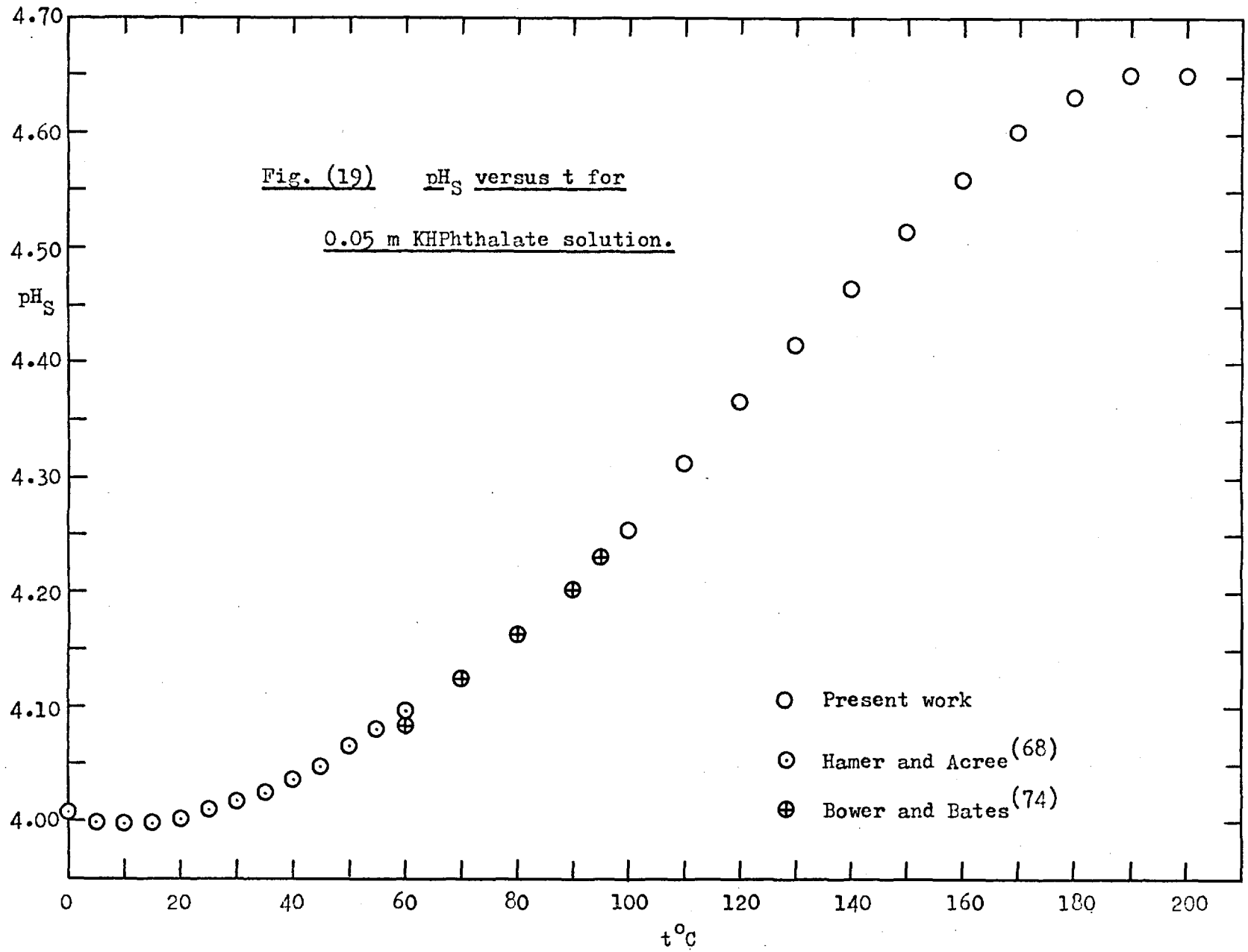


Fig. (19) pH_S versus t for 0.05 m KHPhthalate solution.

4.5 0.025 m Potassium Dihydrogen Phosphate - 0.025 m Disodium Hydrogen Phosphate

An attempt to calibrate this buffer solution containing 0.015 m KCl was made using sheathed Ag-AgCl electrodes and Pd black hydrogen electrodes. However, catastrophic reduction of AgCl occurred and despite the sheaths the final pH of the cooled solution was over 0.05 units lower than that of the original. During the run the buffer was heated to 200°C but inspection of the $p(a_{H}\gamma_{Cl})$ data showed quite clearly that severe reduction had already taken place by 120°C. Work on this solution was therefore abandoned and none attempted on those of higher pH.

4.6 Accuracy and Comparison with Previous Work

The accuracy of the pH_S values is rather difficult to determine. Most of the error in calculating pH_S from $p(a_{H}\gamma_{Cl})^{\circ}$ by equation (11) will derive from uncertainty in the value estimated for the ionic strength. A 10 % error (which should be the maximum) with I = 0.05 leads to an uncertainty of 0.003-0.004 units in pH_S between 100-200°C.

The sources of experimental errors in $p(a_{H}\gamma_{Cl})$ can be seen in equation (8). The cell's potential could be measured to better than 0.1 mV (=0.001 pH units) and another 0.1 mV is allowed for Greeley's values of $E^{\circ}_{Ag-AgCl}$. The temperature was probably accurate to 0.1° (=0.001 units). The error in P_{H_2} is derived from the gauge (0.5 p.s.i.) and also, at higher

temperatures, from an uncertainty in the value of P_{H_2O} (0.5 p.s.i.) due to temperature error. Errors in the barometric pressure are negligible. A further 0.005 pH units is allowed for R and F giving a total on 0.015 units.

The standard error ($1.528\sigma_p$ or $2.198\sigma_p$) of $p(a_H\gamma_{Cl})^\circ$ is merely a measure of the scatter of the data and could certainly be reduced somewhat by further measurements.

Total maximum uncertainties of 0.025, 0.028 and 0.09 units are estimated for the Tetroxalate, Tartrate and Phthalate solutions respectively, the high last value being due to the wide scatter of the data in this case.

Agreement with Bates at 95-100° is regarded as quite satisfactory. pH_S values extrapolated from the present work to 95°C for Tartrate and Phthalate are 0.010 units lower than those of Bates. That for Tetroxalate is 0.027 units lower, which is rather surprising since this data has the lowest standard error.

There is no directly comparable previous data on these solutions. Lepeintre[11] obtained for the Tartrate buffer, at 100, 125 and 150° pH values of 3.68, 3.80 and 3.95 (cf. 3.676, 3.753, and 3.804) using the cell,

$$Pt(H_2)\left|0.01\ m\ HCl\right|\left|\ KCl\ (Sat.\ 25^\circ C)\right|\left|\ Buffer\right|Pt(H_2)$$

and assumed $\gamma_{H^+} = \gamma_{\pm HCl}$. Liquid junction potentials were assumed to cancel but Lepeintre suggestsan accuracy of 0.1 units.

Kryukov, et al[12] obtained values for this solution at these temperatures of 3.69, 3.79 and 3.92 from consecutive, independent measurements on the cells,

$$Pt(H_2)\,|\,0.1\text{ m HCl}\,\|\,\text{Thallium Ref. Electrode}$$

$$Pt(H_2)\,|\,\text{Buffer}\,\|\,\text{Thallium Ref. Electrode}$$

and assuming Greeley's values for the pH of 0.1 m HCl at elevated temperatures[13]. Junction potentials were assumed to cancel. His values at the same temperatures for the pH of the Phthalate solution, 4.24, 4.37 and 4.50 compare rather favourably with those obtained in the present work, 4.254, 4.391 and 4.514. General comparison between all these results is, however, rather difficult since different conventional definitions of the pH have been employed.

4.7 Standard Buffers at Elevated Temperatures

The situation regarding the use of the six standard buffers, A-F, in Table (11), at elevated temperatures can now be summed up as follows. The Tetroxalate and Tartrate solutions can be calibrated but both decompose at relatively low temperatures. The Phthalate solution is thermally very stable and an ideal buffer but subject to reduction by H_2 during its calibration. Phosphate and Borate buffers are probably also satisfactory to high temperatures but their pH is too high for Ag-AgCl electrodes to be used as reference electrodes during their calibration.

The calibration of these latter two buffer solutions at elevated temperatures using a cell not involving a liquid-liquid junction will have to await the development of a suitable stable reference electrode (see Appendix B). The Phthalate

solution can probably also be calibrated to higher temperatures but a particularly inert hydrogen electrode will have to be used. The decomposition of the Tetroxalate buffer is particularly inconvenient in that very few strong, thermally stable, dibasic acids exist which could be used. The most obvious choice is sulphuric acid (pK_2 = 1.98 at 25°C) and a solution of $KHSO_4$ would certainly be satisfactory. (The reason that such a solution has not been used before as a buffer is probably that potassium and sodium bisulphates are very deliquescent and standard solutions are therefore difficult to prepare. However, the choice is so limited in this case that this disadvantage will have to be accepted). This would require a detailed study of the aqueous thermodynamics of H_2SO_4 at elevated temperatures preferable in conjunction with a sulphate based reference electrode.

5. SYMBOLS AND THE PHYSICAL CONSTANTS

Most symbols are defined in the text close to their first appearance in an equation, however, the following general conventions are observed throughout the thesis.

T	Temperature in Kelvin.
t	Temperature in ^{o}C.
c_i	Concentration of i ($m.l.^{-1}$).
M	Molarity ($m.l.^{-1}$).
m_i	Molality of i ($m.kg.^{-1}$).
a_i	Activity of i (invariably $m.kg.^{-1}$).
γ_i	Activity coefficient of i.
x_i	Mole fraction of i.
P_i, p_i	Pressure of i.
f_i	Fugacity of i.
ϕ^o	A function, ϕ, in the prescribed standard state.
$\phi(T)$	A function, ϕ, is a function of T.
I	Ionic Strength (invariably $m.kg.^{-1}$).
E	E.M.F., potential.
log	Logarithm to base 10.
ln	Logarithm to base e.
K	Thermodynamic equilibrium constant.
A, B	Debye-Huckel constants (on molal scale).
N, R, F	Avogardro Number, Gas Constant and Faraday.
e	Electron charge.
Z_i	Valence of ion, i.
σ	Standard error, standard deviation.
$p(\phi)$	$-\log(\phi)$

— (n) Reference number of an electrochemical cell, chemical reaction or identity. No distinction is made between these three for this purpose and numbering is consecutive throughout the thesis.

| Phase boundary in an electrochemical cell.

|| Liquid-liquid junction in an electrochemical cell.

The following values for the physical constants were taken from Taylor, et al[81]

$e = 4.803250\ 10^{-10}$ e.s.u.

$N = 6.022169\ 10^{23}$ $m.^{-1}$

$k = 1.380622\ 10^{-16}$ $erg.deg.^{-1}$

$F = 9.64867\ 10^{4}$ $coulomb.m.^{-1}$

$R = 8.31434$ $J.m.^{-1}deg.^{-1}$

also $\ln 10 = 2.50259$ and therefore

$(R/F).\ln 10 = 0.000198416$ $deg.^{-1}$

To convert p.s.i. to atmospheres: 1 atm. = 14.6960 p.s.i.

6. REFERENCES

(1) Bates, R.G. Determination of pH; Theory and Practice, 2nd Ed. (1973). John Wiley and Sons.

(2) Guggenheim, E.A. The Conceptions of Electrical Potential Difference between Two Phases and the Individual Activities of Ions; I and II. J. phys. Chem. (1929), 33 842-849, ibid, (1930), 34, 1541-1543

(3) Frank, H.S. Single Ion Activities and Ion-Solvent Interaction in Dilute Aqueous Solution. J. phys. Chem. (1963), 67, 1554-1558

(4) Oppenheim, I. Single Electrode Potentials J. phys. Chem. (1964), 68, 2959-2961

(5) Guggenheim, E.A. Studies of Cells with Liquid-Liquid Junctions. Pt. II. Thermodynamic Significance and Relationship to Activity Coefficients. J. phys. Chem. (1930), 34, 1758-1766

(6) Bates, R.G. and Guggenheim, E.A. Report on the Standardisation of pH and Related Terminology. Pure appl. Chem. (1960-1961), 1, 163-168

(7) Hitchcock, D.I. A Measure of Acidity Obtained from the Electromotive Force of a Cell Without Liquid Junction. J. Am. chem. Soc. (1936), 58, 855-856

(8) Bates, R.G. Definition of pH Scales. Chem. Revs. (1948), 42, 1-61

(9) Bates, R.G. and Smith, E.R. Standardisation of the pH Scale. J. Wash. Acad. Sci. (1948), 38, 61-66

(10) Stene, S. Ueber die Bestimmung von pH bei Temperaturen ueber 100°C. Rec. Trav. Chim. Pays-Bas. (1930), 49, 1133-1145

(11) Le Peintre, M.M. Mesure du pH sous Pression et a Temperature Elevee. Soc. Franc. Elect. Bull. (1960), 1, 584-591

(12) Kryukov, P.A., Perkovets, V.D., Starostina, L.I. and Smolyakov, B.S. Standardisation of pH Values of Buffer Solutions at Temperatures to 150°C. Izv. Sib. Otd. Akad. Nauk. SSSR. Ser. Khim. Nauk. (Bull. Siberian Dept. of the Acad. for Sci. SSSR. Series for Chem. Science. which later becomes Siberian J. Chem.) (1966), 7, 29-34

(13) Greeley, R.S. An Operationally Defined pH Scale from 25 to 275°C. Anal. Chem. (1960), 32, 1717-1718

(14) International Thermocouple Reference Tables. Part 3 Iron/Copper-nickel Thermocouples Type J. B.S. 4937: Pt. 3, (1973)

(15) Stimson, H.F. International Practical Temperature Scale of 1948; Text Revision of 1960. J. Res. natn. Bur. Stand. (1961), 65A, 139-145

(16) International Practical Temperature Scale of 1968. Metrol. (1969), 5, 35-44

(17) Ives, D.J.D. and Janz, G.J. Reference Electrodes. (1961) Academic Press

(18) Taniguchi, H. and Janz, G.J. Preparation and Reproducibility of the Thermal-Electrolytic Silver-Silver Chloride Electrode. J. electrochem. Soc. (1957), 104, 123-127

(19) Rule, C.K. and La Mer, V.K. Thermal Type Silver-Silver Chloride Electrodes. J. Am. chem. Soc. (1936), 58, 2339-2340

(20) Raridon, R.J. Measurements of Temperature Coefficients in Aqueous Solutions up to 200°C using Packed Column Techniques. Ph.D. Thesis, Vanderbilt Univ. Tenn. (1959)

(21) Harned, H.S. and Ehlers, R.W. The Thermodynamics of Aqueous Hydrdrochloric Acid Solutions from Electromotive Force Measurements. J. Am. chem. Soc. (1933), 55, 2179-2194

(22) Harned, H.S. and Paxton, T.R. The Thermodynamics of Ionised Water in Strontium Chloride Solutions from Electromotive Force Measurements. J. phys. Chem. (1953), 57, 531-535

(23) Bates, R.G. and Bower, V.E. Standard Potential of the Silver-Silver Chloride Electrode from 0 to 95°C and the Thermodynamic Properties of Dilute Hydrochloric Acid Solutions. J. Res. natn. Bur. Stand. (1954), 53, 283-290, RP. 2546

(24) Lietze, M.H. and Vaughen, J.V. The Behaviour of the Silver, Silver Chloride and the Mercury, Mercurous Chloride Electrodes at High Temperatures. J. Am. chem. Soc. (1955), 77, 876-878

(25) Roychoudhury, R.N. and Bonilla, C.F. Measurement of the Acidity of Aqueous Solutions at High Temperatures and Pressures. J. electrochem. Soc. (1956), 103, 241-246

(26) Izaki, T. and Arai, K. The Behaviour of the Ag-AgCl Electrode at High Temperatures. Suiyokai-Shi. (1968), 16, 367-370

(27) Greeley, R.S., Smith, W.T., Stoughton, R.W., and Lietze, M.H. Electromotive Force Studies in Aqueous Solutions at Elevated Temperatures. I The Standard Potential of the Silver-Silver Chloride Electrode. J. phys. Chem. (1960), 64, 652-655

(28) Lietze, M.H. The Hydrogen Electrode-Silver Chloride System at High Temperatures and Pressures. J. Am. chem. Soc. (1955), 77, 1344-1346

(29) Anderson, N.J. Ph.D. Thesis, Univ. Chicago, Chicago, (1945)

(30) a) Hills, G.J. and Ives, D.J.G. The Hydrogen-Calomel Cell. Pt. I. The Hydrogen Electrode. J. chem. Soc. (1951), 305-310

b) ---------- The Hydrogen Electrode. Nature. (1949), 163, 997

(31) Feltham, A.M. and Spiro, M. Platinised Platinum Electrodes. Chem. Revs. (1971), 71, 177-193

(32) Hamer, W.J. and Acree, S.F. A Comparison of Platinum and Palladium Hydrogen Electrodes in Aqueous Solutions of Acid Potassium Phthalate. J. Res. natn. Bur. Stand. (1944), 33, 87-103

(33) Lewis, G.N. and Broghton, T.B. A Study of Hydrogen and Calomel Electrodes. J. Am. chem. Soc. (1917), 39, 2245-2261

(34) a) Lorch, A.E. Choice of Catalysts for the Hydrogen Electrode. Anal. Chem. (1934), 6, 164-165

b) ---------- and Hammett, L.P. A Study of the Catalytic Properties of Bright Platinum and Iridium Deposits in the Activation of Hydrogen. J. Am. chem. Soc. (1933), 55, 70-80

(35) Reid, F.H. Electrodeposition of the Platinum Group Metals. Metallurgical Revs. (1963), 8, 167-211

(36) Perley, A. and Godshalk, J.B. Improvements in Electrodes for pH Measurement U.S.Pat. No. 2,416,949 U.K.Pat. No. 567,722 June, (1942)

(37) MacNamara, E.L. Method of Electroplating Iridium. U.S.Pat. No. 3,207,680 (1965)

(38) Conn, G.A. Iridium Plating. Plating. (1965), 52, 1258-1261

(39) Skomoraski, R.M. and Paterson, N.J. Iridium Plating. U.S.Pat. No. 3,639,219 (1972)

(40) Ovendon, P.J. An Iridium Plating Solution. Nature (1957), 179, 39

(41) Ignatova, N.V. and Vasserman, B.J. A Bath for Electroplating Metals with Iridium. C.A. (1961), 55, 18396e U.S.S.R.Pat. No. 136,056 (1960)

(42) a) Tyrrell, C.J. The Electrodeposition of Iridium. Trans. Inst. Metal. Finishing. (1965), 43, 161-166

b) ---------- Electrodeposition of Iridium. U.K.Pat. No. 1,022,451 (1964)

(43) Fernelius, W.C. (Ed.) Inorganic Syntheses Vol. II (1946), II, 4-6

(44) Bates, R.G. Electrometric pH Determinations. (1954), John Wiley and Sons, 206

(45) Zimmerman, W. The Preparation of High Purity Silver Chloride. J. Am chem. Soc. (1952), 74, 852-853

(46) Pinching, G.D. and Bates, R.G. Purification of NaCl and KCl for use in Electrochemical Work and the Detection of Small Amounts of Bromides. J. Res. natn. Bur. Stand. (1946), 37, 311-319, RP. 1749

(47) Bates, R.G., Pinching, G.D. and Smith, E.R. pH Standards of High Acidity and High Alkalinity and the Practical Scale of pH. J. Res. natn. Bur. Stand. (1950), 45, 418-429, RP. 2153

(48) Bates, R.G., Bower, V.E. and Smith, E.R. Calcium Hydroxide as a High Alkaline pH Standard. J. Res. natn. Bur. Stand. (1956), 56, 305-312, RP. 2680

(49) Vogel, A.I. Quantitative Inorganic Analysis, 3rd. Ed. (1962). Longmans.

(50) Weast, R.C. Handbook of Chemistry and Physics, 53rd. Ed. (1972) The Chemical Rubber Co.

(51) Bates, R.G. Revised Standard Values for pH Measurements from 0 to 95°C. J. Res. natn. Bur. Stand. (1962), 66A, 179-184

(52) Jolley, L.B.W. Summation of Series, 2nd. Ed. (1961) Dover Publications, Inc.

(53) Greeley, R.S., Smith, W.T., Lietzke, M.H. and Stoughton, R.W. Electromotive Force Measurements in Aqueous Solutions at Elevated Temperatures. II Thermodynamic Properties of Hydrochloric Acid. J. phys. Chem. (1960), 64, 1445-1448

(54) Denbeigh, K. The Principles of Chemical Equilibrium, 3rd. Ed. (1971). Cambridge University Press.

(55) U. K. Committee on the Properties of Steam. U.K. Steam Tables in S.I. Units 1970. Edward Arnold (Publishers) Ltd.

(56) Hildebrand, J.H. and Scott, R.L. Solubility of Nonelectrolytes, 3rd. Ed. (1950) Reinhold Publishing Corp.

(57) Needes, C.R.S. Precipitation of Metals and Alloys from Aqueous Solutions by Hydrogen. Ph.D. Thesis, Imperial College, London. (1969)

(58) Epstein, L.F. Constants in the Equation of State of a Gas. J. chem. Phys. (1952), 20, 1981-1982

(59) Putnam, W.E. and Kilpatrick, J.E. The General Relation between the Density Virial Coefficients and the Pressure Coefficients. J. chem. Phys. (1953). 21, 951

(60) Darken, L.S. and Gurry, R.W. Physical Chemistry of Metals. (1953). McGraw-Hill Book Co. Inc.

(61) Hirschfelder, J.O., Curtiss, C.F. and Bird, R.B. Molecular Theory of Gases and Liquids. (1954) John Wiley & Sons, Inc.

(62) Shaw, H.R. and Wones, D.R. Fugacity Coefficients for H_2 Gas between 0 and 1000°C for Pressures to 3000 atm. Am. J. Sci. (1964), 262, 918-929

(63) Kaye, G.W.C. and Laby, T.H. Tables of Physics and Chemical Constants, 13th Ed. (1966). Longmans, Green & Co.

(64) Harned, H.S. and Owen, B.B. The Physical Chemistry of Electrolytic Solutions, 3rd Ed. Reinhold Publishing Corp.

(65) Akerlof, G.C. and Oshry, H.I. The Dielectric Constant of Water at High Temperatures and in Equilibrium with its Vapour. J. Am. chem. Soc. (1950), 72, 2844-2847

(66) Malmberg C.G. and Maryott, A.A. Dielectric Constant of Water from 0 to 100°C. J. Res. natn. Bur. Stand. (1956), 56, 1-8, RP. 2641

(67) Chatfield, C. Statistics for Technology. (1970) Penguin Books.

(68) Hamer, W.J. and Acree S.F. A Method for the Determination of the pH of 0.05 m Solutions of Acid Potassium Phthalate with or without Potassium Chloride. J. Res. natn. Bur. Stand. (1944), 32, 215-227, RP 1586

(69) Bower, V.E., Bates, R.G. and Smith, E.R. pH of Solutions of Potassium Tetroxalate from 0 to 60°C J. Res. natn. Bur. Stand. (1953), 51, 189-194, RP 2450

(70) Mesmer, R.E., Baes, C.F. and Sweeton, F.E. Acidity Measurements at Elevated Temperatures. VI Boric Acid Equilibria. Inorg. Chem. (1972), 11, 537-543

(71) Manov, G.G., DeLollis, N.J. and Acree, S.F. Ionisation Constant of Boric Acid and the pH of Certain Borax-Chloride Buffer Solutions from 0 to 60°C. J. Res. natn. Bur. Stand. (1944), 33, 287-306, RP 1609

(72) a) Owen, B.B. The Dissociation Constant of Boric Acid from 10 to 60°C. J. Am. chem. Soc. (1934), 56, 1695-1697

b) ---------- and King, E.J. The Effect of Sodium Chloride upon the Ionisation of Boric Acid at Various Temperatures. J. Am. chem. Soc. (1943), 65, 1612-1620

(73) Pinching, G.D. and Bates, R.G. Second Dissociation Constant of Oxalic Acid from 0 to 50°C and the pH of Certain Oxalate Buffer Solutions.
J. Res. natn. Bur. Stand. (1948), 40, 405-416, RP 1885

(74) Bower, V.E. and Bates, R.G. Standards for pH Measurements from 60° to 95°C.
J. Res. natn. Bur. Stand. (1957), 59, 261-264, RP 2797

(75) Bates, R.G., Bower, V.E., Miller, R.G. and Smith, E.R. pH of Solutions of Potassium Hydrogen d-Tartrate from 0° to 60°C.
J. Res. natn. Bur. Stand. (1951), 47, 433-438, RP 2268

(76) Hamer, W.J., Pinching, G.D. and Acree, S.F. First Dissociation Constant of o-Phthalic Acid and Related pH Values of Phthalate Buffers from 0° to 60°C.
J. Res. natn. Bur. Stand. (1945), 35, 539-564, RP 1687

(77) Robinson, R.A. and Stokes, R.H. Electrolyte Solutions, 2nd. Ed. (1959). Butterworths.

(78) Bates, R.G. and Canham, R.G. Resolution of the Dissociation Constants of d-Tartaric Acid from 0° to 50°C.
J. Res. natn. Bur. Stand. (1951), 47, 343-348, RP 2260

(79) Hamer, W.J., Pinching, G.D. and Acree, S.F. pH Standards at Various Temperatures: Aqueous Solutions of Acid Potassium Phthalate.
J. Res. natn. Bur. Stand. (1946), 36, 47-62, RP 1690

(80) Hamer, W.J. and Acree, S.F. Second Dissociation Constant of o-Phthalic Acid and Related pH Values of Phthalate Buffers.
J. Res. natn. Bur. Stand. (1945), 35, 381-416, RP 1678

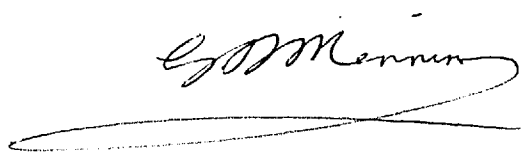
(81) Taylor, B.N., Parker, W.H., and Langenberg, D.N. Determination of e/h, using Macroscopic Quantum Phase Coherence in Superconductors: Implications for Quantum Electrodynamics and the Fundemental Physical Constants.
Rev. Mod. Phys. (1969), 41, 375-469

Acknowledgements

The author wishes to thank his supervisor, Dr. A.R. Burkin, Reader in Hydrometallurgy at the Royal School of Mines, for his advice and encouragement over three years and in particular for his answers to some of the more esoteric questions posed him.

Thanks also go to Mr. J.E.A. Burgess for much practical advice and to Mr. C.D. Waters for his extraordinary patience with the author's inability to program computers correctly. The author also acknowledges the aid received from the staffs of the Chemical Metallurgy Laboratory and the Departmental Workshop and from other members of the Hydrometallurgy Group.

Finally the author wishes to express his appreciation to Rio Tinto Zinc Co. Ltd. for a Research Bursary received throughout this work.



G.D. Manning.

January 1975

Appendix A

The Calculation of the Minimum Dimensions of the Autoclave

The required minimum dimensions of a reaction vessel having two adjacent 3 in. diameter, 3 in. deep cylindrical reaction pots capable of withstanding an internal pressure of 5000 p.s.i. were calculated as follows.

The maximum hoop stress in a thick-walled cylinder subject to an internal pressure, P is

$$f_H = P \frac{(d_2^2 + d_1^2)}{(d_2^2 - d_1^2)}$$

where d_2 and d_1 are the outer and inner diameters. The maximum allowable stress at various temperatures in AISI 316 Stainless Steel (nominal composition: 18 Cr; 10 Ni; 2 Mo) is given in Table A1.

Table A1

$t^\circ F$	$t^\circ C$	Max. allow. Stress in Tension. p.s.i.
200	93	18700
300	149	17900
400	204	17500
500	260	17200
600	316	17100

A maximum working temperature of 300°C was envisaged and therefore substituting f_H = 17100 p.s.i., P = 5000 p.s.i. and d_1 = 3 in. gave d_2 = 4.054 in. equivalent to a wall thickness of at least 0.527 in.

O-rings of diameter 4 in. were to be employed and therefore the total area of the autoclave head subject to the internal pressure was $2.\pi.(2)^2 = 25.14$ in.^{2} and the total force at 5000 p.s.i., 125680 lb. The initial tension in the bolts would have therefore to be at least 125680/15 = 8400 lbf/bolt. The smallest BSF Socket Head Cap Screw with a suitable safty margin was 3/8 in. diameter.

The maximum stress in a flat plate of thickness, t held by a ring of bolts and subjected to an upward pressure, P is

$$f = \frac{d^2 cP}{t^2}$$

where d is the bolt ring diameter (4.429 in.) and c is a constant (0.162). These gave t = 0.964 in.

The actual dimensions of the autoclave body and head are given in Figs. A1 and A2. Six of the seven pressure unions through the head above each reaction pot were situated on two concentric circles about the central unions and staggered at 60°. This arrangement allowed good clearance between each union's gland nut.

After construction the autoclave was successfully hydraulically pressure tested at 5000 p.s.i. for 1 hour.

In the present work, in which the internal pressure was always <300 p.s.i. the Socket Head Caps Screws were tightened to 160 lb.in.

The dimensions and design of the mild steel cooling plates are shown in Fig. A3.

Reference

Perry, J.H. Chemical Engineers Handbook, 4th Ed. (1963)

Section 24, pp 12-17

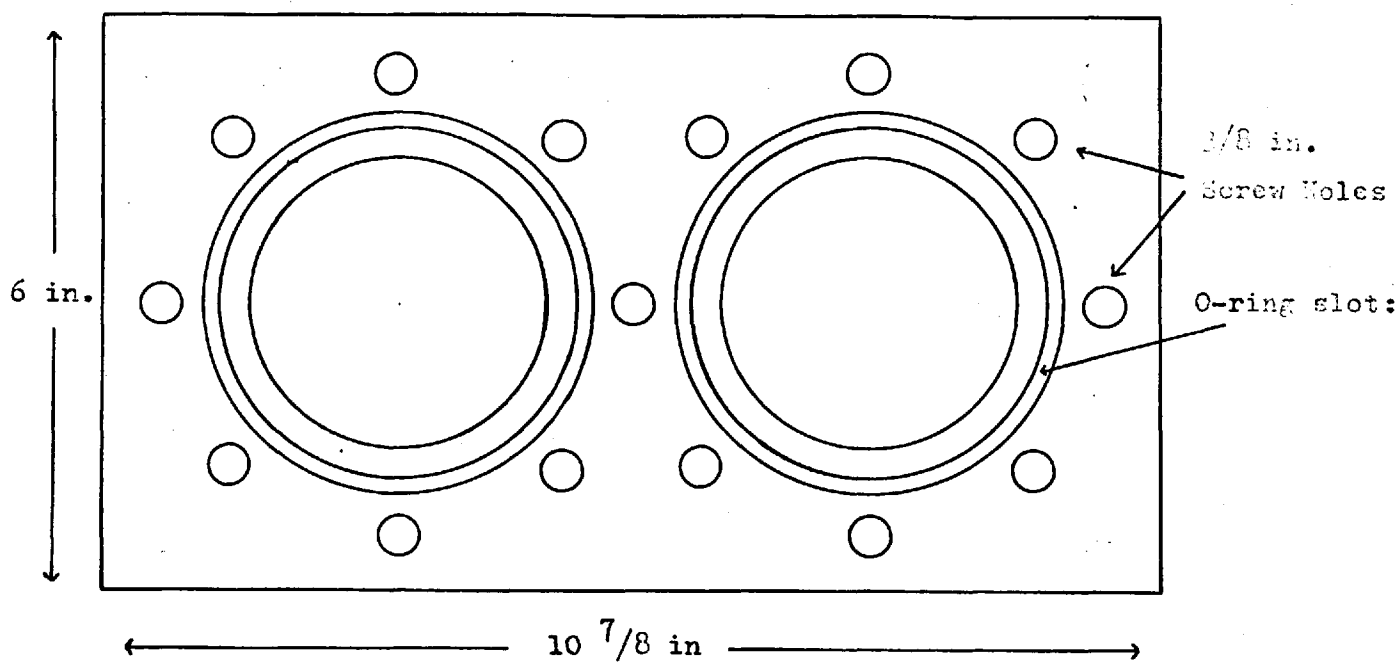
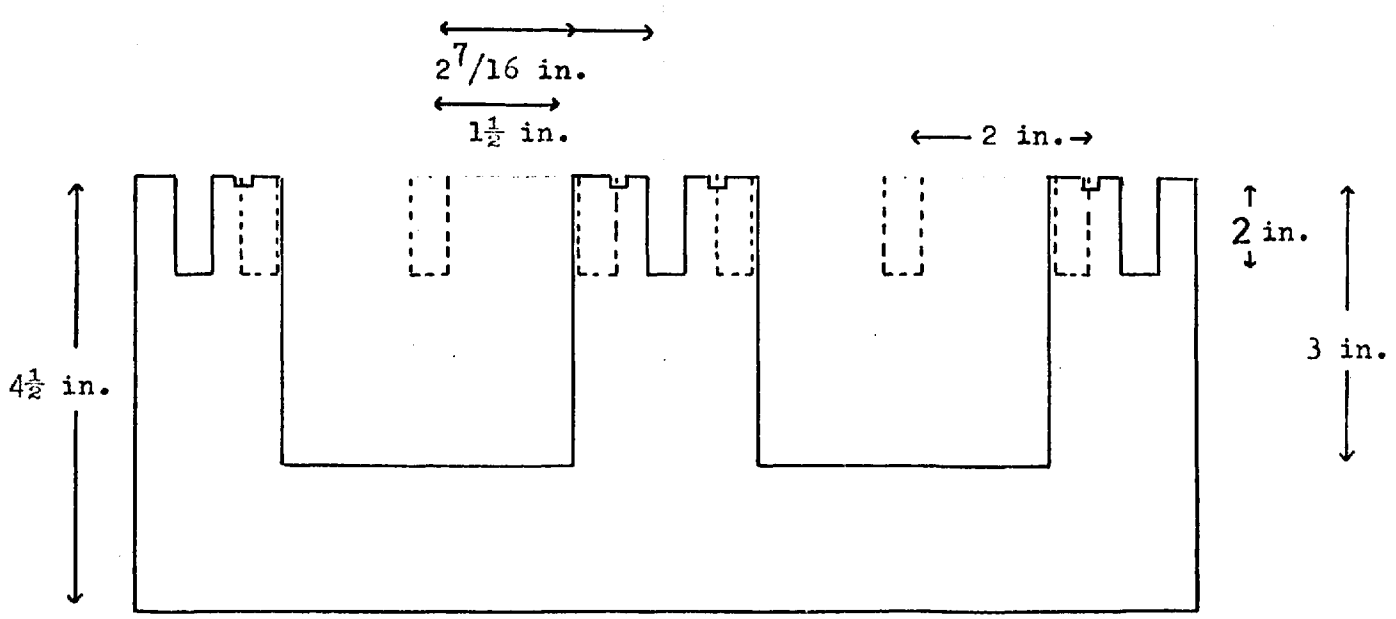
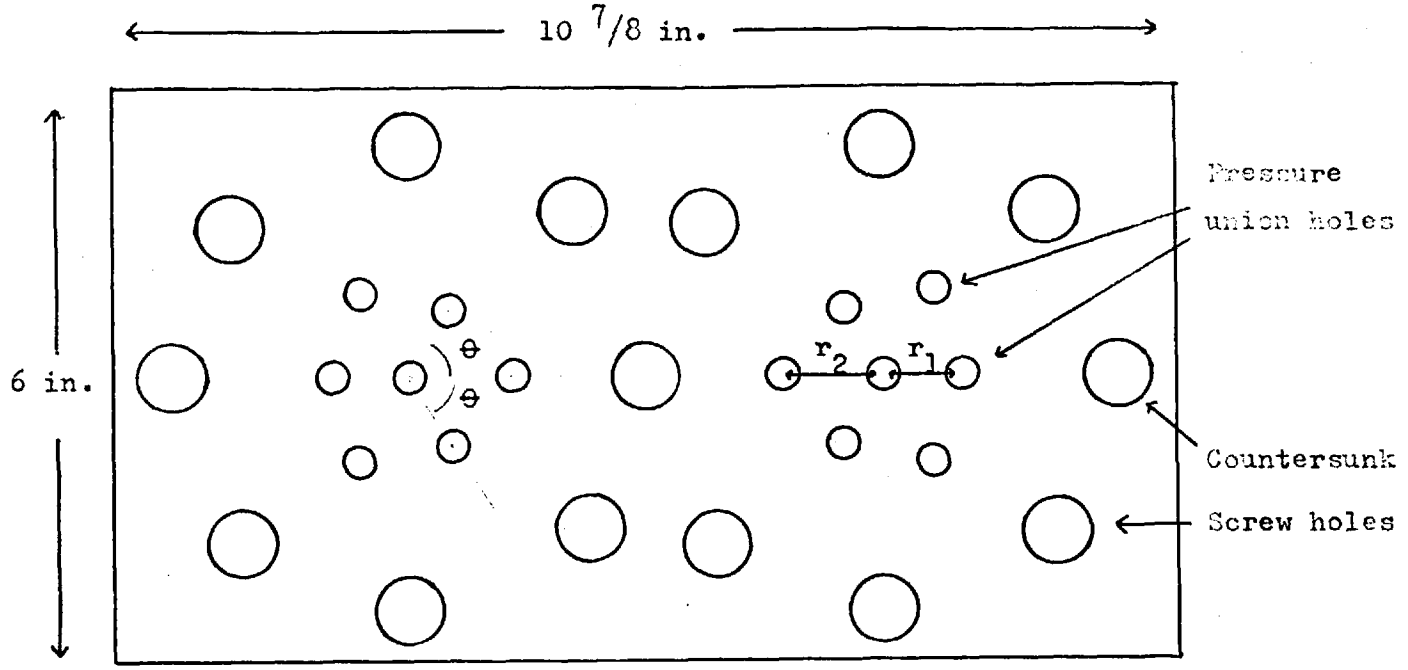


Fig. (A1) Autoclave Body

($\frac{1}{2}$ Scale)





Head: $1\frac{1}{2}$ in. thick.

Unions: Autoclave Engineers, Standard W 125 union.
for $^{1}/_{8}$ in. O.D. Stainless tubing.

$r_1 = {}^{13}/_{16}$ in. $\quad r_2 = 1\ {}^{1}/_{32}$ in. $\quad \theta = 60^{\circ}$

Fig. (A2) Autoclave Head

($\frac{1}{2}$ Scale)

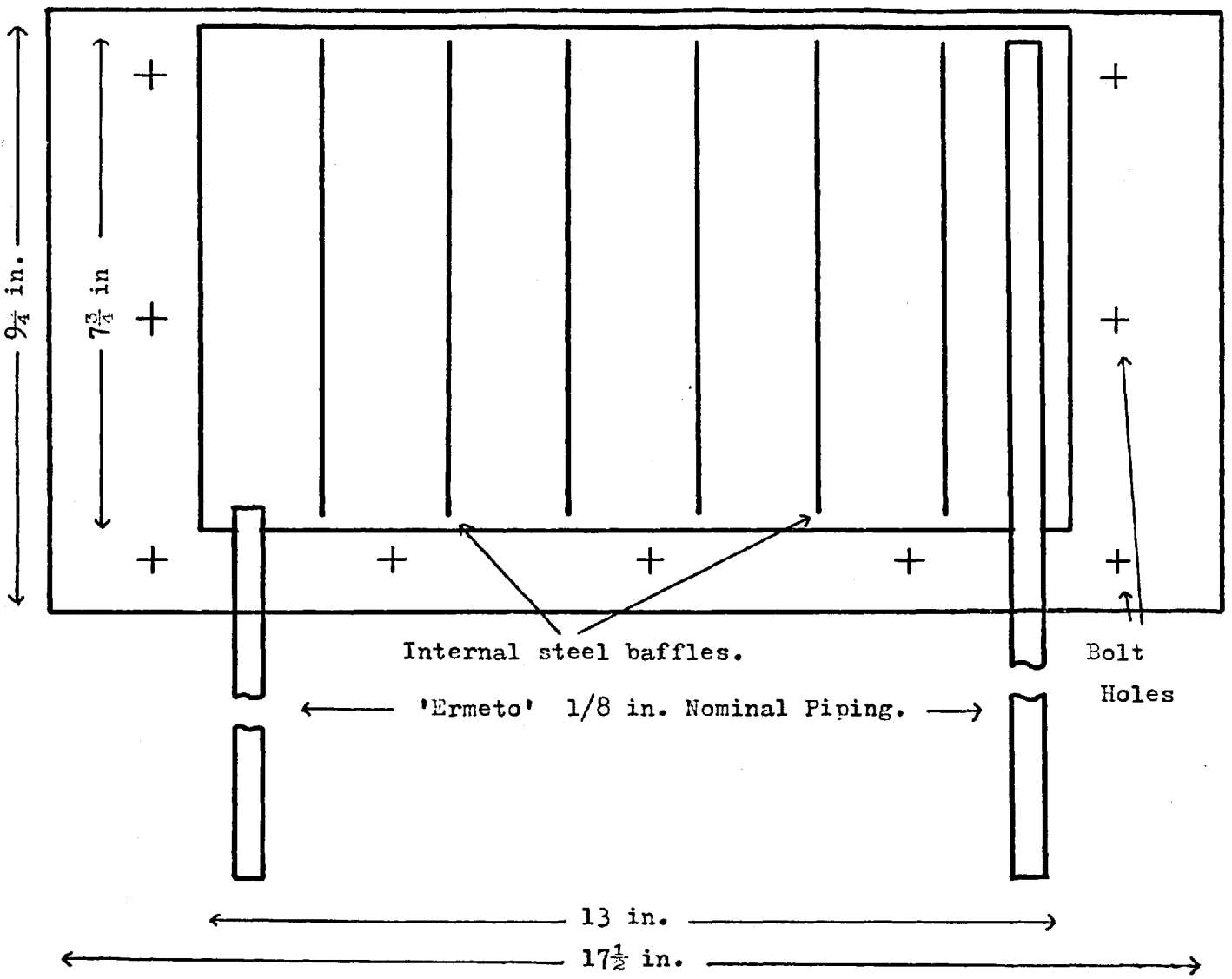


Fig. (A3) Left-hand cooling plate

(Right-hand plate is mirror image)



Appendix B

The Reduction of Silver Chloride by Hydrogen and some Consideration of the Requirements for Reference Electrodes at Elevated Temperatures

The Reduction of Silver Chloride

The reduction of AgCl by H_2 in aqueous solution follows the equation,

$$AgCl + \tfrac{1}{2}H_2 = Ag + H^+ + Cl^- \qquad \text{— (B1)}$$

which is the full-cell reaction when a Ag-AgCl electrode is opposed by a hydrogen electrode. It is this reaction that limits the usefulness of the Ag-AgCl electrode as a reference electrode at elevated temperatures in the presence of H_2. The free energy change and equilibrium constant for reaction (B1),

$$K = \frac{a_{Ag}\, a_{H^+} a_{Cl^-}}{a_{AgCl}\, a_{H_2}^{\frac{1}{2}}} = a_{H^+} a_{Cl^-} \doteqdot m_{HCl}^2$$

(at a_{H_2} = 1 atm.)

may be calculated from Greeley's[B1] values of $E^o_{Ag\text{-}AgCl}$ and these together with the approximate molalities of HCl (i.e. ignoring activity coeffients) in equilibrium with solid AgCl and H_2 at 1 atm. pressure are given in Table (B1). A plot of log m_{HCl} versus t°C is shown in Fig. (B1) and at any conditions of temperature and HCl molality represented below this line AgCl is

Table (B1)

Thermodynamic Data for Reaction (B1) (after Greeley[B1])

$t^{\circ}C$	$E^{\circ}_{Ag-AgCl}$	ΔG(kcal)	log K	log m_{HCl}	m_{HCl}
25	-0.22233	5.127	-3.758	-1.879	0.013
60	-0.1968	4.538	-2.977	-1.489	0.032
90	-0.1696	3.911	-2.354	-1.177	0.067
125	-0.1330	3.067	-1.684	-0.842	0.14
150	-0.1032	2.380	-1.229	-0.615	0.24
175	-0.0708	1.633	-0.796	-0.398	0.40
200	-0.0348	0.803	-0.371	-0.186	0.65
225	0.0051	-0.118	0.052	0.026	1.06
250	0.054	-1.245	0.520	0.260	1.82
275	0.090	-2.075	0.827	0.414	2.59

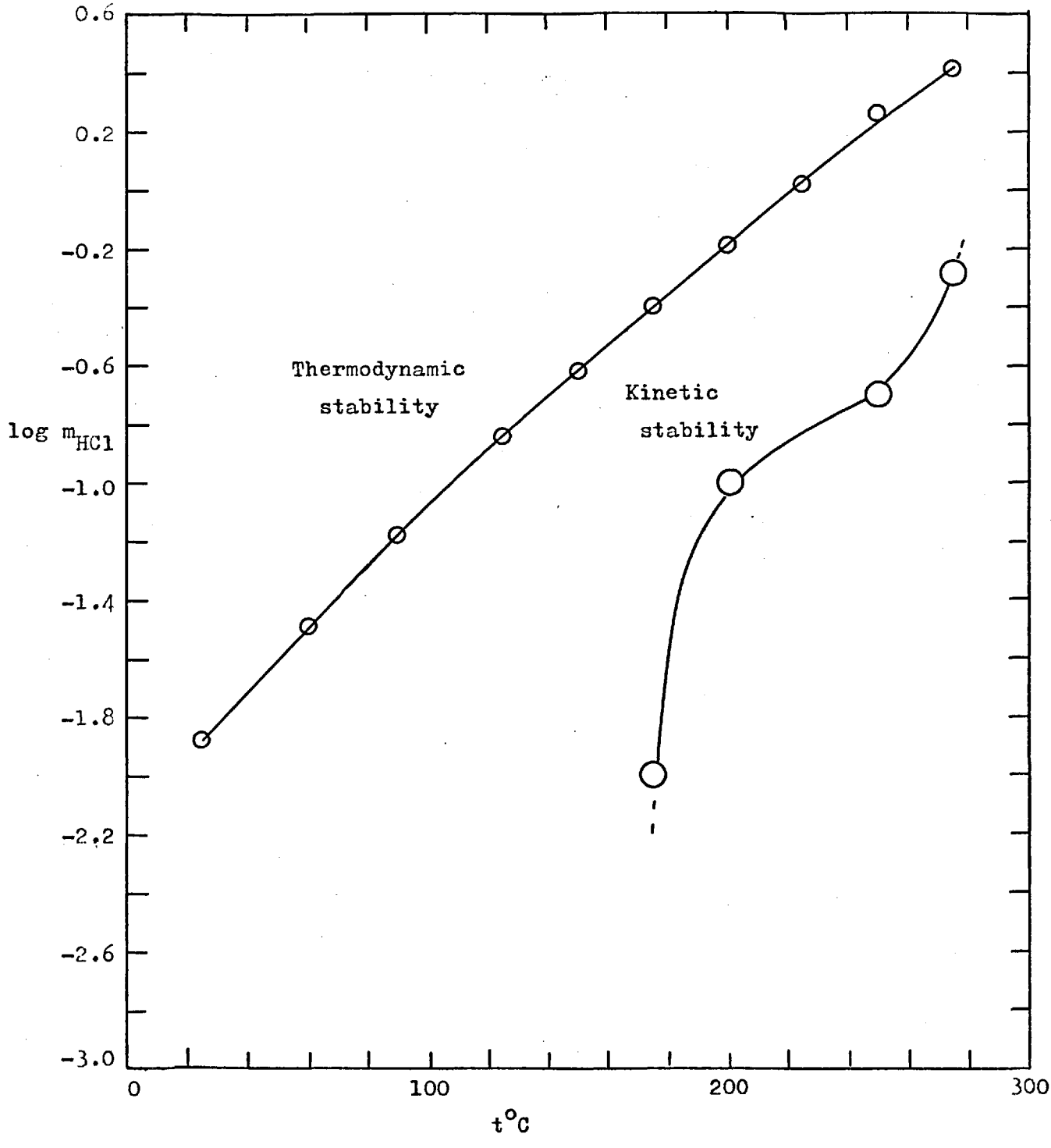


Fig. (B1) Approximate thermodynamic and kinetic stability of solid AgCl in contact with m_{HCl}, at 1 atm. H_2 pressure (after Greeley, et al.[27])

thermodynamically unstable and should be reduced by H_2 at 1 atm. (It is easy to deduce that inclusion of activity coefficients would raise this line to somewhat more positive values of log m_{HCl} at each temperature).

In fact, AgCl is much more stable than this plot suggests because of the slow kinetics of reaction (B1) and some idea of the practical stability of AgCl in HCl solutions under H_2 may be gained from Greeley's observations of potential drifts attributed to AgCl reduction obtained in his work. He quotes the lowest temperature (within 25°) at which AgCl reduction occurs at a significant rate for three values of m_{HCl} and also states that no reduction occurred up to 275°C with $m_{HCl} \geqslant 0.5$. (The H_2 pressure would have been slightly greater than 1 atm. but certainly less than 2 atm.). This curve is also shown in Fig. (B1) and it is below this line that reduction actually occurs to a significant extent. Thus the area between these two lines is a region of kinetic stability for AgCl. At ambient temperatures the lines are relatively far apart, e.g. at 25°C, solid AgCl is thermodynamically unstable in a solution in which $m_{HCl} < 0.013$ (i.e. $a_{H^+} \cdot a_{Cl^-} < 0.00017$) however, Ag-AgCl electrodes work well in 0.001 m HCl versus hydrogen electrodes and for calibration of $Ca(OH)_2$ buffer solution Bates, et al.[B2] have used Ag-AgCl electrodes in a solution of pH = 12.5 containing 0.001 m KCl, i.e. $a_{H^+} \cdot a_{Cl^-} \simeq 10^{-16}$, which was saturated with H_2.

At elevated temperatures the two lines converge and the region of kinetic stability becomes much more narrow as is to be expected. Above 200°C, Ag-AgCl electrodes can only be used for any length of time in solutions whose ionic strengths are becoming too great

to be handled by simple solution theory. The electrode, therefore, looses its usefulness for making accurate thermodynamic measurements in the presence of H_2 under these conditions. It does not, however, loose its usefulness as a general reference electrode (see below).

Reference Electrodes

Reference half-cells are commonly divided into so-called 'kinds' of electrode. Thus the half-cells,

$$Ni|NiSO_4\ (m),$$

and

$$(Pt)H_2|HCl\ (m),$$

are electrodes of the 'first kind' being reversible only to the metal (hydrogen). Examples of electrodes of the 'second kind' are,

$$Hg,Hg_2Cl_2|KCl\ (m),$$

and

$$Ag,AgI|NaI\ (m),$$

which are reversible to both the metal ion and anion. It is possible to go further and have electrodes of the 'third kind' for example,

$$Hg,Hg_2(C_2O_4),Ca(C_2O_4)|Ca(NO_3)_2\ (m),$$

and

$$Hg,Hg_2WO_4,CaWO_4|Ca(NO_3)_2\ (m),$$

which are reversible to two metal ions (in this case Hg_2^{++} and Ca^{++}) and an anion (oxalate or tungstate). These particular half-cells have been used to measure calcium ion concentration in solutions.(B3) It may be noted in passing that if a half-cell,

$$M,MX,HX\,|\,\text{Solution},$$

could be found comprising of a suitable metal, M and a salt, MX and acid HX, both of low solubility, then it would act as a pH electrode. Because,

$$M^+ + e^- = M$$

giving
$$E = E^o_{M^+/M} - \frac{RT}{F} \ln \frac{1}{a_{M^+}} \qquad \text{— (B2)}$$

The solubility products of the salt and acid are

$$K_{MX} = a_{M^+}a_{X^-}$$

$$K_{HX} = a_{H^+}a_{X^-}$$

which on substitution into (B2) give,

$$E = E^o_{M^+/M} - \frac{RT}{F} \ln \frac{K_{HX}}{K_{MX}} - \frac{2.303RT}{F}\,pH$$

or
$$E = E^o_{M/MX/HX} - \frac{2.303RT}{F}\,pH$$

For example, it is possible to regard metal-metal oxide electrodes (which offer some of the best prospects for a high temperature pH electrode) as electrodes of this kind in which the solvent, water, also acts as an acid, of which the metal oxide is a salt. In this case one has,

$$M,M_2O\,|\,H_2O,\ \text{Solution},$$

and therefore, (B2) still applies but in addition,

$$M_2O + H_2O = \text{(hydroxide or some hydrated oxide)}$$

$$= 2M^+ + 2OH^-$$

yielding $$K_{M_2O} = \frac{a_{M^+}^2 a_{OH^-}^2}{a_{H_2O}}$$

and of course $$K'_w = \frac{a_{H^+} a_{OH^-}}{a_{H_2O}}$$

and (B2) becomes,

$$E = E^o_{M^+/M} - \frac{RT}{F} \ln \frac{K'_w}{K_{M_2O}} - \frac{RT}{F} \ln a_{H_2O} - \frac{2.303RT}{F} pH \quad \text{— (B3)}$$

In solutions where the water activity may be taken as unity, K'_w becomes the normal dissociation constant, K_w and (B3) may be reduced to,

$$E = E^o_{M/M_2O/H_2O} - \frac{2.303RT}{F} pH$$

and the half-cell behaves as a pH electrode. (Metal-metal oxide electrodes may also be regarded as special electrodes of the 'second kind' although the final results are, of course, identical to those obtained above).

To return to the general discussion, apart from the hydrogen electrode, electrodes of the 'first kind' have had only limited success. As these electrodes react to metal ion activity in

solution they are potentially very valuable but there are two overriding difficulties. Firstly, most metals whose ions one might wish to monitor in solution, will be corroded by that solution. For example, an electrode reacting to (say) Ni^{++} would be of obvious value and in theory it is necessary only to put a piece of nickel metal into the solution versus a reference electrode, however, generally any solution with a significant Ni^{++} concentration will probably have a pH low enough to cause the metal to be attacked. This effect will become worse at elevated temperatures. In fact electrodes of the 'third kind' neatly avoid this difficulty in that the metal present in the electrode is not that which is being determined in solution. Thus in the examples above a relatively noble metal, Hg, can be used to determine the ionic activity of a reactive metal, Ca, via insoluble salts of the two metals containing a common anion.

Electrodes of the 'second kind' may well be practical as fixed potential reference electrode (type B, see below) since the aqeous solution in contact with the metal is constant and may be suitably chosen e.g.

$$Ni|NiSO_4\ (1\ m)||$$

and the simplicity of such a cell may well have advantages at elevated temperatures when the number of possible systems becomes severely restricted.

The second major difficulty, common to all kinds of electrodes, is the production of a clean, reproducible metal surface in a thermodynamic ground state. Purity is, of course, always a major consideration, e.g. 99.9 % Pb is attacked by acid much more easily

than 99.99 % Pb. Internal strain often makes equilibrium potentials difficult to obtain, but high temperatures will be advantageous in this respect by helping to anneal the metal phase. (For example, thermal strain has been suggested as the cause of the discrepancies between $E^{o}_{Ag-AgCl}$ for different types of Ag-AgCl electrode[B4] but Greeley[B1] has found that thermal cycling improved agreement between different electrodes).

The demand for a clean, reproducible surface has caused metal amalgams (e.g. Pb(Hg), Tl(Hg)) to be extensively used at ambient temperatures, but the high vapour pressure of Hg and the low melting points of amalgams do not make them attractive for work at elevated temperatures. Alloys with noble metals (e.g. Pt, Au) are, however, a distinct possibility. The activity of the metal in the alloy will be less than that of the pure metal, effectively reducing its reactivity towards corrosion by solutions or oxygen. Moreover, any oxide formed may not stick to the surface of the alloy as tenaciously as to that of the pure metal, thus helping to preserve a reproducible potential. Such alloys would be difficult to prepare however and would therefore ideally contain two distinct phases thus fixing the chemical potential of the metal over a range of compositions.

Generally, satisfactory reference electrodes which are reversible to metal ions in solution are difficult to arrange and by far the most successful electrodes are those of the 'second kind' which are reversible to a soluble anion. Of these the most common are Ag-AgCl and $Hg-Hg_2Cl_2$, but other examples are Ag-AgBr, Ag-AgI, $Ag-Ag_2SO_4$, $Hg-Hg_2SO_4$, $Pb-PbSO_4$ and Tl(Hg)-TlCl. all of which have been studied to some extent at elevated

temperatures.[B5,B6] Hg_2Cl_2 disproportionates increasingly to Hg and $HgCl_2$ at above room temperature, AgBr and AgI are subject to aerial oxidation, Hg_2SO_4 hydrolyses to Hg, HgO and H_2SO_4 at elevated temperatures and the Pb-$PbSO_4$ electrode is reproducible to only $\pm$ 10 mV at 250°C.[B7] Ag_2SO_4 is really rather too soluble for satisfactory use in reference electrodes. There is no doubt that the most satisfactory and well tested system (apart from the hydrogen electrode) is Ag-AgCl, which has been calibrated up to 275°C, but the reduction of AgCl by H_2 in solutions with pH > 4-5 causes a real problem. Thus in Section (4.1) it was shown that both the phosphate and borate buffers can be used up to 200°C and probably to even higher temperatures, but without a suitable reference electrode which is stable in opposition to a hydrogen electrode there is no way, at present, of accurately calibrating themusing a cell without liquid junction.

At this point it is convenient to further subdivide reference electrode into two types exemplified by,

$$Ag,AgCl|KCl(m),\text{Solutes } A,B,...| \qquad - A$$

$$Ag,AgCl|KCl(m)\|\ \text{Salt bridge}\| \qquad - B$$

Type A contains no liquid junction, is strictly thermodynamic and capable of high accuracy, reproducibility and precise theoretical definition. However, the solid phases of the electrode are not only in contact with the reversible anion in solution but also with other solutes and phases associated with the opposing half-cell and are thus open to attack by them. This is, of

course, precisely the situation that exists in the cell used above to calibrate buffer solutions.

Type B is a fixed potential reference electrode. It contains a standard solution and a salt bridge although these are often conveniently made identical e.g. 3.5 M KCl. It contains, therefore, at least one liquid-liquid junction and although the half-cell as written has a fixed potential the varying junction potentials at the free end of the salt bridge and any solution beyond it means that the electrodes potential does tend to vary somewhat, although probably within $\pm$ 10 mV. For this reason it is not as amenable to strict thermodynamic definition as Type A and even its standard half-potential is to some extent dependent on the opposing half-cell and associated solutions employed for its calibration. However, electrodes of this type have the great advantage that their solid phases are effectively shielded from attack by external phases by the salt bridge. Thus such systems are extensively used as approximately fixed potential electrodes in opposition to glass pH electrodes (in practical measurement), redox electrodes and other single ion monitoring electrodes.

Because of the restrictions on possible cell systems imposed by the use of elevated temperatures the different requirements of the two types of reference electrodes becomes highly relevant. For Type A is required a half-cell which is very stable and reproducible (to 0.1 mV) but which need not necessarily have a long life, i.e. it may be subject to attack by other cell components as long as it survives for (say) a few hours. (e.g. the Ag-AgCl electrodes in the phthalate buffer at

200°C). For Type B, however, the minimum acceptable requirements are virtually the reverse. Thus it should have a long, useful life (i.e. weeks) but over that time it need not be stable to more than (say) ± 10 mV. Nor indeed need two similar electrodes agree to better than this. It is now obvious that systems suitable for use as Type B will be much easier to find than those for Type A. Thus all that is required is a metal, an insoluble metal compound and a solution which are compatable and thermally stable and which do, of course, give a fairly steady potential. The cell,

$$Pb,PbSO_4 \,|\, \text{Sat. } (NH_4)_2SO_4 \,||$$

($(NH_4)_2SO_4$ is the only common sulphate whose solubility does not decrease at elevated temperatures) could suffice even in the present state of knowledge. Also, as stated above, electrodes of the 'first kind' may well be satisfactory since despite the general restrictions imposed by elevated temperatures, the faster rates of reaction will almost certainly make some systems useful which were rejected at ambient temperatures because they were slow to reach equilibrium. However, the most immediate choice is, [B8]

$$Ag,AgCl \,|\, \text{Sat. LiCl} \,||$$

LiCl is used because of its greater molal solubility compared to KCl thus keeping the product, $a_{H^+}.a_{Cl^-}$ as large as possible so as to oppose any hydrolysis (or reduction on calibration) of AgCl. The solution might also contain (say) 0.01 m HCl for this purpose. Such a reference electrode could almost certainly be calibrated to 300°C versus a hydrogen electrode using the cell,

$$Ag,AgCl|\ Sat.\ LiCl||\ HCl(m)|\ Pt(H_2)$$

as long as H_2 was prevented from entering the Ag-AgCl half-cell (although there must be some diffusion of dissolved H_2 across the liquid-liquid junction). Such a calibration alone would immediately make the measurement of redox in a wide range of solutions possible at elevated temperatures.

The requirements of electrodes of Type A make it virtually necessary to design the electrode with reference to the half-cell which it is to oppose. One case will therefore be considered, which is probably the most important and that in which the reference electrode is stable in opposition to a hydrogen electrode in solutions covering a wide range of pH. In this system there is a fundamental difficulty that any compound of a metal which is noble enough not to be corroded by dilute solutions at elevated temperatures will probably itself be thermodynamically unstable and be reduced.(e.g. Ag and AgCl). Alternatively, any compound which is thermodynamically stable in the presence of H_2 will be one of a relatively reactive metal, e.g. $BaSO_4$. One way out of this vicious circle is to use a kinetically stable compound of a relatively noble metal. Ideally this would contain a univalent anion, avoiding any equilibrium between an acid and neutral salt, but most possible combinations employing the simple anions, Cl^-, Br^-, I^-, etc. have been tried. If divalent anions are admitted then $SO_4^=$ is the obvious choice. Insoluble sulphates are formed by Ag^+, Hg_2^{++}, Tl^+, Pb^{++}, Ba^{++} and Ca^{++} but of these Ba and Ca metals are too reactive. Hg_2SO_4 hydrolyses rather easily[B5] and the solubility of Tl_2SO_4 is ~0.05 m at 25°C

which is already rather too high and in common with that of $(NH_4)_2SO_4$ (although as distinct from virtually all other sulphate solubilities) increases steadily with rising temperature.[B8] The solubility of Ag_2SO_4 is also inconveniently high at room temperature and the author has reason to believe that its solubility will behave similarly to that of Tl_2SO_4. One is left, therefore, with the Pb-$PbSO_4$ system. Some work has been done on this at ambient temperatures[B3] and also up to 250°C[B8] although none has been totally successful. However, it has a number of points in its favour. Lead is a relatively noble, soft metal and interestingly, forms a low melting alloy with platinum. $PbSO_4$ is not easily reduced by hydrogen although it will certainly be hydrolysed somewhat in alkaline solution. However, it may be noted that $PbSO_4$ is isomorphous with $BaSO_4$ (both crystals are orthorhombic, have the same space group and very similar unit cell dimensions) and are co-precipitated from aqueous solution. There seems, therefore, a distinct possibility that a Pb doped $BaSO_4$ phase could be used having the advantages of a very low solubility and resistance to hydrolysis.

It is felt that the above is the sort of specific, Type A electrode that may well have to be developed at elevated temperatures to meet a particular problem.

References

(B1) Greeley, R.S., Smith, W.T., Stoughton, R.W., and Lietze, M.H. Electromotive Force Studies in Aqueous Solutions at Elevated Temperatures. I The Standard Potential of the Silver-Silver Chloride Electrode. J. phys. Chem. (1960), 64, 652-655

(B2) Bates, R.G., Bower, V.E. and Smith, E.R. Calcium Hydroxide as a Highly Alkaline pH Standard. J. Res. natn. Bur. Stand. (1956), 56, 305-312, RP 2680

(B3) Ives, D.J.D. and Janz, G.J. Reference Electrodes. (1961) Acedemic Press Ch. 3, p 174

(B4) Taniguchi, H and Janz, G.J. Preparation and Reproducibility of the Thermal-Electrolytic Silver-Silver Chloride Electrode. J. electrochem. Soc. (1957), 104, 123-127

(B5) Lietzke, M.H. Reference electrodes A paper in the Conference on High Temperature, High Pressure Electrochemistry in Aqueous Solutions. (1973) Surrey University.

(B6) Jones, D.de G. and Masterson, H.G. Techniques for the Measurement of Electrode Processes at Temperatures above 100°C. Advances in Corrosion Science (1971), 1, 1-49

(B7) Lepeintre, M., Mahieu, C and Monjou, J. Electrode de reference utilisable en milieu aqueux jusqu'a 250°C C. R. Acad. Sc. Paris. (1965), 261, (Gp. 7) 3389-3391

(B8) Benrath, von A., Gjedebo, F., Schiffers, B. and Wunderlich H. Über die Loslichkeit von Salzen und Salzgemischen in Wasser bei Temperaturen oberhalb 100° Zeit. anorg. alleg. Chem. (1937), 231, 285-297

Appendix C

Precipitation of Metal Compounds from Aqueous Solutions at Elevated Temperatures

At elevated temperatures many aqueous metal solutions precipitate solids. These may be oxides, hydrated oxides, neutral or basic salts the type of compound precipitating depending on the metal, its oxidation state, the anions present in the solution, temperature and pH. The author has previously reviewed the hydrolysis of aqueous metal solutions at elevated temperatures[Cl] and it is evident that whereas hydrolysis of chloride and nitrate systems will yield (hydrated) oxides e.g. CrOOH, Fe_2O_3, SnO_2, ThO_2, ZrO_2, HfO_2, in sulphate systems (presently the most important in hydrometallurgy) basic salts will be precipitated at moderately low pH. Such precipitation is potentially very important commercially, for example, a process has been proposed for the removal of iron, in the ferric state, from zinc bearing liquors by thermal hydrolysis, a jarosite, $MFe_3(SO_4)_2(OH)_6$, being precipitated. Also a completely acid based process for aluminium recovery from low grade, high iron and silica bauxite has been proposed in which aluminium is precipitated by thermal hydrolysis as an insoluble basic sulphate (similar to the jarosites) in the presence of ferrous iron, which stays in solution. Thus knowledge of the basic sulphates which can be precipitated at elevated temperatures if of considerable importance.

The literature provides ample evidence that many such salts exist, many of which can be prepared at room temperature by simple, careful partial neutralisation of metal sulphate solutions. However,

the conditions for the preparation of stoichiometric salts are usually quite exacting, often involving dilute (<0.1 M) solutions compared to those experienced in hydrometallurgy (0.1-3.0 M). Basic sulphates have relatively complicated formulae and structures and their formation and stoichiometries are expected to depend as much on kinetics as on thermodynamic equilibria, e.g. the rate of diffusion of $SO_4^=$ ions into a metal hydroxide lattice. Indeed, it will be seen below that short time equilibrium in certain nickel solutions at 150° and 200°C produced very similar results although on increasing the reaction time by a factor of seven a completely new solid phase was formed at the higher temperature. However, whether this really indicates a different thermodynamic equilibrium or just slower kinetics at the lower temperature is impossible to decide. It certainly seems likely that for true equilibrium to be attained in such systems, even at 200°C, reaction times of at least days rather than hours are required. However, such questions are not necessarily relevant to hydrometallurgy in which only short term equilibrium (i.e. within minutes) whether thermodynamic or not, is of importance.

Some preliminary experiments have previously been made by the author on the Cr(III), Cu(II) and Zn sulphate systems at 150°C.[C2] Cr(III) forms a rather ill-defined basic sulphate, $Cr_3(SO_4)_2O_6H_7$ reminiscent of the jarosites and alunites ($MFe_3(SO_4)_2(OH)_6$ and $MAl_3(SO_4)_2(OH)_6$) although no evidence for an analogous series of such compounds was found.

Copper sulphate solutions precipitated two basic sulphates identical to two previously determined minerals, Antlerite, $Cu_3(SO_4)(OH)_4$, at low pH and Bronchantite, $Cu_4(SO_4)(OH)_6$ at higher

pH. At still higher pH tenorite, CuO (and not $Cu(OH)_2$) is formed. These results have been subsequently confirmed by Kwok and Robins.(C3)

Zinc sulphate solutions precipitated only one basic sulphate whose X-ray powder pattern was similar to that of Bronchantite and which had a SO_4/Zn mole ratio of approximately 0.25. It was therefore assumed to be $Zn_4(SO_4)(OH)_6$. At high pH zinc oxide was formed.

From these results and other considerations it seems likely that all divalent transition metals will form one or more basic sulphates at elevated temperatures and some preliminary investigations of the Ni, Co(II) and Mn(II) sulphate systems have been made.

Experimental

Thick-walled, pyrex test-tubes were heated in the flame to produce narrow-necked ampoules. 5 ml. of an approximately 1 M metal sulphate solution (the true molarity was found by gravimetric analysis of the respective metal) were pipetted in and the required volume (always <1 ml.) of 10 M NaOH solution (accurately determined by dilution and titration versus standard 0.1 M HCl) added from a graduated 1 ml. pipette. Water was then added to make up the volume to 10 ml. and the ampoule sealed in the flame under air. The sealed tubes were manually or mechanically shaken, to obtain some homogeneity in the slurries, and then heated in an autoclave, two-thirds filled with water to balance the ampoules' internal vapour pressure, to the required temperature. On cooling the tubes were cut open and the contents filtered. Solids were washed with water and acetone (to avoid heating) and selected ones X-rayed.

Solutions were analysed for metal and sulphate and the SO_4/metal mole ratios in the precipitates calculated.

Analyses

Metals in solution were determined by Atomic Absorption Spectroscopy. Gravimetric analysis of Ni in precipitates was performed by dissolving the solids in hot, concentrated hydrochloric acid followed by precipitation with dimethylglyoxime in the usual way. Gravimetric analysis of sulphate in the precipitates was performed by $BaSO_4$ precipitation from similarly prepared solutions. All gravimetric analyses are quoted as the mean of two determinations with the relevant deviations.

Sulphate in solution was determined indirectly by Atomic Absorption. The recommended procedure involves precipitation of $BaSO_4$ and subsequent determination of the excess Ba metal. However, a barium A.A. lamp was not available during this work and so a method was devised involving $PbSO_4$ precipitation.

$PbSO_4$ is appreciably soluble in water at room temperature (30-40 mg./l.) however, its solubility is greatly reduced by the addition of ethanol, a 50 % by volume mixture seeming to lower its solubility to a suitable level (see Table (C1)).

The analysis was carried out as follows. Solutions were prepared by mixing in the following order, 10 ml. 1200 p.p.m. Pb solution ($Pb(NO_3)_2$ in 0.1 M HNO_3), x ml. (usually 0.75-1.0 ml.) of the sulphate solution (containing 2.5-5.0 g/l. SO_4), and 50 ml. of ethanol and the whole made up to 100 ml. with water. (Precipitation of $PbSO_4$ rarely occurred before the addition of the ethanol). The solution was centrifuged and the clear liquor

Table (C1)

Solubility of $PbSO_4$ in Ethanol-Water Mixtures at 25°C

Vol. % Ethanol	$PbSO_4$ Solubility: mg/l.
0	30
10	11
20	4.3
30	1.5
40	0.51
50	0.32
60	0.20
70	0.06

analysed for Pb by A.A. in the usual way but using a 50 % ethanol-water mixture as a blank. (The presence of ethanol seemed to have very little effect on the acetylene-air flame). Initially a calibration curve was drawn of % absorption versus sulphate concentration (that is the sulphate concentration in the 100 ml. of solution were the $PbSO_4$ actually dissolved) from results with known standards (see Fig. (C1)). The method seemed completely satisfactory and reproducible giving a basically linear calibration graph. It may well have advantages over $BaSO_4$ precipitation, which is notoriously temperamental although further tests on chemical interferences would have to be made. One particularly important interference was, however, checked. The pH of the final ethanol-water solution to be analysed must not be too low otherwise the equilibrium

$$H^+ + SO_4^{=} = HSO_4^-$$

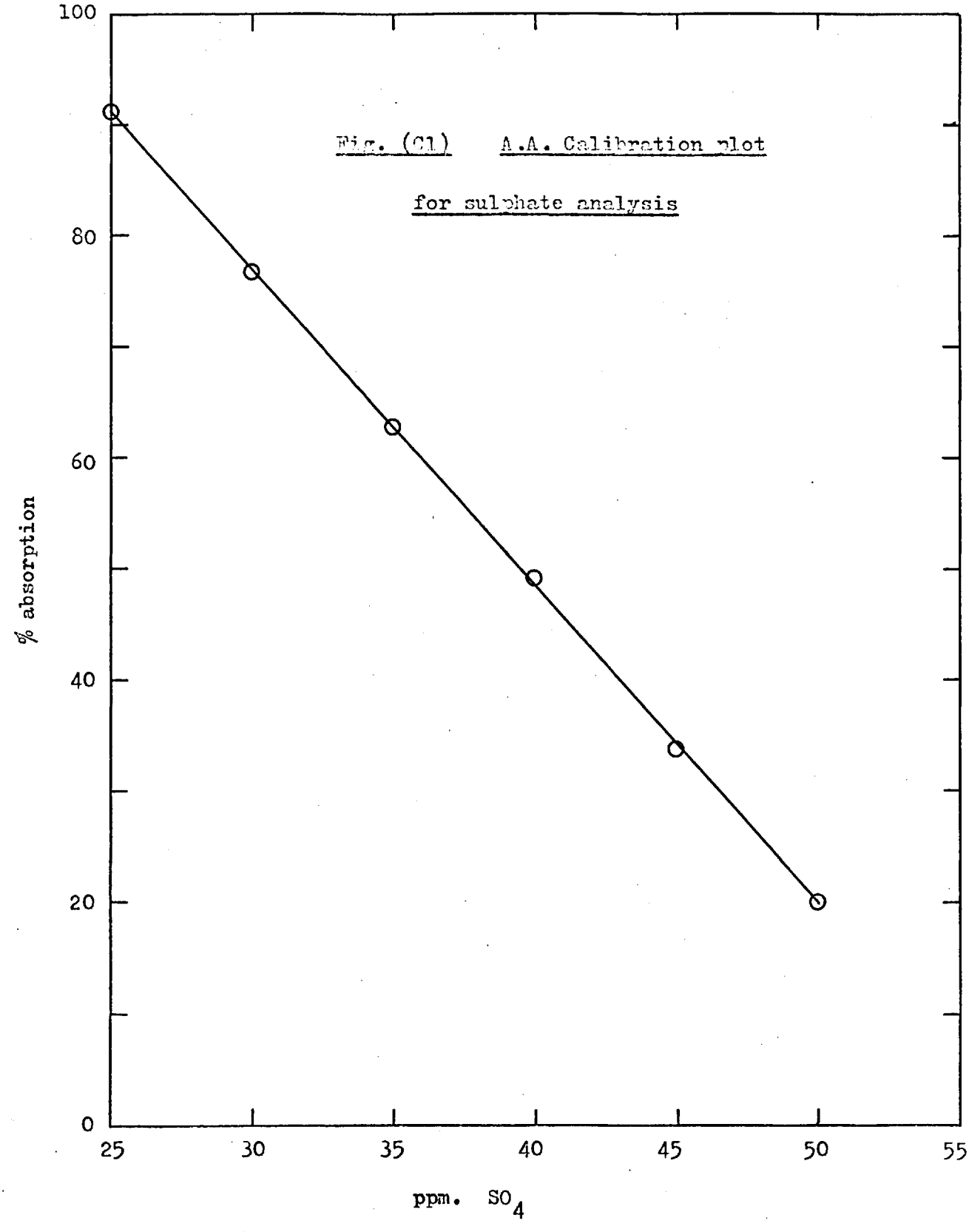


Fig. (C1) A.A. Calibration plot for sulphate analysis

will be forced to the right, greatly increasing the solubility of $PbSO_4$ (due to bisulphate formation) and leading to low sulphate analyses.

25-50 p.p.m. SO_4 standards were prepared as described above and therefore containing 0.01 M free HNO_3. Two other 25 p.p.m. standards were also prepared containing 0.1 and 0.5 M free HNO_3. The latter of these two solutions gave no precipitate of $PbSO_4$ even after standing for 3 days showing that the presence of the free acid had increased the solubility of $PbSO_4$ in the ethanol-water mixture to at least 79 mg/l. The solution containing 0.1 M HNO_3 gave a precipitate as normal but on A.A. analysis gave a significantly higher absorbance than the 25 p.p.m. standard containing containing only 0.01 M HNO_3, whose absorbance was in good linear agreement with the other standards. Indeed on the basis of this plot the standard containing 0.1 M HNO_3 would contain only 22.5 p.p.m. SO_4, corresponding to an increase in the solubility of $PbSO_4$ of 8 mg/l. Thus low pH can have a significant effect, although the original sulphate solution would have to have a very high acid concentration (>10 M). The effect would probably be most noticeable with solutions containing much free acid but little SO_4, in which case a simple expedient might be the addition of a drop of a suitable pH indicator to the ethanol-water solution and addition of dilute alkali to pH 2-3 just before making up to the 100 ml. mark.

The above test does not, of course, prove that the presence of only 0.01 M free acid does not also cause some increase in $PbSO_4$ solubility, however it seems unlikely to be large in view of the relatively small effect of 0.1 M acid. Moreover, SO_4 analyses

by this method of the original 1 M metal sulphate solutions (which would have had the lowest pH of any to be analysed in this work) were always in good agreement with SO_4 calculated from the gravimetric determinations of the metal in the solutions.

Results

Nickel

The results from the first tests carried out at 150°C are given in Fig. (C2) which shows per cent nickel precipitated (% Ni ppt) and the SO_4/Ni mole ratios in the precipitated solids (calculated from solution analyses) as a function of the per cent stoichiometric sodium hydroxide addition (% sNa) to the original solution. The SO_4/Ni curve clearly indicates that three different phases are being precipitated, I at below 40 % sNa having a maximum SO_4/Ni ratio of 0.34, phase II at between 50–80 % sNa with a maximum ratio of 0.19 and a third phase containing no SO_4 at 100 % sNa. The % Ni ppt curve also clearly shows this behaviour, where a steady increase in % Ni ppt with % sNa corresponds to the precipitation of a single phase but an inflexion occurs when one phase is changing into another, e.g. between 40–50 % sNa and 80–90 % sNa.

X-ray powder photographs of the solids from 20, 70 and 100 % sNa confirm these conclusions. The precipitate from 100 % sNa has d spacings identical to those of $Ni(OH)_2$. A search of the ASTM X-Ray pattern index based on the pattern of phase I (20 % sNa) revealed a close similarity to the pattern of the mineral Devillite,

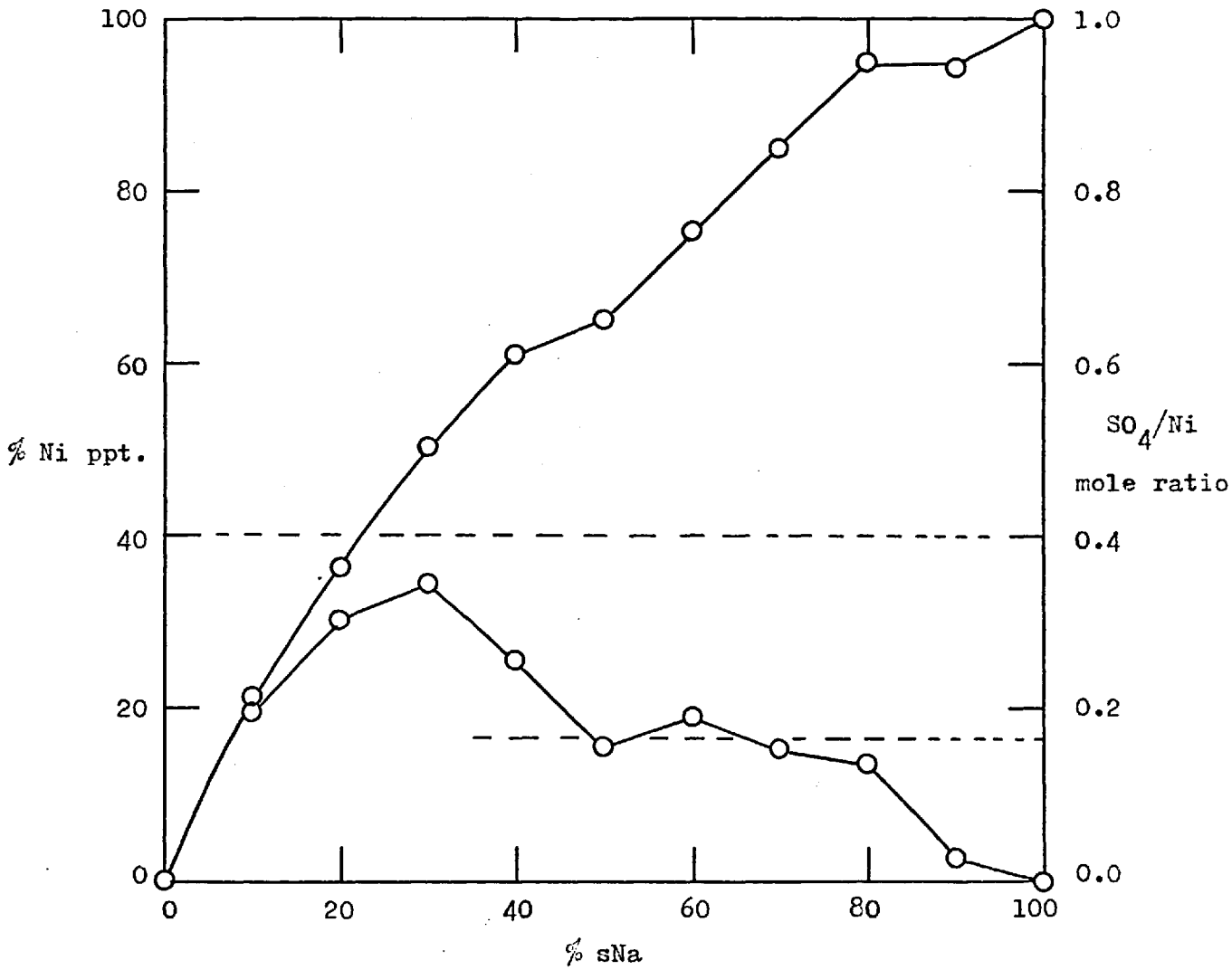


Fig. (C2) Precipitation of Ni compounds from 0.5 M $NiSO_4$ solutions at 150°C.

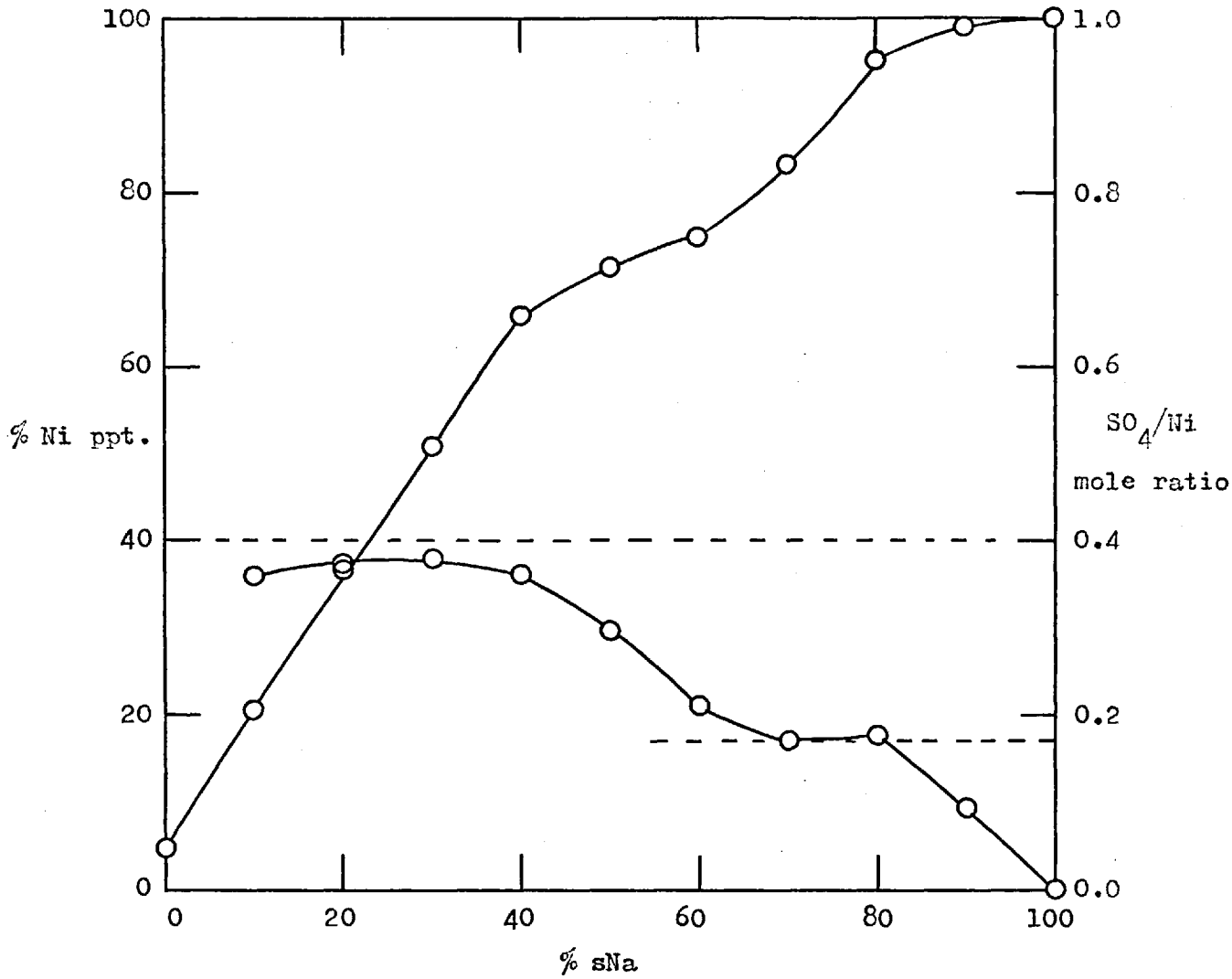


Fig. (C3) Precipitation of Ni compounds from 0.5 M $NiSO_4$ solutions at 200°C.

$Cu_4Ca(SO_4)_2(OH)_6 \cdot 3H_2O$. Isomorphism therefore suggests that phase I is the nickel analogue, $Ni_5(SO_4)_2(OH)_6 \cdot nH_2O$, having a SO_4/Ni ratio of 0.4. In fact the actual value of the ratio in the solid formed from 20 % sNa was 0.30, which must be expected to be correct to within $\pm$ 10 %. However, this discrepancy between the real and suggested theoretical ratio may be explained by considering the way in which the precipitate was actually formed. The initial addition of (in this case) 0.2 ml. of 10 M NaOH to a solution of 1 M $NiSO_4$ would be expected to precipitate mostly $Ni(OH)_2$ due to the high local pH. Thus if a basic sulphate is the stable phase at equilibrium it is going to be formed by the absorption of $SO_4^=$ ions from the solution and not by homogenous precipitation. This may well be a difficult and slow process even at 200°C and therefore during the reaction time a non-stoichiometric salt is formed although the basic lattice has been created. Further evidence for this idea is given below.

The X-ray pattern of phase II (70 % sNa) was found to be very similar to that of $Mg_6(SO_4)(OH)_{10} \cdot 3H_2O$ (C4) suggesting the analogue $Ni_6(SO_4)(OH)_{10} \cdot nH_2O$ having a SO_4/Ni ratio of 0.17 in good agreement with the value of 0.15 found for this precipitate.

The whole series of tests was repeated at 200°C to see if phases nearer to the stoichiometries now expected could be obtained. The results are shown in Fig. (C3). The SO_4/Ni curve shows even more clearly the ranges of % sNa corresponding to each phase and the characteristic shape of the % Ni ppt curve is again obtained. Phase I (20-40 % sNa) has a SO_4/Ni ratio of 0.36-0.38 (considerably nearer to 0.4) and phase II (70-80 % sNa) a ratio of 0.17-0.18. X-ray data for the solids from 20 and 70 % sNa showed patterns

visually identical to those obtained at the lower temperature. The pattern for the 50 % sNa solid was a combination of these two patterns confirming that this precipitate is merely a mixture of phases I and II. (It also means that at this point the solution is in equilibrium with two solid phases both containing the same ions. This is not a common occurrence in aqueous chemistry.)

The solutions from these tests were also analysed (by A.A.) for Na and were found to contain all the initially added metal (the lowest value was 96.2 %) proving that no sodium was present in the solid phases.

A closer study of the d spacings of the two phases prepared at 150°C revealed that the pattern of phase I could be correlated to the pattern of a basic nickel sulphate prepared by Marshall (C5) (who produced a total of four different solids) and also to the pattern of a solid prepared by Kwok and Robins (who produced two different solids.) The correlation between the patterns of phase I prepared in the present work (GDM I), phase III prepared by Marshall (M III) and phase I prepared by Kwok and Robins (KR I) together with that of Devillite is shown in Table (C2). It can be seen that all four patterns are very similar and there can be no doubt that the three nickel phases are identical notwithstanding some discrepancies at high d values and some absent lines between the patterns. Kwok and Robins had previously noted the similarity between KR I and M III.

The X-ray pattern of the second phase produced in the present work (GDM II) could be correlated to patterns of other solids prepared by these two sets of investigators namely M IV and KR II. The patterns for these and for $Mg_6(SO_4)(OH)_{10}\cdot 3H_2O$ are shown in

Table (C2)

GDM I		M III		KR I		Devillite	
d	I/I_o	d	I/I_o	d	I/I_o	d	I/I_o
10.15	vs	10.10	vs	10.12	s	10.2	vs
6.16	vw	6.20	vw	5.91	vw	5.89	vvw
						5.66	vvw
5.37	w	5.40	w	5.44	w	5.34	vvw
5.07	vs	5.10	s	5.10	vs	5.06	s
5.01	w					4.96	vvw
						4.83	vvw
4.64	vw	4.65	w	4.66	w	4.68	w
						4.58	vvw
						4.47	vvw
				4.35	w	4.38	vvw
				4.21	w	4.26	vw
4.066	vw	4.05	w	4.05	w		
4.012	vw						
3.938	vw					3.87	w
3.781	vw	3.80	vw				
						3.52	w
3.37	vw	3.40	m	3.40	m	3.38	s
3.264	Bw	3.28	vw				
3.075	vvw	3.09	w	3.09	w		
3.059	vvw						
3.016	vw						
2.923	vw	2.92	vvw	2.93	w		
2.74	vw			2.82	w	2.76	vw
2.692	vw	2.70	m	2.70	m	2.70	vvw
2.669	vw			2.64	w	2.65	m
2.623	w	2.62	m			2.63	w
2.594	w					2.58	m
2.546	w	2.55	w	2.56	m		
2.496	vvw	2.50	m	2.51	m	2.50	m
2.485	vw	----------		2.48	w	2.48	w
2.428	w			2.43	w		

d	I/I_o
2.369	w
2.337	vw
2.297	vw
2.246	vvw
2.216	vw
2.13	vw
2.102	w
2.032	w
1.977	Bw
1.927	Bvw
1.729	Bw
1.690	w
1.614	w
1.553	m
+ 3 lines to	
1.456	vw
+ 2 lines	

d	I/I_o
2.39	w
2.34	m
2.26	w
2.16	w
2.12	w
2.03	s
1.90	w
1.74	vw
1.71	vw

d	I/I_o
2.37	w
2.28	vw
2.22	w
2.20	w
2.15	vvw
2.09	vvw
1.99	vw
1.96	w
1.84	w
1.74	vw
1.70	vvw
1.69	vvw
1.68	vvw
1.67	vvw
1.63	vvw
1.61	vvw
1.57	m
+ 5 lines to	
1.46	vw

Table (C3)

GDM II		M IV		KR II		$MgSO_4 \cdot 5Mg(OH)_2 \cdot 3H_2O$	
d	I/I_o	d	I/I_o	d	I/I_o	d	I/I_o
				11.63	m		
				10.28	m		
8.10	Bvs	7.75	v	8.04	m	7.77	w
6.81	Bm	6.70	vs	6.81	s	6.88	vs
						6.11	vw
				5.79	m	5.70	vw
5.06	Bm	5.05	m	5.07	vs	5.13	vs
						4.76	?
				4.15	m	4.30	w
				3.93	s		
3.841	w	3.82	m	3.85	s	3.87	s
						3.62	vw
3.386	Bw	3.37	w			3.42	w
3.297	Bw					3.30	vw
						3.07	w
2.944	s	2.93	w	2.94	s	2.97	m
						2.87	vw
2.748	m	2.73	w	2.74	s	2.78	m
2.651	w	2.62	vvw			2.61	Bm
2.574	w	2.56	w	2.56	s		
2.493	w	2.49	vw	2.46(?)	m	2.461(?)	w
		2.42	vw			2.381	vw
2.225	vs	2.22	s	2.23	vs	2.248	vs
2.133	w						
2.079	vw					2.083	w
2.066	vw	2.05	vvw				
2.039	w						
1.988	m	1.98	w	1.99	m	2.001	Bm
						1.934	vw
1.874	Bw	1.86	vw			1.884	w
		----------				1.823	w
1.753	Bw					1.759	m
1.693	Bw					1.701	m

d	I/I_o	d	I/I_o	d	I/I_o
1.651	Bw			1.662	m
1.593	vBw			1.606	m
				1.572	w
1.538	vw	1.54	m	1.548	w
1.496	Bw			1.509	w
+ 5 lines to					
1.321	vw				

Table (C3). In this case Kwok and Robins had not noticed the similarity between their phase and that of Marshall although it is perhaps not surprising when one considers these two patterns alone, in view of the total absence of the two highest d values of KR II in M IV and the discrepancies between some of the lines' relative intensities. There can be no doubt however that these two phases and GDM II are basically identical.

An attempt was made to prepare a sample of GDM I in sufficient quantity so that it could be analysed directly. 2.553 ml. of 9.796 M NaOH (25 % sNa) were added to 50 ml. of 1.0 M $NiSO_4$ solution and the whole made up to 100 ml. and sealed in a large phial (total volume about 250 ml.) made in the flame from 1 in. diameter pyrex tubing. The slurry was mixed thoroughly by mechanical agitation and heated in an autoclave, as in the previous tests, to 200°C for 4 hours. On cooling the phial was again shaken and returned to the autoclave for reheating. This cycle was repeated.

After the first heating the precipitate was pale green and visually identical to GDM I. After the third heating a lime-green band of solid, quite distinct from the rest of the precipitate beneath it, was present at the solid-liquid interface. On shaking this new phase settled faster than the original one. (It was subsequently found that the new solid consisted of distinguishable crystals under moderate magnification whereas GDM I never appeared as more than an amorphous powder, even under high magnification). As the number of heating cycles increased the proportion of the new phase became greater until after 7 x 4 hours at 200°C the solid seemed to be totally converted. (Some large colourless

crystals were also present but were assumed to be sodium sulphate).

The phial was cut open, its contents filtered, washed with water and acetone: the yield was 4.516 g. Gravimetric analysis of this solid gave Ni: 40.64 ± 0.03 % and SO_4: 40.84 ± 0.01 % giving a SO_4/Ni ratio of 0.614. Assuming OH^- ions balance the charge and H_2O the equivalent weight these results correspond to a formula $Ni_3(SO_4)_{1.84}(OH)_{2.31}\cdot 2.27H_2O$ or $Ni_{3.26}(SO_4)_2(OH)_{2.51}\cdot 2.46H_2O$. If it is assumed that the lattice is SO_4 deficient rather than Ni excessive then the former stoichiometry becomes the most likely suggesting the theoretical formula $Ni_3(SO_4)_2(OH)_6\cdot 2H_2O$ (containing 40.18 % Ni and 43.83 % SO_4).

The X-ray pattern of this compound (GDM III) could be fitted to that of $Mg_3(SO_4)_2(OH)_6\cdot 3H_2O$ and also to that of another of Marshall's products (M I) as shown in Table (C4). This is also confirmed by Marshall's estimate of 1.5 for the NiO/SO_3 mole ratio in his compound. (It may be noted in passing that the similarity of the X-ray powder patterns, and therefore the structures, of two pairs of Ni and Mg sulphates must be due in part to the two metal ions' similar size: Ni^{2+} - 0.69 Å, Mg^{2+} - 0.66 Å).

The failure to produce a sample of GDM I at 200°C led to a repetition of the above experiment at 150°C. 2.042 ml. of 9.796 M NaOH (25 % sNa) plus 40 ml. of 1.0 M $NiSO_4$ solution made up to 80 ml. were sealed in a phial as before and an identical procedure followed leading to a total of 30 hours at 150°C. No second solid ever formed visably and the precipitate kept its light green colour throughout. The yield was 1.710 g. Gravimetric analysis of the product gave Ni: 47.32 ± 0.01 % and SO_4: 29.95 ± 0.04 % corresponding to a SO_4/Ni ratio of 0.387

which leads to the formulae $Ni_5(SO_4)_{1.93}(OH)_{6.13}\cdot 2.04H_2O$ or $Ni_{5.17}(SO_4)_2(OH)_{6.34}\cdot 2.10H_2O$. These indicate a theoretical formula $Ni_5(SO_4)_2(OH)_6\cdot 2H_2O$ (47.06 % Ni and 30.80 % SO_4) confirming previous conclusions.

An X-ray photograph of this sample was taken some three months after its preparation during which time it had been kept in a sealed, but not necessarily air-tight, container. The pattern obtained was not that of the previously prepared GDM I but much closer to GDM II plus some other lines. The correlation is shown in Table (C5). This is interpreted as meaning that $Ni_5(SO_4)_2(OH)_6\cdot 2H_2O$ is not stable in air at room temperature and changes in part to $Ni_6(SO_4)(OH)_{10}$. (In previous work $Zn_4(SO_4)(OH)_6$ was observed to decompose within a few days at room temperature forming, among other things, ZnO). The decomposition reaction is not clear although a straightforward equation could be written,

$$2Ni_5(SO_4)_2(OH)_6 = Ni_6(SO_4)(OH)_{10} + 3NiSO_4 + Ni(OH)_2$$

However, no pattern of nickel hydroxide, nickel sulphate and its hydrates or any other basic nickel sulphate could be fitted with confidence to the X-ray powder photograph.

In light of the success in fitting the powder patterns of phases prepared in the present work to patterns of salts of other metals the pattern of the fourth phase (M II) prepared, but not identified by Marshall was re-examined but no obvious fit to any other salt was observed. Marshall estimated a NiO/SO_3 ratio of 2.5 (i.e. $Ni/SO_4 = 0.4$) for this compound, which is odd since the same ratio has been proved for GDM I and M III. However, there is no reason to doubt Marshall's estimate since his one for

Table (C4)

GDM III		M I		$2MgSO_4 \cdot Mg(OH)_2 \cdot 3H_2O$	
d	I/I_o	d	I/I_o	d	I/I_o
				8.05	vvw
7.14	s	7.10	s	7.22	m
6.33	m	6.30	w	6.37	m
5.75	s	5.70	m	5.78	m
5.24	vw			5.32	m
4.84	vw	4.70(?)	w	4.80	m
4.74	w			4.62	vw
		4.33	w	4.28	m
4.005	s	4.00	s	4.07	m
3.833	vw	3.80	w	3.89	m
3.574	vvw	3.60	vw	3.59	w
		3.52	vw		
3.400	m	3.39	w	3.41	Bm
3.179	m	3.22	w	3.21	Bm
		3.07	w	3.08	vw
2.941	vs	2.92	s	2.97	s
2.897	m			2.90	vw
2.875	m	2.86	s		
		2.80	w	2.80	m
2.775	m	2.76	w		
2.648	s	2.64	m	2.66	Bm
2.625	vvw			2.58	vw
2.484	s	2.47	m	2.497	m
2.420	w	----------			
2.381	vvw			2.385	m
2.372	w				
2.352	vvw				
2.301	w			2.313	m
2.275	vw				
2.260	vw			2.254	vvw
2.174	vw			2.183	vvw
2.130	vvw				
2.111	w			2.108	w

d	I/I_o	d	I/I_o
2.100	w		
2.083	vvw		
2.027	w	2.029	m
2.015	w	1.997	w
1.980	w		
1.935	vvw		
1.919	vw	1.919	m
1.910	vw		
1.895	vw		
1.870	vw	1.870	w
1.857	w	1.856	vvw
1.817	vw		
1.787	vw		
1.772	vvw		
1.759	vvw		
1.749	vw	1.747	vvw
1.740	vw		
1.714	vvw		
1.709	vvw	1.701(?)	m
1.693	w	1.701(?)	m
1.650	vvw		
1.640	w	1.646(?)	w
1.621	vvw	1.621	m
1.610	vw		
1.601	vvw		
1.592	vvw	1.587	m
+ 6 lines to			
1.518	vw	1.518	Bw
+ 20 lines to			
1.233	vw		

Table (C5)

See text.		GDM II	
d	I/I_o	d	I/I_o
10.30	vs		
7.94	vw	8.10	Bvs
6.82	s	6.81	Bm
5.41	vw		
5.12	s	5.06	Bm
3.850	vw	3.841	w
3.408	m	3.386	Bw
3.303	vvw	3.297	Bw
3.085	vvw		
2.994	vvw		
2.945	w	2.944	s
2.752	vw	2.748	m
2.708	vw		
2.684	w		
2.647	vvw	2.651	w
2.625	vw		
2.584	vvw	2.574	w
2.553	vvw		
2.515	m		
2.486	vvw	2.493	vs
2.436	vw		
2.392	vw		
2.353	vvw		
3.315	vvw		
2.261	w		
2.232	m	2.225	w
2.201	vvw		
2.165	vvw		
2.114	vvw		
2.074	vvw	2.079	vw
		2.066	vw
2.044	vw	2.039	w

d	I/I_o	d	I/I_o
1.979	vBm	1.988	m
1.898	vvw		
1.882	vvw	1.874	Bw
1.867	vvw		
1.821	vvw		
1.760	vvw	1.753	Bw
1.739	vvw		
1.698	w	1.693	Bw
1.654	vvw	1.651	Bw
1.623	vvw		
1.593	vw	1.593	vBw
1.560	ms		
1.541	vw	1.538	vw
1.524	vw		
1.499	Bvw	1.496	Bw
1.463	Bvw	1.465	vw
		+ 3 lines to	
		1.321	Bvvw

Table (C6)

M II		M III	
d	I/I_o	d	I/I_o
10.00	f	10.10	s
		6.20	vf
		5.40	f
5.25	s	5.10	s^-
		4.65	f^+
		4.05	f
		3.80	f^-
3.42	vvf	3.40	m
3.20	vf	3.28	vf
		3.09	f
2.85	vvf	2.92	vvf
2.74	m	2.70	m
2.62	m^+	2.62	m^-
		2.55	f
		2.50	m
2.42	f	2.43	f
		2.38	f
2.27	f		
2.18	vvf		
2.09	m^-		
1.90	vvf		
1.75	f		
1.60	m^-		

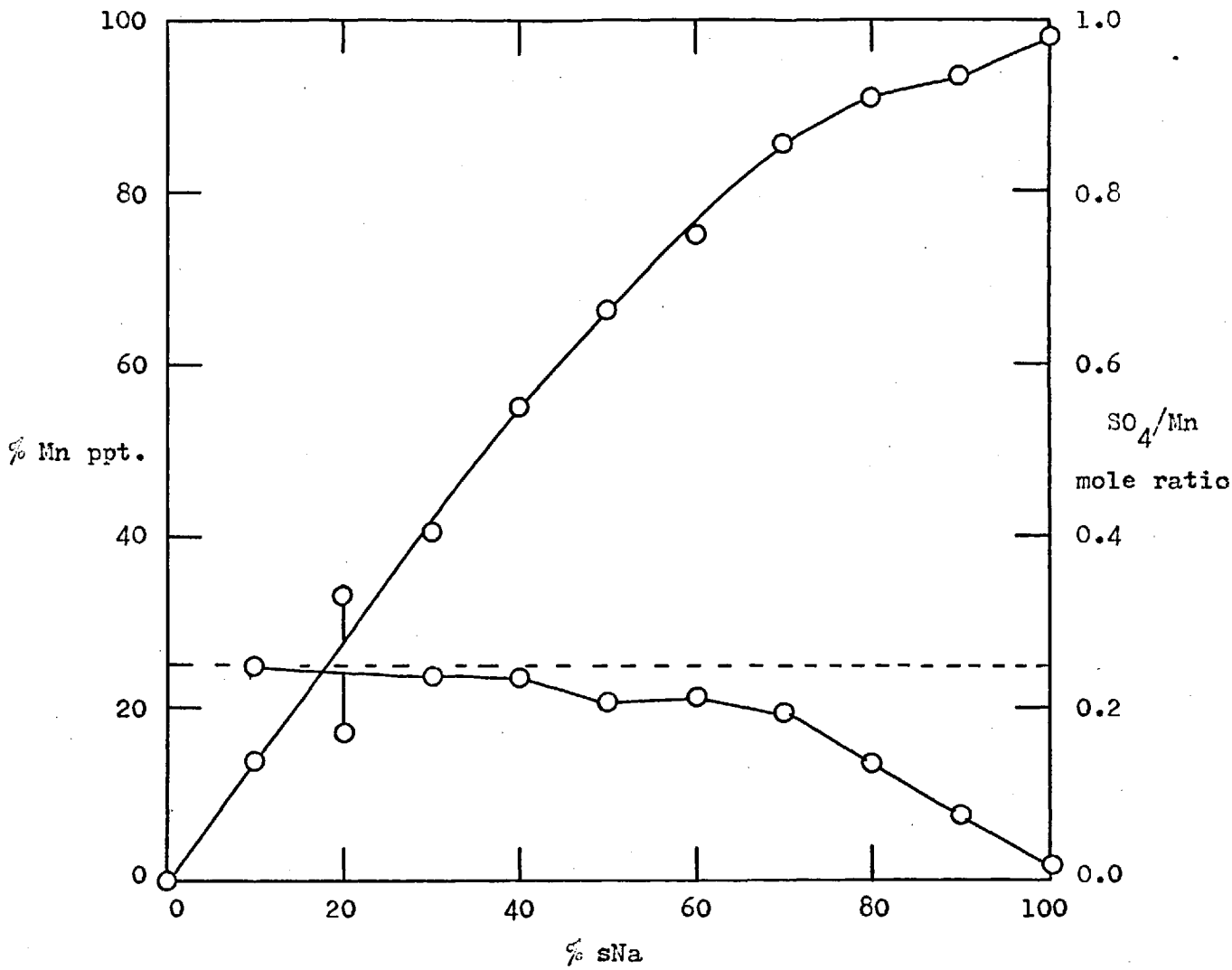


Fig. (C4) Precipitation of Mn compounds from 0.5 M $MnSO_4$ solutions at 150°C.

phase M I has been confirmed above. In view of these facts it seems possible that M II and M III are basically the same compound and the correlation between the two X-ray patterns shown in Table (C6) (Marshall's data) demonstrates that this is not too unreasonable.

Manganese

Unfortunately the initial addition of strong NaOH solution to the 1 M $MnSO_4$ caused some oxidation by air to occur, either Mn(III) or Mn(IV) oxides being formed which gave all the solids a brown colour. The results for the 0.5 M $MnSO_4$ solutions at 150°C are shown in Fig. (C4) and are somewhat inconclusive.

A SO_4/Mn mole ratio of nearly 0.25 is observed at low % sNa (the point at 20 % sNa is believed erroneous) which drops to 0.2 at between 50-60 % sNa and then steadily falls to zero at 100 % sNa.

X-ray data were unsatifactory. The compounds fluoresced badly in the radiation from the cobalt target available giving a high background intensity and making measurement difficult. Moreover, the patterns were themselves weak indicating low crystallinity in the solids. Table (C7) shows the fit of the d spacings of $Mn(OH)_2$ to the pattern obtained from the precipitate formed from 100 % sNa. It can be seen that the agreement is not very good and that some other phase may be present. Patterns from the solids formed from 30, 60 and 80 % sNa appeared virtually identical (apart from some $Mn(OH)_2$ lines present) which seems to exclude the possibility that two distinct phases with SO_4/Mn ratios of 0.25 and 0.2 exist. Also considering the % Mn ppt curve, if the point at 20 % sNa is

Table (C7)

Solid from 100 % sNa		$Mn(OH)_2$	
d	I/I_o	d	I/I_o
4.93	w	4.72	s
3.09	w		
2.89	vw	2.87	m
2.77	m		
2.49	m	2.45	vs
2.37	mw	2.36	vvw
1.80	w	1.83	m
		1.66	mw
1.58	w	1.57	w
1.54	w	+ 11 lines.	

Table (C8)

Solid from 60 % sNa

d	I/I_o	d	I/I_o
12.9	m	3.03	mw
7.49	w	2.988	mw
6.04	m	2.947	vw
5.30	w	2.774	vw
4.94	w	2.672	vw
4.37	w	2.651	vw
3.76	w	2.493	vw
3.56	vw	2.477	mw
3.34	mw	2.361	w
3.32	vw	2.231	w
3.29	vw	1.874	w
3.23	vw	1.703	w
3.09	vw	1.651	w
3.06	vw		

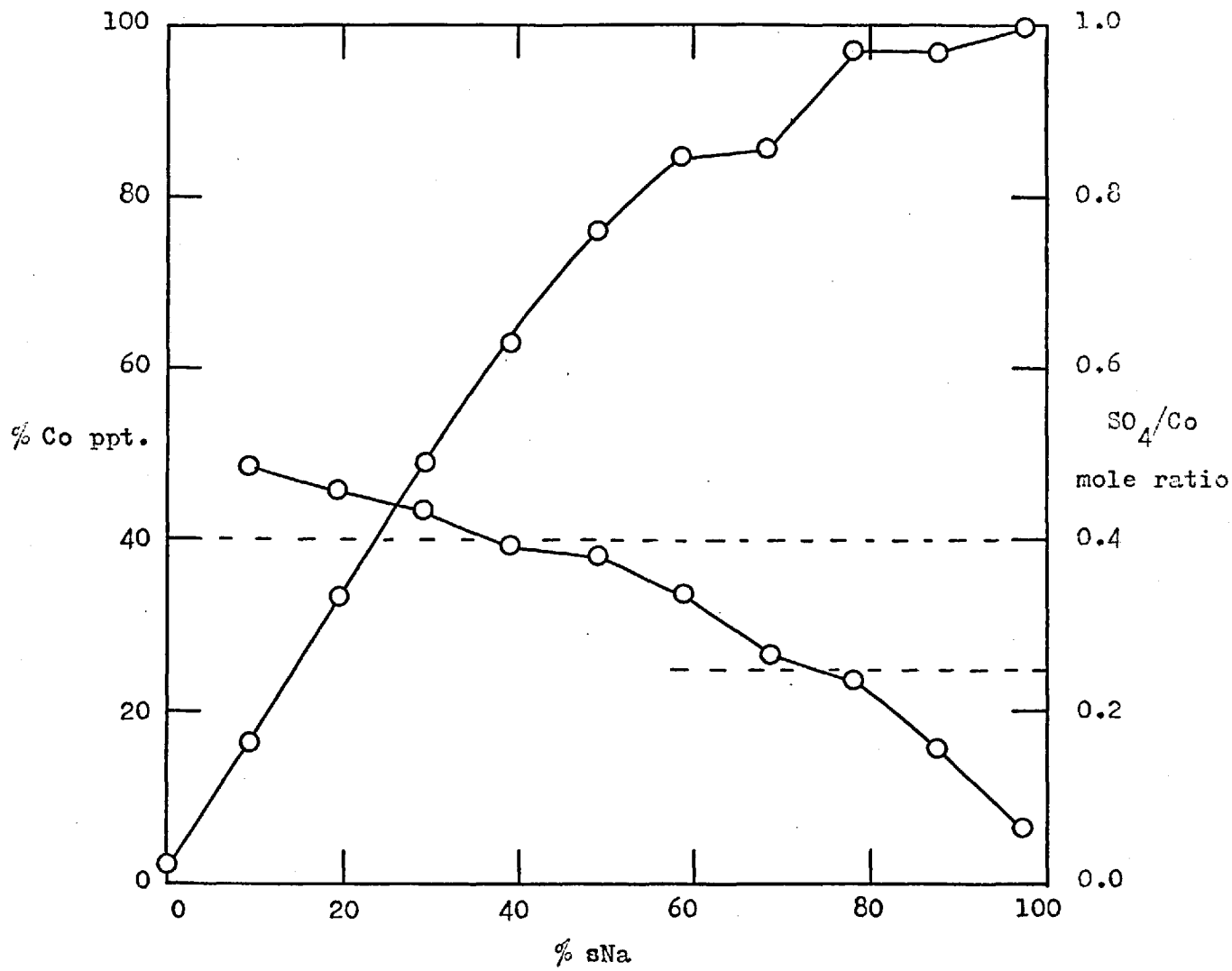


Fig. (C5) Precipitation of Co compounds from 0.5 M $CoSO_4$ solutions at 150°C.

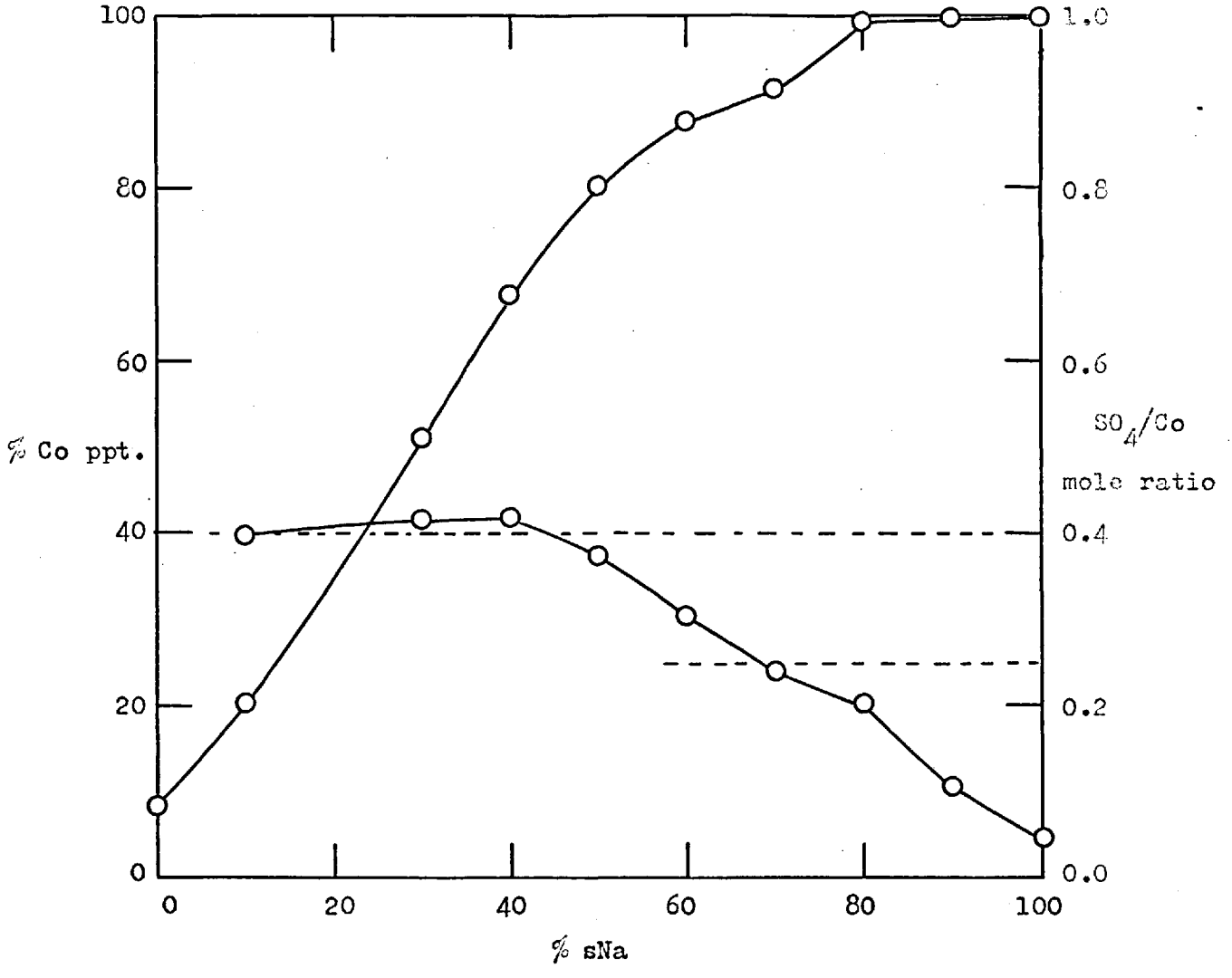


Fig. (C6) Precipitation of Co compounds

from 0.5 M $CoSO_4$ solutions at 200°C.

regarded as erroneous (i.e. too high, which would account for the low SO_4/Mn ratio at this point, the sulphate analyses showing a smooth curvature through this region) then the curve increases steadily to 70 % sNa at which point it flattens, corresponding to the formation of $Mn(OH)_2$. There is no inflexion at between 40 and 50 % sNa which would be expected if a new phase was forming at this point. It seems, therefore, that there is no real plateau in the SO_4/Mn curve at 50-60 % sNa and that the only sulphate phase formed is $Mn_4(SO_4)(OH)_6.nH_2O$, possibly like the Cu(II) and Zn compounds of similar stoichiometry, although the d spacings of these compounds could not be convincingly fitted to the X-ray pattern of the solid formed from 60 % sNa shown in Table (C8).

Cobalt

As with manganese, the initial addition of concentrated NaOH solution to the 1 M $CoSO_4$ caused some oxidation of the metal to occur, in this case to Co(III). This resulted in brown-black scaly deposits (almost certainly Co_3O_4) being formed during heating which stuck to the glass ampoule. The results obtained with the 0.5 M $CoSO_4$ solutions at 150° and 200°C are shown in Figs. (C5) and (C6).

The % Co ppt and SO_4/Co ratio curves clearly indicate the formation of three compounds at both temperatures. Compound I at below 50 % sNa, compound II at between 70-80 % sNa and $Co(OH)_2$ at 100 % sNa. Despite the rather higher values obtained at 150°C below 30 % sNa, the most likely value of the SO_4/Co ratio in I is 0.4, corresponding to $Co_5(SO_4)_2(OH)_6.nH_2O$ (cf. Mg and Ni).

Table (C9)

Solid from 97 % sNa		$Co(OH)_2$*	
d	I/I_o	d	I/I_o
7.06	vvw		
4.66	vs	4.66	s
2.756	s	2.76	m
2.438	vw		
2.370	vs	2.38	vs
		2.34	vvw
2.322	vw		
2.134	w		
2.025	vvw		
1.775	s	1.78	s
1.587	s	1.60	m
1.550	vw	1.56	vvw
1.502	s	1.51	m
1.427	vw		
1.374	m	1.38	vvw
1.351	m	1.36	m
		+ 8 lines to	
		1.01	m

* ASTM Card No. 3-913

Table (C10)

$Co_5(SO_4)_2(OH)_6 \cdot nH_2O$

d	I/I_o
17.8	s
8.80	vs
8.11	vw
7.36	vw
7.05	s
6.66	vw
5.87	w
5.78	vvw
5.67	vw
5.56	vw
5.44	w
4.60	w
4.02	vvw
3.85	vvw
3.82	vvw
3.61	vw
3.52	m
3.40	m
3.34	vvw
3.21	vw
3.16	m
3.13	vw
3.10	vvw
2.972	vvw
2.929	vvw
2.898	w
2.875	vvw
2.848	w
2.793	vw
2.764	vw
2.719	vs
2.697	vvw

d	I/I_o
2.653	vvw
2.607	s
2.566	s
2.520	Bvvw
2.496	vvw
2.422	m
2.450	vw
2.430	m
2.406	w
2.366	vw
2.318	vw
2.306	vw
2.282	vvw
2.262	vvw
2.240	w
2.192	w
2.156	m
2.131	vvw
2.103	vvw
2.082	vvw
2.059	vvw
2.028	m
2.002	vw
1.984	Bvw
1.960	vvw
1.944	vvw
1.923	vvw
1.896	vw
1.851	
1.844	w
1.809	vw
1.794	vvw
1.766	vvw
1.756	w
1.737	w
1.709	vvw

d	I/I_o
1.701	vvw
1.696	vvw
1.670	vw
1.653	vvw
1.639	vvw
1.604	vvw
1.587	vvw
1.573	vs
1.562	m
1.549	s
1.534	m
1.519	Bm
1.499	Bw
1.477	Bw
1.461	Bvvw
1.445	vw
1.435	vw
1.418	vw
1.405	vvw
1.379	vvw
1.362	w
1.356	vw
1.270	vvw

For compound II a SO_4/Co ratio of 0.25 looks probable which corresponds to $Co_4(SO_4)(OH)_6.nH_2O$ (cf. Cu(II), Zn and Mn).

X-ray data of solids produced at 150°C qualitatively confirm these results. The pattern from the solid formed by 97 % sNa could be matched to that of $Co(OH)_2$ (see Table (C9)) although some extra lines are present. The patterns of solids formed by 30 and 80 % sNa are shown in Tables (C10) and (C11) and are quite distinct but very complex, that of compound I having over 100 lines. The particularly high d spacing of 17.8 for compound I, indicating a very large unit cell, is also noteworthy. However, due partially to their complexity no unambiguous fit to any other compound could be made.

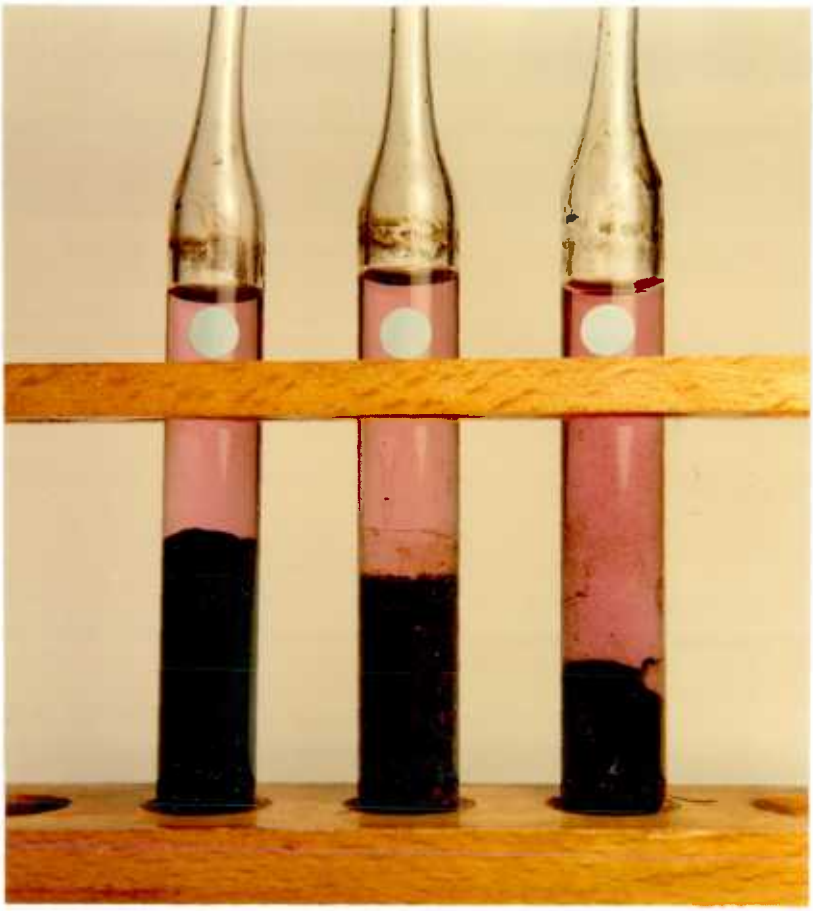
Perhaps the most striking aspect of this system is its colour variations. The slurries initially produced at room temperature were all dark blue but after heating to either temperature solids produced at below 40 % sNa (I) were dark red, whereas solids formed at between 70-90 % sNa (II) were blue. The $Co(OH)_2$ formed at 100 % sNa was pink. Between 40 and 60 % sNa, where the solutions are in equilibrium with both I and II the two phases were clearly distinguishable in the precipitated solids. Moreover, as produced in the ampoules (i.e. without stirring) the layer of II was always below the layer of I, the boundary between them being sometimes strikingly sharp. If this really does indicate the order of formation of the two compounds (i.e. II first) then it is precisely that which would be expected due to the slow absorption of $SO_4^=$ ions from solution by the solid. The high local pH produced initially by the addition of strong NaOH solution precipitates either

Table (C11)

$Co_4(SO_4)(OH)_6 \cdot nH_2O$

d	I/I_o
10.38	s
5.50	m
5.34	m
5.14	m
3.89	vvw
3.83	vvw
3.43	w
3.35	vvw
3.27	Bvvw
3.19	Bvvw
3.12	vvw
2.953	vvw
2.841	Bvvw
2.815	vvw
2.779	vvw
2.749	vs
2.719	vw
2.671	vs
2.650	vvw
2.599	vvw
2.573	vw
2.539	vvw
2.517	vvw
2.471	vvw
2.454	m
2.413	vvw
2.390	w
2.346	vw
2.302	vvw
2.175	w
2.135	vw
2.109	w

d	I/I_o
2.075	m
2.044	vw
2.024	vw
1.976	vvw
1.963	vvw
1.905	vw
1.890	vvw
1.847	vvw
1.805	vvw
1.789	vvw
1.770	vvw
1.755	vvw
1.740	vvw
1.723	vvw
1.713	vvw
1.705	vvw
1.671	Bvvw
1.643	vvw
1.623	w
1.580	vs
1.571	vw
1.552	vw
1.544	w
1.534	vvw
1.522	Bvw
1.481	vw
1.431	vw
1.393	vw
1.384	vw
1.368	m
1.349	m



A B C

Fig. (C 7)

$Co(OH)_2$ or $Co_4(SO_4)(OH)_6$ (probably the latter since the slurries were blue) which quickly settles to the bottom of the ampoule. Subsequently, on heating, the precipitates in those ampoules with a sufficiently low % sNa slowly absorb $SO_4^{=}$ from solution (and this will obviously start at the solid-solution interface) producing compound I. A reaction can be written,

$$5Co_4(SO_4)(OH)_6 \text{ (II)} + 3SO_4^{=} = 4Co_5(SO_4)_2(OH)_6 \text{ (I)} + 6OH^{-}$$

although, of course, it merely represents the change of stoichiometry and says nothing about a mechanism. At low % sNa this convertion is complete, but at 40-60 % sNa only partial convertion can occur and therefore the two distinct layers are preserved. (Precisely the opposite order of precipitation would be expected if NaOH were added slowly, in which case phase I would be formed initially and then phase II, as the pH increased on addition of more NaOH.)

The effect is clearly shown in Fig. (C7). Phials A, B and C contained originally 0.5 M $CoSO_4$ plus 60, 50 and 40 % sNa respectively and were heated to 150°C for 4 hours. In A, blue phase II is seen with a thin layer of dark phase I (in reality rather more red than here reproduced) at the solid-solution boundary. In B almost equal quantities of I and II are present although with I definitely above II and in C virtual total convertion has occurred and only I in visible. (Scales of Co_3O_4 (?) can also be seen on the glass above the liquid level).

References

(C1) Manning, G.D. Pressure Hydrolysis - A Survey
Stevenage: Warren Spring Laboratory, (1970),
LR 134 (ME)

(C2) Manning, G.D. The Hydrolysis of Chromium, Copper and Zinc Sulphate Solutions at Elevated Temperatures
Stevenage: Warren Spring Laboratory, (1971)
LR 165 (ME)

(C3) Kwok, O.J. and Robins, R.G. Thermal Precipitation in Aqueous Solutions.
International Symp. on Hydromet. (Ed. Evans, D.J.I. and Shoemaker, R.S.) A.I.M.M.P.E. N.York, (1973),
39, 1033-1080

(C4) Demediuk, T. and Cole, W.F. A Study on Magnesium Oxysulphates. Aust. J. Chem. (1957), 10, 287-294

(C5) Marshall, W.L., Gill, J.S. and Slusher, R.
Aqueous Systems at High Temperature - VI. Investigations on the System $NiO-SO_3-H_2O$ and its D_2O Analogue from 10^{-4} to 3 m SO_3, 150-450°C
J. inorg. nucl. Chem. (1962), 24, 889-897